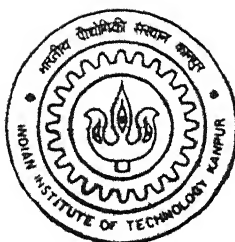


9871702

First Principle Calculation on Point Defects in GaAs

by
Kaushik Nandi

TH
MS/2001/M
N1537

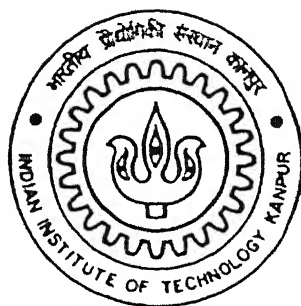


DEPARTMENT OF MATERIALS SCIENCE
INDIAN INSTITUTE OF TECHNOLOGY, KANPUR
January, 2001

First Principle Calculation on Point Defects in GaAs

By

Kaushik Nandi



DEPARTMENT OF MATERIALS SCIENCE
INDIAN INSTITUTE OF TECHNOLOGY KANPUR

January, 2001

300/

33733



A133733

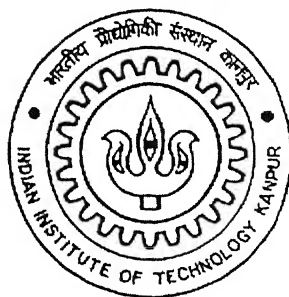
First Principle Calculation on Point Defects in GaAs

*A Thesis Submitted
in partial fulfillment of the requirements
for the degree of*

Master of Technology

By

Kaushik Nandi

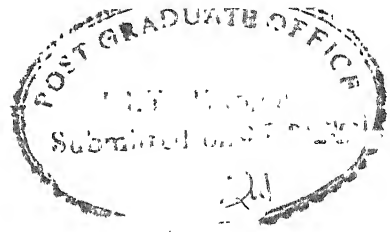


To the

DEPARTMENT OF MATERIALS SCIENCE

INDIAN INSTITUTE OF TECHNOLOGY KANPUR

January, 2001



Certificate

It is certified that the work contained in the thesis entitled *First principle calculation on point defects in GaAs* by **Kaushik Nandi** has been carried out under my supervision and this thesis work has not been submitted elsewhere for a degree.

Deepak

Dr. Deepak Gupta

Asst. Professor,

Deptt. of Materials and Metallurgical Engg.,

Indian Institute of Technology,

Kanpur, 208016

Table of Contents

Abstract.....	iv
Acknowledgement.....	v
List of Figures.....	vi
List of Tables.....	viii

Charter 1: Introduction

1.1 Background	1
1.2 Literature Review	2
1.3 Objectives of the present study	4

Chapter 2: Electronic structure calculation

2.1 The problem of the structure of matter	5
2.1.1 Adiabatic approximation (Born-Oppenheimer approximation)	6
2.1.2 Quantum many body theory	6
2.1.3 Density functional theory	8
2.1.4 Dynamics of ions	9
2.2 The concept of pseudopotential	10
2.2.1 General background and formulation	12
2.2.2 Atomic all electron calculation	13
2.2.3 Screened norm-conserving pseudopotential	15
2.2.4 Construction of Bachlet-Hamann-Schlüter pseudopotential	16
2.3 Defects in Semiconductors	19

Chapter 3: The *fhi96md* and *fhi98pp* code

3.1 The <i>fhi96md</i> program structure	21
3.1.1 Input and output files	25
3.2 Effect of various parameters used in the <i>fhi96md</i> code	27
3.3 The <i>fhi98pp</i> program structure	30

Chapter 4: Results and Discussion

4.1 Optimization of Gallium Arsenide structure	49
4.2 Optimization of Arsenic structure	54
4.3 Optimization of Gallium structure	65
4.4 Heat of formation of GaAs	74
4.5 Defect formation energy in GaAs	76

Chapter 4: Conclusions 81

Appendix A : Input file used for the optimization of GaAs	83
Appendix B : Input file used for the generation of the Ga, As, Si and C pseudopotential... 86	
Appendix C : Files <i>start.inp</i> and <i>inp.mod</i> used in the total energy calculation of GaAs	88
Appendix D : Input file used for the optimization of As	91
Appendix E : Neural network inputs used for the optimization of arsenic.....	95
Appendix F : Input file used for the optimization of Ga	100
Appendix G : Neural network inputs used for the optimization of gallium.....	104
Bibliography	109

Abstract

We have carried out *ab initio* total energy calculations using the density-functional theory to study the native defects in GaAs material. First principle pseudopotentials for Ga and As were generated according to the Bachlet-Hamann-Schlüter scheme using the computer code *fhi98pp*. These pseudopotentials were fully separable and norm conserving in nature. In order to ensure the accuracy of the results hard pseudopotentials were generated. The total energy calculation was performed with another code *fhi96md*. Lattice constants of Ga, As and GaAs were optimized on the basis of total energy minimization. All the calculations were done at 20 Ry cutoff and only the electron minimization scheme was employed using the second order damped Joannopoulos algorithm. The supercells for the calculations were constructed from four cells of Ga and As each and eight cells of GaAs. For exchange and correlation local density approximation (LDA) was employed. Heat of formation of GaAs was calculated for these optimized structures by subtracting the bulk energies of Ga and As from the bulk energy of GaAs. Though the individual energies of the materials concerned are close to those published in the literature, our results show that the heat of formation is 0.36 eV where as the experimental result is 0.74 eV. Various point defects were introduced in a GaAs crystal by physically removing the atoms. The formation energies for defects at different charge states have also been examined.

Acknowledgements

I wish to take this opportunity to express my sincere gratitude to my thesis supervisor, Dr. Deepak Gupta, for his expert guidance and valuable suggestions.

My gratitude is due to Prof. Rajendra Prasad, whose collaboration has been very useful. I would like to thank Prof. R. Prasad's students, Bala and Nitya, for their kind cooperation. Special thanks my lab junior Anshu for his kind support and help in every possible stages of my thesis. Apart from them, I would also like to acknowledge the influence of my friends Rajib, Santosh, Surajit, Samit, Khatua, and seniors Anirbanda, Alokeda and Pradyotda for giving me a good company and making my stay at IIT Kanpur a pleasant and memorable one.

Kaushik Nandi

List of Figures

Chapter 3

Fig 3.1. Flow chart of the program <i>flr96md</i>	22
Fig.3.2. Plot for Gallium pseudo 1s and all electron 4s wavefunction	33
Fig 3.3. Plot for Gallium 1s pseudopotential	34
Fig 3.4. Plot for Gallium pseudo 2p and all electron 4p wavefunction	35
Fig 3.5. Plot for Gallium 2p pseudopotential	36
Fig 3.6. Plot for Arsenic pseudo 1s and all electron 4s wavefunction	37
Fig 3.7. Plot for Arsenic 1s pseudopotential	38
Fig 3.8. Plot for Arsenic pseudo 2p and all electron 4p wavefunction	39
Fig 3.9. Plot for Arsenic 2p pseudopotential	40
Fig 3.10. Plot for Silicon pseudo 1s and all electron 3s wavefunction.....	41
Fig 3.11. Plot for Silicon 1s pseudopotential	42
Fig 3.12. Plot for Silicon pseudo 2p and all electron 3p wavefunction	43
Fig 3.13. Plot for Silicon 2p pseudopotential	44
Fig 3.14. Plot for Carbon pseudo 1s and all electron 2s wavefunction	45
Fig 3.15. Plot for Carbon 1s pseudopotential	46
Fig 3.16. Plot for Carbon pseudo 2p and all electron 2p wavefunction	47
Fig 3.17. Plot for Carbon 2p pseudopotential	48

Chapter 4

Fig 4.1. Plot for total energy as a function of cutoff energy for a GaAs supercell containing 32 gallium and 32 arsenic atoms	52
--	----

Fig 4.2. Plot for total energy as a function of lattice parameter for a GaAs supercell containing 32 gallium and 32 arsenic atoms	53
Fig 4.3. Plot for As structure	55
Fig 4 4. Plot for variation of the total energy with $2a$ for a fixed value of c and a family of values of z	58
Fig 4.5. Plot for variation of the total energy with $2a$ for a fixed z and a family of values of c	59
Fig 4.6. Plot for variation of the total energy with c for a fixed value of $2a$ and a family of values of z	60
Fig 4.7. Plot for variation of the total energy with c for a fixed values of z and a family of values of c	61
Fig 4.8. Plot for variation of the total energy with z for a fixed c and a family of values of $2a$	62
Fig 4.9. Plot for variation of the total energy with z for a fixed value of $2a$ and a family of values of c	63
Fig.4.10. Plot for Ga structure	66
Fig.4.11. Plot for total energy of gallium as a function of parameter c	69
Fig.4.12. Plot for total energy of gallium as a function of parameter z	71
Fig.4.13. Plot for total energy of gallium as a function of parameter a	72

List of Tables

Chapter 3

Table 3.1 Variation of the convergence time with the parameter *delt*29

Table 3.2 Variation of the convergence time with the parameter *gamma*.....30

Table.3.3 Comparison of the all electron and pseudo wavefunctions along with
the cutoff radius for Gallium, Arsenic, Silicon and carbon32

Chapter 4

Table 4.1 Variation of total energy with cutoff radius51

Table 4.2 Variation of total energy with lattice parameter.....51

Table 4.3 Calculated total energies at the neighboring points of the approximate
minimum as predicted by the neural network57

Table 4.4 Total energies around the point of minimum energy64

Table 4.5 Calculated total energies at the neighboring points of the approximate
minimum predicted by the neural network67

Table 4.6 Variation of total energy with parameter *c*68

Table 4.7 Variation of total energy with parameter *z*70

Table 4.8 Variation of total energy with parameter *2a*70

Table 4.9 Total energies around the point of minimum energy73

Table 4.10 Bulk energies of Ga, As and GaAs and the heat of formation of GaAs
.....75

Table 4.11 Calculated total energies of a defect supercell at different charge states
along with the perfect cell77

Table 4.12 Calculated defect formation energies of GaAs containing a Ga vacancy defect at different charge states along with the ionization energies	78
---	----

Chapter 1

Introduction

1.1 Background

The calculation of total energy using the density functional theory (DFT) [1.1] is the most commonly used tool in condensed matter physics and materials science. This method has been successfully applied to molecules, bulk solids and surfaces and the results are in very good agreement with the experiments. The basic essence of this theory is that, given an external potential, we are in a position to determine the electronic density, energy and any ground state property. Electronic structure theory, i.e., the theoretical prediction of materials properties from fundamental quantum mechanics without recourse to empirical parameters, has advanced significantly in recent years, serving basic science as well as applied research in numerous industries. The applicability of current methods and their spin-offs covers an extraordinarily wide range of fields and interdisciplinary research topics that embrace Condensed Matter Physics, Materials Science, Computer Science, Chemistry, and Biology.

Defects in semiconductor are particularly important in the context of optical and electrical conductivity. As an example, the semi-insulating GaAs has applications in heterostructure bipolar transistors and optical devices.

In ‘*ab-initio*’ or ‘first-principle’ calculations an exact description of the system is used i.e. no empirical parameters are used. In atomic *ab-initio* calculations only some basic data such as atomic numbers and masses are used as inputs. The ground state of the system is then obtained from DFT using the Born-Oppenheimer approximation [1.2]. The

corresponding equation describing the system is known as the Kohn-Sham equation [1.3]. The ground state energy is then obtained by minimizing the energy functional. The DFT formulation of the Kohn-Sham equation is an exact one. However, the exact form of the exchange-correlation energy as appearing in this equation is not known. Certain physical approximations are made to approximate these energies. A widely used approximation is the local density approximation (LDA). Though LDA underestimates the band gap energies of the semiconductors, it accurately predicts the ground state geometries, charge densities and most importantly, gives the physical trends correctly. Beyond LDA, an alternative method, generalized gradient approximation (GGA) [1.4] was presented, which gives accurate results for the semiconductor systems. But these GGA calculations are computationally more intensive.

1.2 Literature Review

A good description of the *fhi96md* code, which we use here, was given by Bockstedte *et. al.*[1.5]. The formulation and the generation of the corresponding pseudopotentials using *fhi98pp* code was described by Fuchs *et. al.* [1.6].

Chadi and others [1.7] had calculated the total energy and the equilibrium lattice constant for Ga, As and GaAs in a different context (surface reconstruction of the GaAs (100) surface). They had also calculated the heat of formation as a check for their optimized structure. The chemical potential, μ is defined as the derivative of the Gibbs free energy, $G = E + PV - TS$, with respect to the number of particles. Here the term PV is negligible and at temperature $T = 0$, $G = E$. The heat of formation of GaAs is

given by, $\Delta H_f = \mu_{GaAs(bulk)} - \mu_{Ga(bulk)} - \mu_{As(bulk)}$. Since LDA gives accurate results when the energy differences are concerned, they had calculated the total energy of the concerned materials independently and used the difference of the energies to get the heat of formation.

They had observed that though this kind of calculations are mainly done at a cutoff of 12-18 Ry. But since, the surface contains large number of atoms, which for equivalent number of plane waves requires a smaller cutoff energy, surface related calculations could be done at 6 Ry. Instead of doing the surface calculation at 6 Ry cutoff with hard pseudopotentials, Chadi and others had carried out the calculations with softer pseudopotentials, which converges at 6 Ry cutoff. They had modified the earlier Kerker approach [1.8] by choosing a larger cutoff radius and thus producing a softer pseudopotential. The pseudopotentials still are norm conserving. In order to ensure the accuracy of this softer pseudo-potential, various bulk properties were calculated. The GaAs structure and related properties were calculated first. The calculation was done with 8 special k-points. The results show that when a hard pseudopotential predicts a lattice constant of 5.42 Å and 5.55 Å at 6 and 12 Ry cutoff, respectively, the same is 5.48 Å and 5.52 Å for the corresponding softer one. The phonon frequencies calculated at a higher cutoff of 18 Ry had a difference of only 2.5%. Similarly the heat of formation for these two cases were compared and the results are fairly in good agreement with experiment. This will be discussed in a greater detail in chapter 4.

The As structure related calculations were done according to the method prescribed by Nielsen and others [1.9]. According to Nielsen, the ground state of As is A7 structure. The structure may also be described according to simple cubic structure, but

this structure is not a stable one. Chadi had calculated the As total energy using the experimental structure with 44 inequivalent k points.

The structure of Ga in its ground state is orthorhombic in nature. The total energy for this structure is calculated using 75 inequivalent k points at a cutoff of 6 Ry.

1.3 Objectives of the present study

The objective of the present work is to estimate the various point defect formation energies in GaAs. For this purpose, a norm conserving fully separable pseudopotentials for Ga and As are generated using the computer code *fhi98pp*. The pseudopotentials and the pseudo wavefunctions are input to another code *fhi96md* for calculating the total energies of the Ga, As and GaAs. The structures are to be optimized on the basis of total energy calculation. The accuracy of the structures is verified by calculating the heat of formation. Then the various defects of GaAs are studied.

Chapter 2

Electronic structure calculation

2.1 The problem of the structure of matter

The microscopic description of the physical and chemical properties of a material system is a complex problem. In general, these systems involve a collection of atoms interacting with each other. These systems may be isolated, extended or a combination of both. The Hamiltonian of such a system may be written as,

$$\begin{aligned}\hat{H} = & -\sum_{I=1}^P \frac{\hbar^2}{2M_I} \bar{\nabla}_I^2 - \sum_{i=1}^N \frac{\hbar^2}{2m} \bar{\nabla}_i^2 + \frac{e^2}{2} \sum_{I=1}^P \sum_{J \neq I}^P \frac{Z_I Z_J}{|\bar{\mathbf{R}}_I - \bar{\mathbf{R}}_J|} \\ & + \frac{e^2}{2} \sum_{i=1}^N \sum_{j \neq i}^N \frac{1}{|\bar{\mathbf{r}}_i - \bar{\mathbf{r}}_j|} - e^2 \sum_{I=1}^P \sum_{i=1}^N \frac{Z_I}{|\bar{\mathbf{R}}_I - \bar{\mathbf{r}}_i|}\end{aligned}\quad (2.1)$$

where $\bar{\mathbf{R}} = \{\bar{\mathbf{R}}_I\}, I=1,2,\dots,P$, is a set of P nuclear coordinates, $\bar{\mathbf{r}} = \{\bar{\mathbf{r}}_i\}, i=1,2,\dots,N$, is a set of N electronic coordinates and e is the electronic charge. Z_I and M_I are the charge and mass of the I th nucleon while m is the mass of the electron. In principle, all the properties of the system can be derived if we can solve the following Schrödinger equation,

$$\hat{H}\Psi(\bar{\mathbf{r}}, \bar{\mathbf{R}}) = E\Psi(\bar{\mathbf{r}}, \bar{\mathbf{R}}) \quad (2.2)$$

where E being the eigenvalue corresponding to the eigenfunction $\Psi(\bar{\mathbf{r}}, \bar{\mathbf{R}})$. In practice, this problem is impossible to solve in the full quantum mechanical framework. And there are very few possible cases where the above equation can be solved analytically or numerically. Common is solution in the ground state of such a problem under certain

approximations. The usual choice is to use some realistic approximation.

2.1.1 Adiabatic approximation (Born-Oppenheimer approximation)

The first observation is that all the nuclei, being heavier than the electrons, move much slower than the associated electrons. As a result, at any instant, the nucleus may be considered to be at rest while the electrons are rotating around them. In other words, as the nuclei follow their dynamics, the electrons associated with them adjust their respective wave functions according to the nuclear wave function. If we substitute,

$$\Psi(\vec{r}, \vec{R}, t) = \sum_n \Theta_n(\vec{R}, t) \Phi_n(\vec{r}, \vec{R}) \quad (2.3)$$

where $\Theta_n(\vec{R}, t)$ is the nuclear and $\Phi_n(\vec{r}, \vec{R})$ is the electronic eigenfunction, the electronic and nuclear part separates out. This approximation is valid for $m/M \approx 10^{-4}$ or 10^{-5} . The corresponding electronic Hamiltonian can be written as,

$$\hat{H}_e(\vec{r}, \vec{R}) = - \sum_{i=1}^N \frac{\hbar^2}{2m} \vec{\nabla}_i^2 + \frac{e^2}{2} \sum_{i=1}^N \sum_{j \neq i}^N \frac{1}{|\vec{r}_i - \vec{r}_j|} - e^2 \sum_{I=1}^P \sum_{i=1}^N \frac{Z_I}{|\vec{R}_I - \vec{r}_i|} \quad (2.4)$$

and the Schrödinger equation reads as,

$$\hat{H}_e \Phi(\vec{r}, \vec{R}) = E_e \Phi(\vec{r}, \vec{R}) \quad (2.5)$$

where E_e is the energy eigenvalue associated with the electron. The above approximation is known as the adiabatic approximation or the Born-Oppenheimer approximation [1.2].

2.1.2 Quantum many body theory

In order to solve Eq. 2.5, the first approximation method was proposed by Hartree [2.1]. According to this theory, the many body wave function can be written as a product

of one-electron wave functions i.e.

$$\Phi(\vec{r}, \vec{R}) = \prod_i \varphi_i(\vec{r}, \vec{R}) \quad (2.6)$$

In this theory, the atom-electron interaction is replaced by a effective potential.

$$\left[-\frac{\hbar^2}{2m} \vec{\nabla}^2 + V_{\text{eff}}(\vec{r}, \vec{R}) \right] \varphi_i(\vec{r}, \vec{R}) = \varepsilon_i \varphi_i(\vec{r}, \vec{R}) \quad (2.7)$$

with

$$V_{\text{eff}}(\vec{r}, \vec{R}) = V_{\text{ext}}(\vec{r}, \vec{R}) + \int \frac{\sum_{j=1}^N \rho_j(\vec{r}')}{|\vec{r} - \vec{r}'|} d\vec{r}' \quad (2.8)$$

where

$$\rho(\vec{r}) = |\varphi_j(\vec{r}, \vec{R})|^2 \quad (2.9)$$

is the electronic density associated with the j th electron. The total energy of the system

is given by,

$$E_H = \sum_{n=1}^N \varepsilon_n - \frac{1}{2} \iint \frac{\rho(\vec{r}) \rho(\vec{r}')}{|\vec{r} - \vec{r}'|} d^3\vec{r} d^3\vec{r}' \quad (2.10)$$

The above method is known as self-consistent Hartree (SCH) method. The main problem with the Hartree theory is that it treats the electrons as distinguishable particles. The indistinguishability of the electrons was taken into account in Hartree-Fock (HF) theory [2.2, 2.3]. Here, instead of writing the many electron wave function as a simple product, the total wave function is written in the form of Slater determinant,

$$\Phi(\vec{r}, \vec{R}) = SD\{\varphi_i(\vec{r}, \vec{R})\} = \frac{1}{\sqrt{N!}} \begin{vmatrix} \varphi_1(\vec{R}, \vec{r}_1) & \varphi_1(\vec{R}, \vec{r}_2) & \cdots & \varphi_1(\vec{R}, \vec{r}_N) \\ \varphi_2(\vec{R}, \vec{r}_1) & \varphi_2(\vec{R}, \vec{r}_2) & \cdots & \varphi_2(\vec{R}, \vec{r}_N) \\ \vdots & \vdots & \ddots & \vdots \\ \varphi_N(\vec{R}, \vec{r}_1) & \varphi_N(\vec{R}, \vec{r}_2) & \cdots & \varphi_N(\vec{R}, \vec{r}_N) \end{vmatrix} \quad (2.11)$$

However, the Hartree-Fock theory totally ignores the Coulomb correlation, which arises due to the repulsion between the electrons. The most straightforward way to introduce the electronic repulsion is to write the many body wave function as a linear combination of the Slater determinants (i.e. Hartree-Fock wave functions). This method is known as configuration-interaction method (CI).

2.1.3 Density Functional Theory

Parallel to the development of this Hartree and related theories, Thomas and Fermi [2.4, 2.5], at the same time as of Hartree, proposed that the full electronic density is the fundamental variable, instead of the wave function. They derived a different differential equation for the density without resorting to the one-electron orbitals. A firm and exact theoretical formulation of such description was provided by Hohenberg and Kohn [1.1] in 1964 and is know as the Density Functional Theory (DFT). In 1965, Kohn and Sham [1.3] proposed the idea of replacing the kinetic energy term in Eq. 2.5 by an equivalent of a non-interacting system. Kohn-Sham defined the density $\rho(\vec{r})$ as,

$$\rho(\vec{r}) = \sum_{i=1}^{\infty} \sum_{s=1}^2 n_{i,s} |\varphi_{i,s}(\vec{r})|^2 \quad (2.12)$$

where $n_{i,s}$ is the occupation number of the orbital $\varphi_{i,s}(\vec{r})$. Such a procedure brings us to self-consistent Kohn-Sham equations:

$$\left[-\frac{\bar{\nabla}^2}{2} + V[\rho; \vec{r}] \right] \varphi_{i,s}(\vec{r}) = \varepsilon_{i,s} \varphi_{i,s}(\vec{r}) \quad (2.13)$$

where the effective potential $V[\rho; \vec{r}]$ is written as,

$$\begin{aligned}
V[\rho; \vec{r}] &= V_{\text{ext}}(\vec{r}) + \int \frac{\rho(\vec{r}')}{|\vec{r} - \vec{r}'|} d^3 \vec{r}' + V_{\text{xc}}[\rho] \\
&= -\frac{Z}{r} + V_H[\rho; \vec{r}] + V_{\text{xc}}[\rho(\vec{r})]
\end{aligned} \tag{2.14}$$

$\phi_{i,s}(r)$ are known as Kohn-Sham orbitals and they may or may not have any physical significance. V_{xc} is the functional derivative of the exchange and correlation energy, E_{xc} . The total energy of the system is then given by,

$$E = \sum_i \varepsilon_{i,s} - \frac{1}{2} \iint \frac{\rho(\vec{r}) \rho(\vec{r}')}{|\vec{r} - \vec{r}'|} d^3 \vec{r} d^3 \vec{r}' + E_{\text{xc}}[\rho] - \int V_{\text{xc}}[\rho] \rho(\vec{r}) d^3 \vec{r} \tag{2.15}$$

The problem with Eq. 2.15 is that the exact form of E_{xc} (or V_{xc}) is not known. Some physical approximations are made to calculate these quantities. These approximations are known as Local Density Approximation (LDA) and are very successful in electronic structure calculation. Using LDA, V_{xc} is written as,

$$V_{\text{xc}}[\rho] = \frac{\partial E_{\text{xc}}^{\text{LDA}}[\rho]}{\partial \rho(\vec{r})} = \frac{d}{d\rho} [\varepsilon_{\text{xc}}^{\text{LDA}}[\rho] \rho(\vec{r})] \tag{2.16}$$

$\varepsilon_{\text{xc}}^{\text{LDA}}[\rho]$ is known as the exchange and correlation energy density and it has been calculated by using quantum Monte Carlo method by Ceperley and Alder [2.6] and parameterized by Perdew and Zunger [2.7]. These are considered to be most accurate to date and are being used in our calculation.

2.1.4 Dynamics of ions

Once the ground state of the electrons are calculated as described in the above section, the atomic equation of motion is integrated with standard molecular dynamics (MD) techniques. The choice of the scheme depends on the type of the application.

Among various MD methods, the most popular ones are Verlet [2.8] and predictor-corrector [2.9] method.

2.2 The concept of pseudopotential

The electron-nuclear interaction in an atom is defined by the Coulomb interaction. The electrons in an atom can be classified into two classes: one of them moves freely through the nucleus and are responsible for the chemical properties of the matter i.e. the valence electrons, while the others are tightly bound to the nucleus and are called the core electrons. In a calculation where both of them are taken into account is called *all-electron* calculation. Since the core electrons do not take part in the chemical bonding i.e. does not guide the chemical properties of the atom it is possible to integrate out the corresponding effects of the core electrons as a screening effect between the valence electron and the *ionic cores* i.e. the nucleus and the core electrons. This type calculation is called the *pseudopotential* calculation.

The valence states, due to the orthogonalization of the core states of same symmetry, show remarkable oscillatory behavior with a number of nodes equal to the $(n - \ell - 1)$, where 'n' is the principal quantum number and ' ℓ ' is the angular quantum number. On the other hand, though the nodeless wavefunctions are non-oscillatory, due to the lack of orthogonality, they can approach the nucleus easily and as a result they create strongly bound states near the nucleus, which are sharply peaked close to the nucleus. These features are totally undesired from the point of view of the computational calculations, as a large number of plane waves (basis functions) are required to describe these noded wavefunctions, which in turn translates into vast amount of computer time

(the matrix to be diagonalized is too large).

Thus the pseudopotential theory is constructed in two parts:

- Core electrons are removed from the calculation and the interaction of the valance electrons with the nucleus plus the core electrons (including orthogonalization) is replaced by an effective, screened potential.
- The full ion-electron interaction, which includes the orthogonality of the valance wavefunction with the core states, is replaced by a weaker pseudopotential that acts on pseudo wavefunctions rather than the true wavefunction.

It is quite clear from the above discussion that the construction of pseudopotential can be done arbitrarily. As a matter of fact, the construction of the empirical pseudopotentials have been obtained in past by fitting with experimental values. But these pseudopotentials lacked a very fundamental property, namely that of transferability. The first transferable pseudopotential was constructed by Hamann, Schüter and Chiang [2.10]. The modern pseudopotentials are constructed according to the recipe prescribed by them. These are as follows:

1. The pseudo wavefunctions should be node less and it should be identical to the all electron wavefunction outside a suitably chosen cut-off radius, r_c :

$$\varphi_{ps}(r) = \tilde{\varphi}_{ps}(r) \quad \text{for } r < r_c$$

and

$$\varphi_{ps}(r) = \varphi_{ae}(r) \quad \text{for } r \geq r_c$$

2. The first and second derivatives of the pseudo wavefunction are continuous at r_c .
3. The eigenvalues of the pseudo wavefunction should be same as that of the all-

electron wavefunction.

4. The norm of the true and the pseudo wavefunctions inside the core radius should be same.
5. Other conditions for the smoothness of the pseudo wavefunctions.

Several schemes were proposed to generate first-principle pseudopotentials. Among them the most popular ones are Bachelet, Hamann and Schüter [2.11], Troullier-Martins [2.12] and Vanderbilt [2.13].

The Bachelet, Hamann and Schüter type of pseudopotential is the most common type of pseudopotential and are being used in the present calculation.

2.2.1 General background and formulation

In generating a good pseudopotential for a material the following considerations are taken into account. (i) **Transferability**: the transferability of a pseudopotential is its ability to describe the valence electron configuration when placed in different environments. This is a major difference with the earlier empirical pseudopotentials. These empirical pseudopotentials were designed for some specific environments and were inevitably very less or almost not transferable to different environments. (ii) **Efficiency**: one other important issue is the efficiency of the pseudopotential i.e. how it reduces the computational load. That means the lesser the number of basis functions it takes to compute the wavefunction and the charge densities, the more efficient it is.

The transferability of a pseudopotential depends on (a) correct scattering properties, (b) the choice of the cutoff radius r_c , (c) the adequate account of the exchange-correlation between the core and the valence states, (d) the Kleinman-Bylander

form [2.15] of non-local pseudopotential, (e) the frozen core approximation and (f) the treatment of higher angular momentum components. The choice of cutoff radius is a crucial factor. The increase in the value of r_c produces a softer pseudopotential, which converges more rapidly. As a result this becomes less transferable as the pseudo wavefunction, at the bonding radius, becomes less accurate. On the other hand r_c should be greater than the outermost node of the corresponding all electron calculation. Choosing r_c close to that node produces bad pseudopotential.

2.2.2 Atomic all electron calculation

The present pseudopotentials are constructed from atomic all electron calculation. The all electron wavefunctions are obtained by self-consistently solving the Kohn-Sham Eq. 1.3 (here only the radial part is considered as the solution of the angular part is trivial),

$$\left[-\frac{1}{2} \frac{d^2}{dr^2} + \frac{\ell(\ell+1)}{2r^2} + V[\rho; r] \right] r\Phi(r) = \varepsilon_{nl} r\Phi(r) \quad (2.17)$$

where $V[\rho; r]$ is the one electron potential.

$$V[\rho; r] = -\frac{Z}{r} + V_H[\rho; r] + V_{xc}^{LDA}(\rho(r)) \quad (2.18)$$

Here $-\frac{Z}{r}$ is the well known coulomb interaction, $\rho(r)$ is the sum of the electronic charge densities of the occupied states, $V_H[\rho; r]$ is the Hartree potential and $V_{xc}^{LDA}(\rho(r))$ is the local density approximation for the exchange-correlation potential. The total energy of the system is given by,

$$E[\rho] = \sum_i \varepsilon_{i,s} - \frac{1}{2} \iint \frac{\rho(r)\rho(r')}{|r-r'|} d^3r d^3r' + E_{xc}[\rho] - \int V_{xc}^{LDA}(\rho(r))\rho(r) d^3r \quad (2.19)$$

$$= T_0[\rho] + E_H[\rho] + E_{xc}[\rho] + \int -\frac{Z}{r} \rho(r) d^3r \quad (2.20)$$

where $T_0[\rho]$ is the kinetic energy of the non-interacting electrons,

$E_{xc}[\rho]$ is the exchange and correlation energy,

$E_H[\rho] = \frac{1}{2} \int \frac{\rho(r)\rho(r')}{|r-r'|} d^3r d^3r'$ is the electrostatic or Hartree energy.

The ground state is obtained by minimizing the total energy with respect to the density functional $\rho(r)$ i.e.

$$\frac{\partial \{E[\rho] - N\}}{\partial \rho(r)} = 0 \quad (2.21)$$

subject to, $\int \rho(r) d^3r = N$.

This equation gives,

$$\left[-\frac{1}{2} \nabla^2 + V_{eff}[\rho; r] - \varepsilon_i \right] \varphi_i(r) = 0 \quad (2.22)$$

where $V_{eff}[\rho; r] = \int \frac{\rho(r')}{|r-r'|} d^3r' + \frac{\partial E_{xc}[\rho]}{\partial \rho(r)} + V(r)$ is the effective potential.

$\rho(r) = \sum_i n_i |\varphi_i(r)|^2$, φ_i is known as the Kohn-Sham orbital which may or may not

have any physical significance. In order to solve the above secular Eq. 2.22, a spherically symmetric electronic charge distribution is assumed. As a result the Kohn-Sham orbitals separates out as,

$$\varphi_i(r) = \left[\frac{R_{n_i, \ell_i}(\varepsilon_i; r)}{r} \right] Y_{\ell_i, m_i}(\theta, \varphi) \quad (2.23)$$

where $Y_{\ell_i, m_i}(\theta, \varphi)$ is the spherical harmonics. The solution of the angular part relating to

$Y_{\ell, m_\ell}(\theta, \varphi)$ is straightforward and will be dropped in the later discussion. The radial

equation, with the relativistic correction, relating $R_{n, \ell}$, becomes,

$$\left[\frac{1}{2M(r)} \left\{ -\frac{d^2}{dr^2} - \frac{1}{2M(r)c^2} \frac{dV(r)}{dr} r \frac{d}{dr} + \frac{\ell(\ell+1)}{r^2} \right\} + V(r) - \varepsilon_i \right] r R_{n, \ell}(\varepsilon_i; r) = 0 \quad (2.24)$$

where the relativistic electron mass is given by, $M(r) = 1 + \frac{(\varepsilon_i - V(r))}{2c^2}$ with $\frac{1}{c} = \frac{1}{137.036}$

is the fine structure constant. The exchange-correlation potential is derived from the exchange-correlation energy density using

$$E_{xc}^{LDA}[\rho] = \int \varepsilon_{xc}^{LDA}[\rho] \rho(r) dr \quad (2.25)$$

The exchange-correlation energy density can be splitted into two parts. The exchange density term has been calculated by Dirac [2.14] and is given by,

$$\varepsilon_x^{LDA}[\rho] = -\frac{3}{4} \left(\frac{3}{\pi} \right)^{1/3} \rho^{1/3} = -\frac{3}{4} \left(\frac{3}{4\pi^2} \right)^{1/3} \frac{1}{r_s} = -\frac{0.458}{r_s} \text{ (a.u.)} \quad (2.26)$$

r_s is the average radius containing one electron, $\rho^{-1} = (4\pi r_s^3 / 3)$. For the correlation part, we have used the Ceperley and Alder [2.6] approximation parameterized by Pedrew and Junger [2.7].

$$\varepsilon_c^{LDA}[\rho] = \begin{cases} \frac{-0.1432}{1 + 1.0539\sqrt{r_s} + 0.3334r_s} & \text{for } r_s \geq 1 \\ -0.0480 + 0.0311 \ln r_s - 0.0116r_s \\ + 0.0020r_s \ln r_s & \text{for } r_s < 1 \end{cases} \quad (2.27)$$

2.2.3 Screened norm-conserving pseudopotential

Once the all electron potential and wavefunctions are obtained by solving Eq. 3.7, the pseudopotential is constructed from it. The radial pseudo wavefunction is then

wavefunction satisfies the one electron Schrödinger equation with the screened potential

$$V_\ell^{ps,scr},$$

$$\left[-\frac{1}{2} \frac{d^2}{dr^2} + \frac{\ell(\ell+1)}{2r^2} + V_\ell^{ps,scr}(r) - \varepsilon_\ell^{ps} \right] u_\ell^{ps}(\varepsilon_\ell^{ps}; r) = 0 \quad (2.28)$$

The screened pseudopotential is obtained by inverting the Schrödinger equation.

$$V_\ell^{scr,ps}(r) = \varepsilon_\ell^{ps} - \frac{\ell(\ell+1)}{2r^2} + \frac{1}{2u_\ell^{ps}(r)} \frac{d^2}{dr^2} u_\ell^{ps}(r) \quad (2.29)$$

2.2.4 Construction of Bachlet-Hamann-Schlüter pseudopotential

The Bachlet-Hamann-Schlüter norm conserving pseudopotentials are constructed in five steps :

- (i) Kohn-Sham equation, as corrected by Dirac for relativistic effects, is solved for a given atomic configuration ν ,

$$\left[-\frac{1}{2} \frac{d^2}{dr^2} - \frac{\kappa(\kappa+1)}{2r^2} + V^\nu(r) \right] G_\kappa(r) = \varepsilon_\kappa G_\kappa(r) \quad (2.30)$$

- (ii) Then the first step pseudopotential \hat{V}_{1j}^ν is obtained by cutting of the singularity at origin from the all electron potential.

$$\hat{V}_{1j}^\nu(r) = V^\nu(r) \left[1 - f\left\{ \frac{r}{r_{cj}} \right\} \right] + c_j^\nu \left\{ \frac{r}{r_{cj}} \right\} \quad (2.31)$$

where, $f\left(\frac{r}{r_{cj}}\right) = \exp\left[-\left(\frac{r}{r_{cj}}\right)^\lambda\right]$ is a smooth cut-off function, which approaches 0 as

$r/r_{cj} \rightarrow \infty$, cutting off around $r \approx r_{cj}$ and approaches 1 as $r \rightarrow 0$. The optimum

value of the parameter λ is taken as 3.5. The constant c_j^ν is adjusted to give a node

less wavefunction $\omega_{1j}^\nu(r)$ with the same eigenvalue as that of the all electron wavefunction. The optimum value of r_{cj} is determined by scaling down from the radius(r_{\max}) of the outer most peak of the radial wavefunction G_κ , $r_{cj} = r_{\max} / cc$, where cc is in the range 1.5 - 2.

(iii) Once the first steps pseudo wavefunction $\omega_{1j}^\nu(r)$ is obtained, the second step involves modification of the same for the norm conservation correction for $r > r_{cj}$. The second step pseudo wavefunction is given by,

$$\omega_{2j}^\nu(r) = \gamma_j^\nu(r) [\omega_{1j}^\nu(r) + \delta_j^\nu r^{l+1} f(r/r_{cj})] \quad (2.32)$$

with $(\gamma_j^\nu)^2 \int [\omega_{1j}^\nu(r) + \delta_j^\nu r^{l+1} f(r/r_{cj})]^2 dr = 1$, being the normalization condition from which the parameter δ_j^ν is to be determined.

(iv) In the third step the final screened pseudopotentials $\hat{V}_{2j}^\nu(r)$ is obtained by inverting the Schrödinger equation for the node less eigenfunction $\omega_{2j}^\nu(r)$ with the eigenvalue ε_j .

$$\hat{V}_{2j}^\nu(r) = \hat{V}_{1j}^\nu(r) + \frac{\delta_j^\nu r^{l+1} f}{2\omega_{2j}^\nu(r)} \times \left[\frac{\mathcal{L}^2 (r/r_{cj})^{2\lambda} - [2\lambda\ell + \lambda(\lambda+1)](r/r_{cj})^\lambda}{r^2} + 2\varepsilon_j - 2\hat{V}_{1j}^\nu(r) \right] \quad (2.33)$$

(v) Finally the screened pseudopotentials $\hat{V}_{2j}^\nu(r)$ are unscreened using the node less pseudo wavefunction $\omega_{2j}^\nu(r)$.

$$\hat{V}_j^{\text{ion}}(r) = \hat{V}_{2j}^\nu(r) - \int \frac{\rho^\nu(r')}{|r-r'|} dr' - \frac{\delta E_{\text{xc}}[\rho^\nu]}{\delta \rho^\nu(r)} \quad (2.34)$$

where $\rho^v(r) = \sum_{\substack{\text{occupied} \\ \text{valance} \\ \text{states}}} \left| \frac{\omega_{2j}^v(r)}{r} \right|^2$ is the pseudo charge density.

The average potential is calculated from the different degenerate states of

$$j = \ell \pm 1/2,$$

$$\hat{V}_\ell^{\text{ion}}(r) = \frac{1}{2\ell+1} \left[\ell \hat{V}_{\ell-1/2}^{\text{ion}}(r) + (\ell+1) \hat{V}_{\ell+1/2}^{\text{ion}}(r) \right] \quad (2.35)$$

The total ionic pseudopotential is the sum of the ionic part and the spin-orbit coupling term as given by,

$$\hat{V}_{ps}^{\text{ion}}(r) = \sum_\ell |\ell\rangle \left[\hat{V}_\ell^{\text{ion}}(r) + \hat{V}_\ell^{\text{so}}(r) \bar{L} \cdot \bar{S} \right] \langle \ell| \quad (2.36)$$

where the spin-orbit term is,

$$\hat{V}_\ell^{\text{so}}(r) = \frac{2}{2\ell+1} (\hat{V}_{\ell+1/2}^{\text{ion}} - \hat{V}_{\ell-1/2}^{\text{ion}}) \quad (2.37)$$

For a high precision fit, the Bachlet-Hamann-Schlüter pseudopotential is split up into a long-range ($\hat{V}_{\text{core}}(r)$, ℓ independent) and a short-range ($\Delta \hat{V}_\ell^{\text{ion}}(r)$, ℓ dependent) term. The core part is given by,

$$\hat{V}_{\text{core}}(r) = -\frac{Z_v}{r} \left[\sum_{i=1}^2 c_i^{\text{core}} \text{erf}[(\alpha_i^{\text{core}})^{1/2} r] \right] \quad (2.38)$$

where $c_1^{\text{core}} + c_2^{\text{core}} = 1$. And the ionic part of the same is given by,

$$\Delta \hat{V}_\ell^{\text{ion}}(r) = \sum_{i=1}^3 (A_i + A_{i+3}) e^{\alpha_i r^2} \quad (2.39)$$

The parameters c_i^{core} and A_i for different elements are calculated and tabulated in the literature.

2.3 Point defects in semiconductors

There are mainly three different types of defects present in a semiconductor. The most common type is the *vacancy* defect, which is formed when an atom is missing from an otherwise perfect crystal. *Interstitial* defects are those defects in which a host atom is present in the interstitial site. In addition, the *antisite* defects are present in AB type of semiconductors, where an A type of atom is present at the site of atom B and vice-versa.

Point defects in semiconductor act as a trap to the electrons and holes. As a result, these defects can be in different charge states. The energy required for the transition from one charge state to other can be studied by means of total energy calculation. Here, the Fermi level acts as the reservoir.

In actual calculation, when a defect is inserted in an otherwise perfect crystal, by means of periodic boundary condition of Bloch's theorem, the defect is translated to an uniform array of repeated defects. This condition necessitates the use of large supercells in this type of calculation.

The defect formation energy is defined as the energy required to create a defect in a perfect lattice. The defect formation energy in a GaAs is given by,

$$\Omega(\mu_e, \mu_{Ga}, \mu_{As}) = E_D + Q_D(E_v + \mu_e) - n_{Ga}\mu_{Ga} - n_{As}\mu_{As} \quad (2.40)$$

where n_{Ga} and n_{As} are the number of Ga and As atoms in the defect cell and μ 's are their respective chemical potentials. μ_e is the chemical potential of the electrons (i.e. the Fermi energy) and E_D is the total energy of a supercell containing one defect at charge state Q_D . Using, $\mu_{GaAs} = \mu_{Ga} + \mu_{As}$, which is valid in equilibrium condition, equation (2.40) may be written as,

$$\Omega(\mu_e, \mu_{Ga}, \mu_{As}) = E'_D + Q_D(E_v + \mu_e) - \frac{1}{2}(n_{Ga} - n_{As})\Delta\mu \quad (2.41)$$

where,

$$E'_D = E_D - \frac{1}{2}(n_{Ga} + n_{As})\mu_{GaAs(bulk)} - \frac{1}{2}(n_{Ga} - n_{As})(\mu_{Ga(bulk)} - \mu_{As(bulk)}) \quad (2.42)$$

and
$$\Delta\mu = (\mu_{Ga} - \mu_{As}) - (\mu_{Ga(bulk)} - \mu_{As(bulk)}) \quad (2.43)$$

E'_D values have been calculated by Northrup and Zhang [2.16]. Here, all the total energies are calculated about a common reference energy level. In supercell calculations, no absolute reference of energy or eigenvalues is present [2.17]. But, the common practice is to chose the top of the valance band maximum as the point of reference.

The defect related total energy calculations, involving the periodic boundary conditions, needs special attention. This is due to the fact that, an uncompensated charge in this type of calculation, will be repeated in every possible direction and would lead to misleading results. To avoid this, an uniform background charge of opposite sign is generally supplied in the background.

Chapter 3

The *fhi96md* and *fhi98pp* code

3.1 The *fhi96md* program structure

The program structure of the computer code *fhi96md* is given in figure 3.1. The different blocks are self-explanatory. The basic idea of the program is to solve the Kohn-Sham equation self-consistently, which is described in the left hand side. The right hand side deals with the dynamics of the atoms.

In the initialization part, the input files i.e. *inp.mod*, *start.inp* and pseudopotential files are read and the initializing input file *inp.ini* is being generated. Then the structure factors and phase factors are calculated. The initial electron density and both local and non-local contribution to the energy, potential and forces are calculated thereafter. Now, if the atoms are allowed to move, the atoms are moved according to structural optimization or molecular dynamics schemes. The electronic wave functions are calculated self-consistently, satisfying energy (*epsel*) or density (*epsekin*) convergence criterion, for this new positions of the atoms. The calculation is repeated for different k-points. The charge density and forces are calculated once again. If the force convergence criterion is not met, the atoms are moved again and procedure is repeated till the criterion is satisfied. The program is terminated on convergence or if the number of iterations or cputime is exceeded. However, if termination occurs without convergence, we change the convergence criteria until it is satisfied. A very good description of the *fhi96md* code is given by Bockstedte and others [1.5].

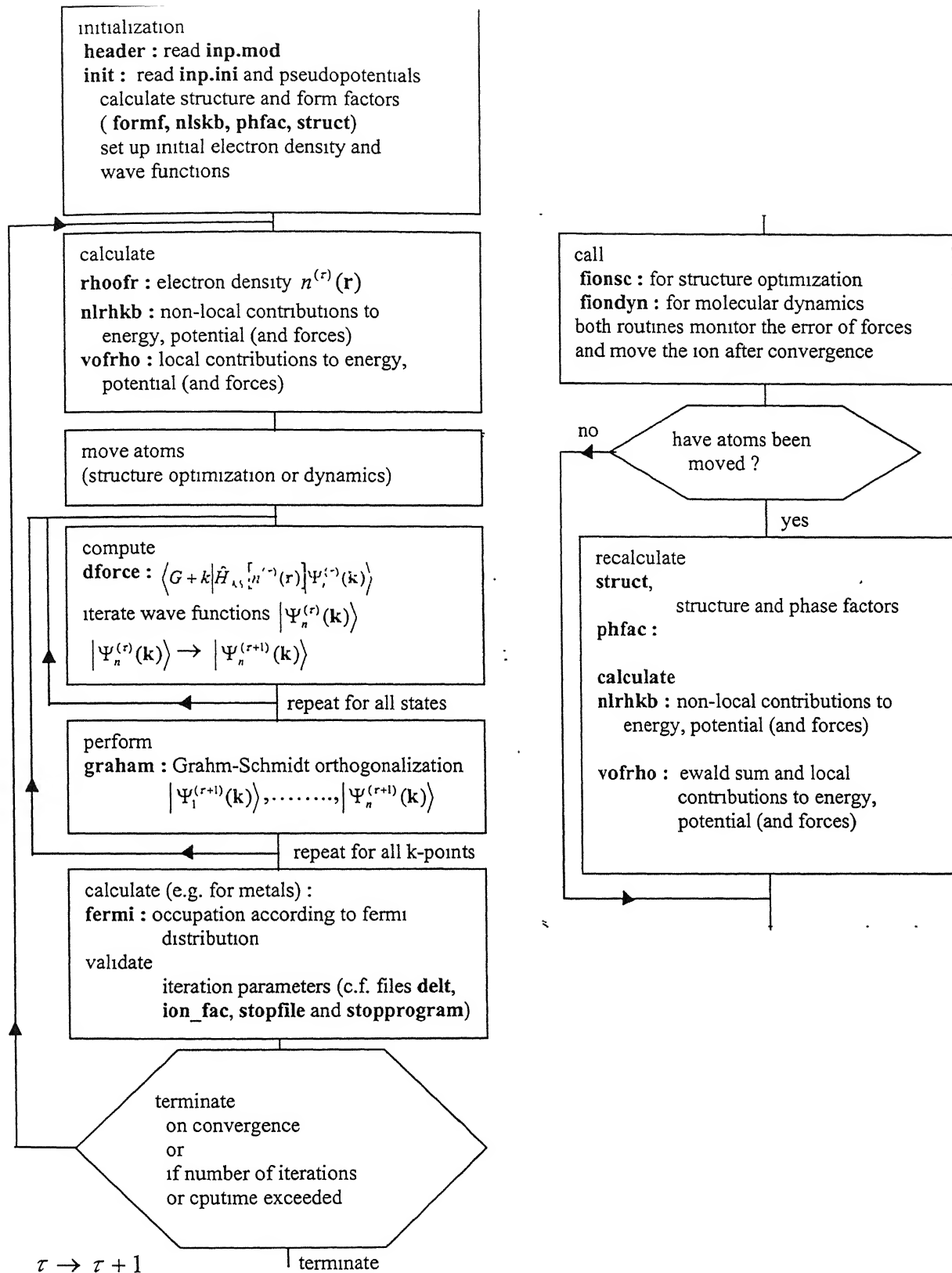


Fig.3.1. Flow chart of the program *fhi96md* (from Bockstedte et.al. [1.5])

Solving the Kohn-Sham equation: Solving the Kohn-Sham equation is the most important part in this type of computer codes. The essential idea is to minimize the energy functional with respect to the wave function. At first, a starting guess is made for the initial choice of the wave functions. Then the energy minimization scheme is employed in terms of the equation of motions of the wave functions. The most popular and simplest one of them is the steepest descent method. The equation of motion is given by,

$$\frac{d}{d\tau}|\phi^{(\tau)}\rangle = (\tilde{\varepsilon} - \hat{H}_{KS})|\phi^{(\tau)}\rangle \quad (3.1)$$

where $|\phi^{(\tau)}\rangle$ is the wave function at time τ and $\tilde{\varepsilon}$ is the Lagrange parameter. The damping is incorporated in Eq. 3.1 by the following way,

$$\frac{d^2}{d\tau^2}|\phi^{(\tau)}\rangle + 2\gamma \frac{d}{d\tau}|\phi^{(\tau)}\rangle = (\tilde{\varepsilon} - \hat{H}_{KS})|\phi^{(\tau)}\rangle \quad (3.2)$$

where γ is the damping parameter. The main draw back of steepest descent method is that one can get stuck to a local minima. In another method, the damped Joannopoulos method [3.1], the new wave function at time $\tau+1$ is calculated from those at time $\tau-1$ and τ .

$$\begin{aligned} \langle G+k|\phi^{(\tau+1)}\rangle = & \langle G+k|\phi^{(\tau)}\rangle + \beta_G \langle G+k|\phi^{(\tau)}\rangle \\ & + \gamma_G \langle G+k|\phi^{(\tau)}\rangle - \eta_G \langle G+k|\hat{H}_{KS}|\phi^{(\tau)}\rangle \end{aligned} \quad (3.3)$$

where the coefficients β_G, γ_G and η_G are given by the following,

$$\beta_G = \frac{\tilde{\varepsilon}(h(\alpha)-1) - \langle G+k|\hat{H}_{KS}|G+k\rangle e^{-\gamma\alpha}}{\tilde{\varepsilon} - \langle G+k|\hat{H}_{KS}|G+k\rangle} \quad (3.4)$$

$$\gamma_G = e^{-\gamma \tilde{\alpha}} \quad (3.5)$$

$$\eta_G = \frac{h(\tilde{\alpha}) - e^{-\gamma \tilde{\alpha}} - 1}{\tilde{\varepsilon} - \langle G+k | \hat{H}_{KS} | G+k \rangle} \quad (3.6)$$

where the function $h(\tilde{\alpha})$ is given by,

$$h(\tilde{\alpha}) = \begin{cases} e^{-(\gamma/2)\tilde{\alpha}} \cos(\omega \tilde{\alpha}) & \text{if } \omega^2 \geq 0 \\ e^{-(\gamma/2)\tilde{\alpha}} \cosh(\sqrt{|\omega^2|} \tilde{\alpha}) & \text{if } \omega^2 < 0 \end{cases} \quad (3.7)$$

with $\omega^2 = \tilde{\varepsilon} - \langle G+k | \hat{H}_{KS} | \phi^{(\tau)} \rangle - \gamma^2/4$. Though the damped Joannopoulos method is more efficient than the first order steepest descent method, limited usage of this method is due to the fact that the process requires an additional storage for the wave function at time $\tau-1$. In order to avoid this additional storage, the William-Soler algorithm [3.2] is used. Here the coefficients in Eq. (2.19) are given by (with $\gamma_G = 0$),

$$\beta_G = \frac{\tilde{\varepsilon} e^{\tilde{\varepsilon} - \langle G+k | \hat{H}_{KS} | G+k \rangle}}{\tilde{\varepsilon} - \langle G+k | \hat{H}_{KS} | G+k \rangle} \quad (3.8)$$

$$\eta_G = \frac{e^{\tilde{\varepsilon} - \langle G+k | \hat{H}_{KS} | G+k \rangle}}{\tilde{\varepsilon} - \langle G+k | \hat{H}_{KS} | G+k \rangle} \quad (3.9)$$

Solving the ionic equation of motion: In order to solve the atomic equation of motion, the Verlet algorithm [2.8] is the most common choice. The Verlet algorithm is given by,

$$r(t + \Delta t) = 2r(t) - r(t - \Delta t) + a(t)\Delta t^2 + O(\Delta t^4) \quad (3.10)$$

where $a(t) = -(1/m)\nabla V(r(t))$ is the acceleration. The truncation error here is of the order of Δt^4 . But when the velocity is calculated from this equation from,

$$v(t) = \frac{r(t + \Delta t) - r(t - \Delta t)}{2\Delta t} \quad (3.11)$$

the error associated with this expression is of the order of Δt^2 , rather than that of Δt^4 . A different variant of Velet algorithm, known as velocity Verlet algorithm is used to handle this problem. Predictor-corrector [2.9] is another commonly used algorithm for this purpose. In this scheme, from the positions and their time derivatives, all known at time t , one “predicts” the position and its time derivatives at a later time $t + \Delta t$, by means of Taylor expansion. The forces are then calculated by taking the gradient at the predicted positions. The difference between the “predicted” and calculated acceleration is the “error signal”, which is used to correct the positions.

3.1.1 Input and Output files

There are three main input files for this program viz. *start.inp*, *inp.mod* and the pseudopotential files. The formulation and generation of the pseudopotential file using the *fhi98pp* code will be discussed in the next section. The file *start.inp* mainly deals with the structure of the atoms in the concerned system while the file *inp.mod* deals with the dynamics of the atom.

In the file *inp.mod*, the scheme for the generation of the wave function is provided. The generation of the wave function can be done by actually solving the Kohn-Sham equation or from file *fort.70* (in case of restarting the program or in the case of dynamics of the atom where the program can be started from the self-consistent electron densities). The step length of electronic iteration (*delt*) and the damping factor (*gamma*) is provided in this file. It is a common practice to choose the above two to be very large initially and change it to a smaller one when the self-consistency is almost reached. Apart

from this, various convergence criteria such as energy (*epsel*), kinetic energy (*epsekin*) and force (*epsfor*) is to be provided in it. This program supports three different schemes to iterate the electronic wave functions, viz. steepest descent, damped Joannopoulos algorithm and William-Soler algorithm. For solving ionic equation of motion, any one of predictor-corrector or Verlet algorithm may be used. The exchange and correlation energy can be calculated by LDA or GGA approximation.

The other input file is *start.inp*. The cell type (*ibrav*) i.e. simple cubic lattice, bcc lattice, fcc lattice and others, and the point group symmetry (*pgind*) is provided in this file. An automatic search option of point group symmetry is also provided, which is useful in case of cells with unknown symmetry. The cell dimensions are to be given according to the choice of the cell type. The unit is atomic unit (a.u., 1 a.u. = 0.52918 Å). The special k-points, generated either by Chadi-Cohen [3.3] or Monkhorst-Pack [3.4] can be used.

The main output file is *fort.6*, which contains information about the total and interaction energies. A complete protocol of the run (electron energy minimization or molecular dynamics) is also stored in this file. Among the other output files, *fort.1* contains the instantaneous atomic positions. The binary format output files *fort.71* contains complete restart information. Other important binary format output files are *fort.72* and *fort.73*, which contains the electronic charge density and total effective potential. Another output file *fort.21* contains the positions and velocities in binary format, when molecular dynamics is done. After the job is done, the following convergence criteria should be checked :

- The difference between the total energy and harris energy should not be more than the parameter *epsel* provided in the file *inp.mod*.
- The program should stop before the CPU time limit exceeded.
- The program should stop before the maximum number of electronic iteration (*nomore*) or atomic movement (*nstepe*).

3.2 Effect of the various parameters used in the *fhi96md* code

The effect of various parameters, which control execution of calculation of total energy, is discussed below with a purpose of learning about the code. Here all the calculations are done using a single unit cell of GaAs. The plane wave cutoff energy used is 8 Ry and the experimental lattice constant of GaAs, 5.64191 Å (10.6616 a.u.) [3.5] is used in all the cases. For reference, input files are attached in appendix A.

File : Start.inp

1. *nel_exe* : *nel_exe* is the number of excess electrons present in the system. For an excess electron we put it as +1 while for an excess hole we put it as -1. For a neutral cell the total energy is -33.998000 a.u.. When an excess electron is present in the system, the total energy becomes -33.863005 a.u., while with an excess hole the energy is -34.059153 a.u..
2. *ibrav* : This parameter *ibrav* determines the type of the lattice to be used in the program. As the GaAs cell is similar to zinc sulfide (interpenetrating fcc) in nature, using an fcc cell (*ibrav* = 2) is the best choice. For this case, we have to specify the position of the Ga (0,0,0) and the position of the As ($\frac{1}{4}, \frac{1}{4}, \frac{1}{4}$). But, ultimately we are interested in incorporating vacancy defects in the cell. In that case, when we try to remove one Ga or one As atom from the cell, all the atoms of the given type are removed. To handle this

problem, the cell is chosen as simple cubic one ($ibrav = 1$). In this cell, 4 Ga atoms are placed at $(0,0,0)$ $(\frac{1}{2}, \frac{1}{2}, 0)$ $(\frac{1}{2}, 0, \frac{1}{2})$ $(0, \frac{1}{2}, \frac{1}{2})$ while the 4 As atoms at $(\frac{1}{4}, \frac{1}{4}, \frac{1}{4})$ $(\frac{3}{4}, \frac{3}{4}, \frac{1}{4})$ $(\frac{3}{4}, \frac{1}{4}, \frac{3}{4})$ $(\frac{1}{4}, \frac{3}{4}, \frac{3}{4})$. In this case, removing one atom from a specific site, still keeps the remaining atoms. The transformation from fcc to simple cubic structure is to be done in such a way that the total energy per pair should remain the same. For a cell with simple cubic symmetry, the total energy is -33.998000 a.u.. This energy is for 4 pairs of GaAs. Thus, the energy per pair is -8.4995 a.u. When the same calculation is repeated for a cell with fcc symmetry, the energy per pair is -8.499501 a.u. The difference in energy of $\sim 10^{-6}$ a.u. is minor.

3. *k*-point : The choice of the special *k*-point is a structure specific issue. The special *k*-points are generated either according to the Chadi-Cohen [3.3] mesh or according to Monkhorst-Pack [3.4] mesh. Since GaAs has fcc symmetry, here we have used the special *k*-point for the fcc structure (0.5, 0.5, 0.5). The total energy obtained is -33.998000 a.u.. When the same calculation is repeated for a special *k*-point (0.0, 0.0, 0.0), the energy obtained is -34.002714 a.u.

4. *fold parameter* : The fold parameter denotes the folding of the *k* points. A (3 3 3) folding means there is a (3×3×3) folding of the *k*-point used. Accuracy of the calculation is better with large folding. In order to reduce the computational load, we have used a (1×1×1) folding or no folding of the *k*-point in our calculation. When a (3×3×3) folding is used, the total energy obtained is -34.355107 a.u. (compare with -33.998000 a.u., used in our calculation with (1×1×1) folding).

5. *Cutoff energy* : The effect of cutoff energy will be discussed in detail in chapter 4.

6. *ekt* : The parameter *ekt* denotes the temperature of the artificial Fermi smearing of the electrons. This is measured in eV. When this parameter is changed to 0.01 from that of its original value at 0.004, total energy remains the same (-33.998000 a.u.). But when this is changed to 1.0, total energy becomes -33.773929 a.u..

7. *T-ion* : Changing the parameter *T-ion*, which denotes the ionic temperature, has no effect on the total energy.

8. *T_init* : The parameter *T_init*, denoting the temperature of initial velocities in K, has no effect on the calculated total energy.

9. *Q* : *Q* denotes the mass of the thermostat in a.u. and has no effect on the calculated total energy.

File : inp.mod

1. *delt* : The parameter *delt* determines the time step of the electronic iteration. The effect of the parameter *delt* is shown in table 3.1.

Table 3.1 Variation of the convergence time with the parameter *delt*

<i>delt</i>	time taken for convergence (sec)	Total Energy (a.u.)
10.0	38.77	-33.997989
20.0	34.70	-33.998000
30.0	32.32	-33.998012
40.0	32.04	-33.998012
50.0	28.72	-33.998013

2. *gamma* : The parameter *gamma* is the damping parameter used in the damped Joannopoulos algorithm. The effect of this parameter is shown in table 3.2.

Table 3.2 Variation of the convergence time with the parameter γ

γ	time taken for convergence (sec)	Total Energy (a.u.)
0.5	28.96	-33.998013
0.7	29.68	-33.998010
0.9	26.53	-33.998000
1.1	46.26	-33.998013
1.3	47.83	-33.998014

3. ι_{edyn} : ι_{edyn} denotes the scheme for the iteration of the wavefunctions. The total energies obtained using the steepest descent method, William Soler algorithm and damped Joannopoulos are -33.997984 a.u., -33.997999 a.u. and -33.998000 a.u., respectively. The difference in the three cases are $\sim 10^{-5}$ a.u..

3.3 The *fhi98pp* program structure

The program *fhi98pp* is needed to generate the pseudopotentials. The Fortran program *fhi98pp* has two main utilities: (i) a UNIX C-shell script *psgen* with related program *fhipp* and (ii) another C-shell script *pswatch* with associated program *pslp*. The program *fhipp* calculates the ionic pseudopotential for an element while *pslp* tests the transferability of the pseudopotentials thus generated. The input file (input files for the generation of the Ga, As, Si and C pseudopotential are attached in appendix B) is provided with the atomic number, number of core and valence states, atomic configuration and the type of exchange-correlation approximation used. Artificial atoms with fractional atomic number can be handled with this program. Both, Bachelet-Hamann-Schüter and Troullier-Martins type of pseudopotentials can be generated by this

program. The default cutoff radius for the pseudo wavefunction is provided with the shell script utility *psgen*. For Bachelet-Hamann-Schüter case, it is r_l^{\max} of the outer most maximum of the all electron wavefunction and for Troullier-Martins, it is $0.6r_l^{\max}$ if some core states are present with the same angular momentum or $0.4r_l^{\max}$ otherwise. The default cut-off radius can be changed according to the need. Another shell script utility *pswatch* is used after the pseudopotential is generated by *psgen*. It performs a self-consistent calculation of the pseudo atom, computes the logarithmic derivatives of the all electron potential and pseudopotential and carries out analysis for ghost states for Kleinman-Bylander form of non-local pseudopotential. There are several parameters that control the evaluation of the logarithmic derivatives and the fully separable pseudopotential.

All electron and pseudo wavefunction plots of gallium (fig.3.2-3.5), arsenic (fig.3.6-3.9), silicon (fig.3.10-3.13) and carbon (fig.3.14-3.17) along with their pseudopotentials are shown in the following section. From the plots of the wavefunction it is clear that all the pseudo wavefunctions thus generated are nodeless and beyond a certain cutoff radius, all the pseudo wavefunctions exactly matches with the corresponding all electron wavefunctions. As a final check, we compare the pseudo wavefunction eigenvalues with the corresponding all electron valance wavefunctions. All the results along with the cutoff radius are given in table 3.3.

Table.3.3 Comparison of the all electron and pseudo wavefunctions along with the cutoff radius for Gallium, Arsenic, Silicon and carbon

Element	ℓ value	Cutoff radius (a.u.)	Eigenvalues	
			All electron	Pseudo
Gallium	0	1.2234	-9.1703234 (4s)	-9.1703246 (1s)
	1	1.4870	-2.7331192 (4p)	-2.7331193 (2p)
Arsenic	0	1.149	-14.6997676 (4s)	-14.6997684 (1s)
	1	1.1776	-5.3417404 (4p)	-5.3417406 (2p)
Silicon	0	1.046	-10.8791848 (3s)	-10.8791853 (1s)
	1	1.2714	-4.1628555 (3p)	-4.1628555 (2p)
Carbon	0	0.7205	-13.6394102 (2s)	-13.6394110 (1s)
	1	0.4644	-5.4159021 (2p)	-5.4159025 (2p)

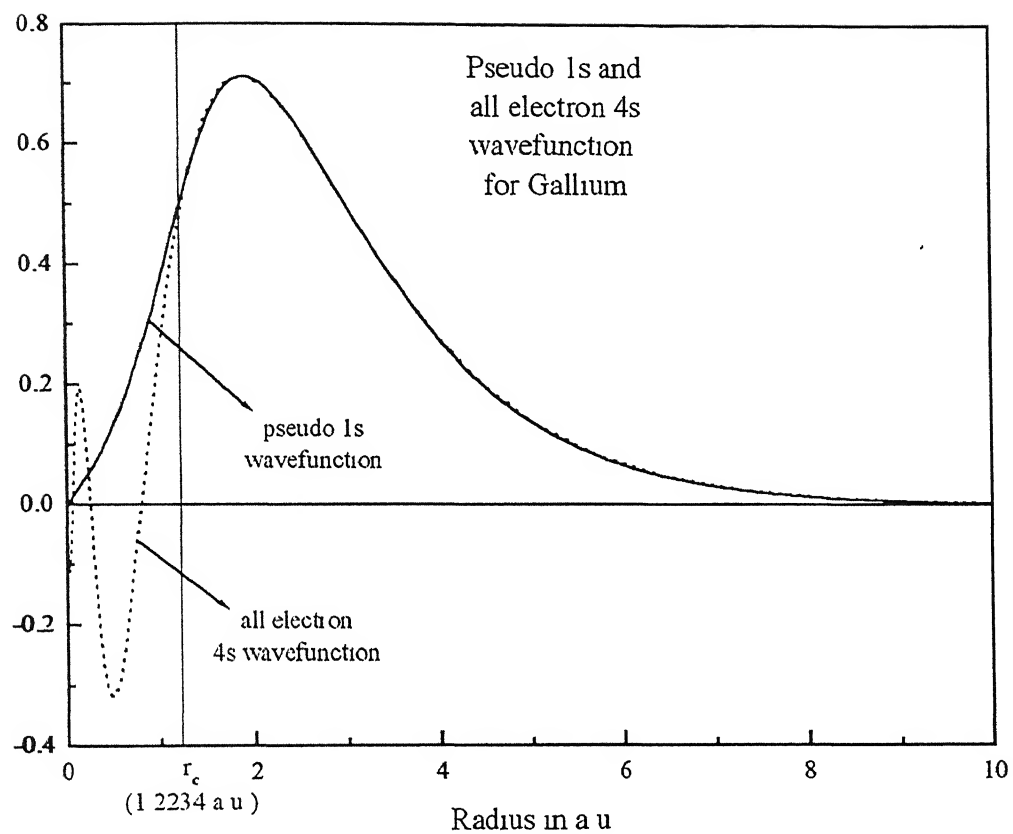


Fig.3.2. Plot for Gallium pseudo 1s and all electron 4s wavefunction

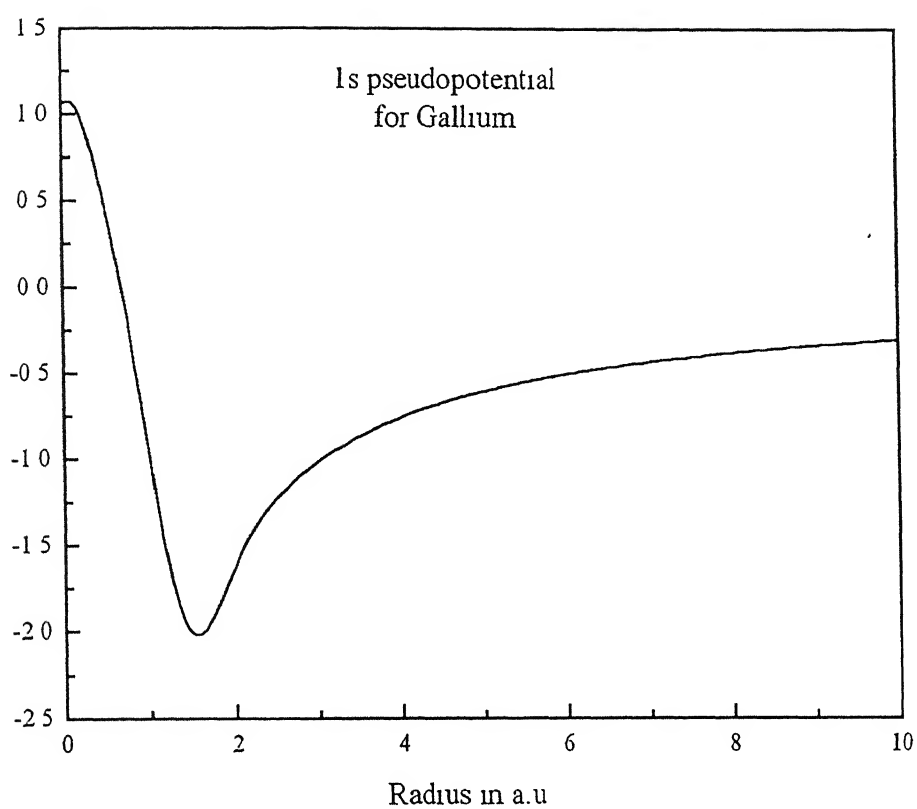


Fig.3.3. Plot for Gallium 1s pseudopotential

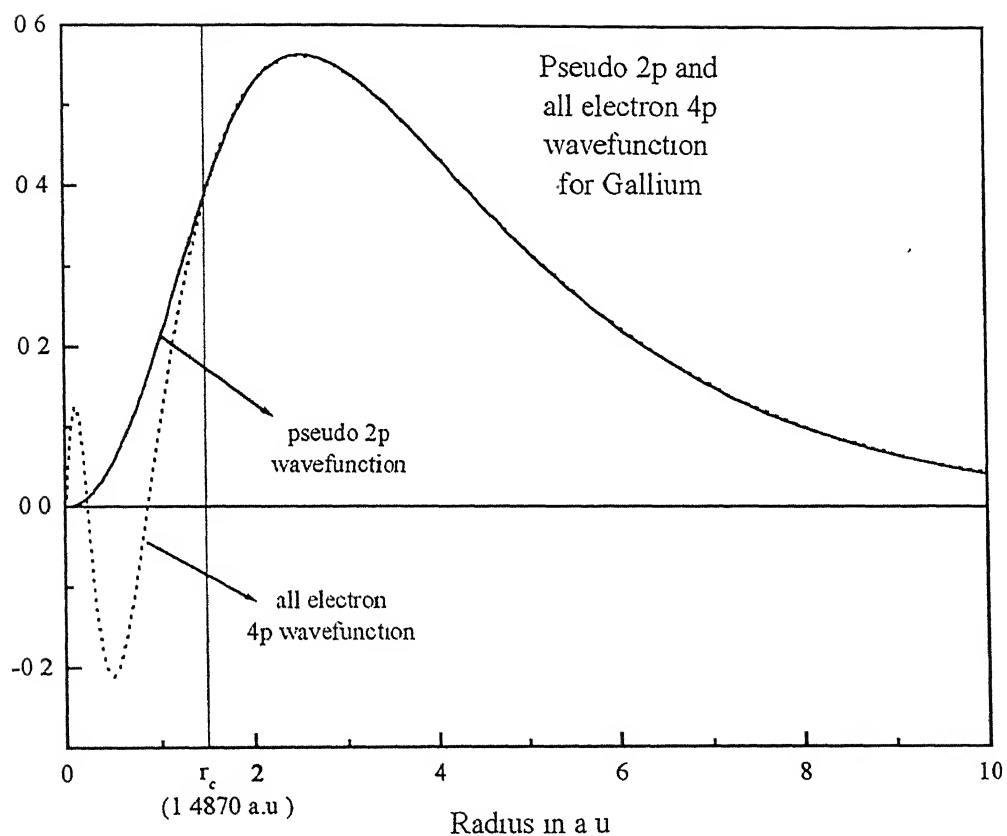


Fig.3.4. Plot for Gallium pseudo 2p and all electron 4p wavefunction

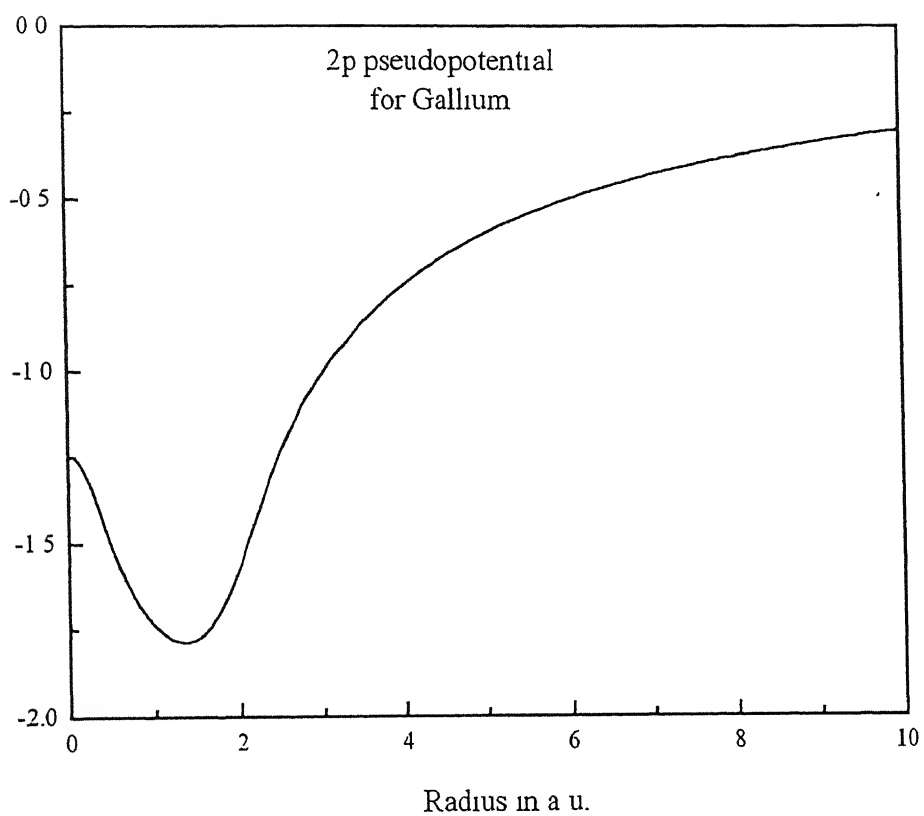


Fig.3.5. Plot for Gallium 2p pseudopotential

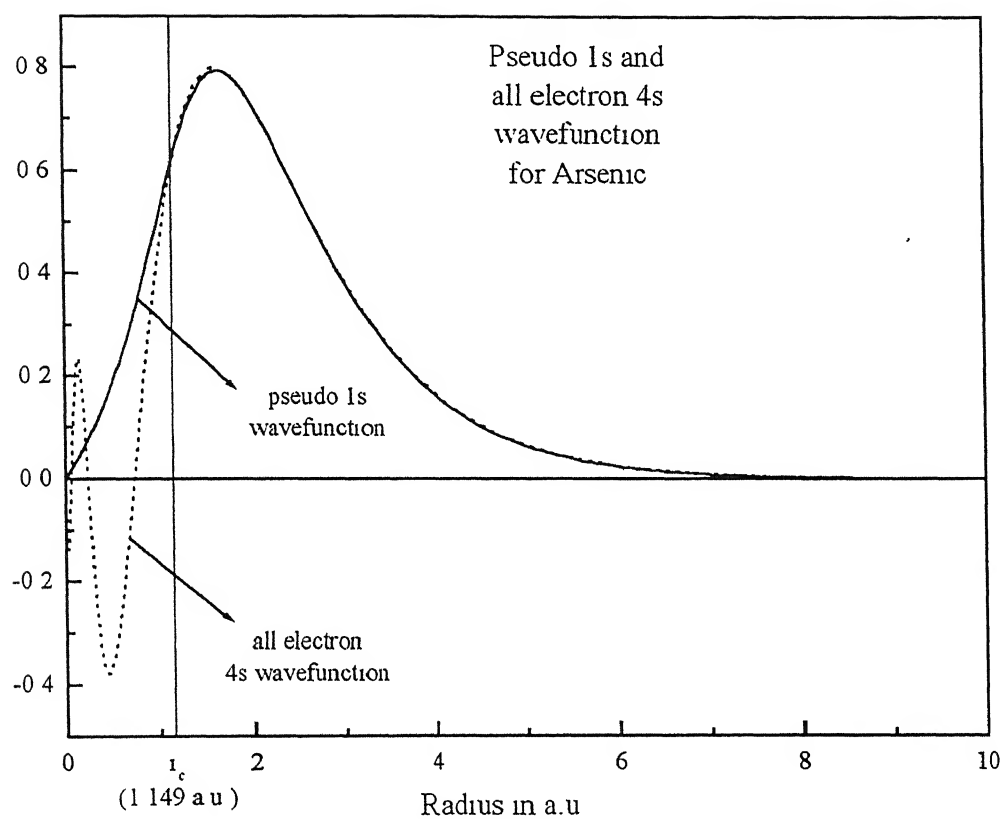


Fig.3.6. Plot for Arsenic pseudo 1s and all electron 4s wavefunction

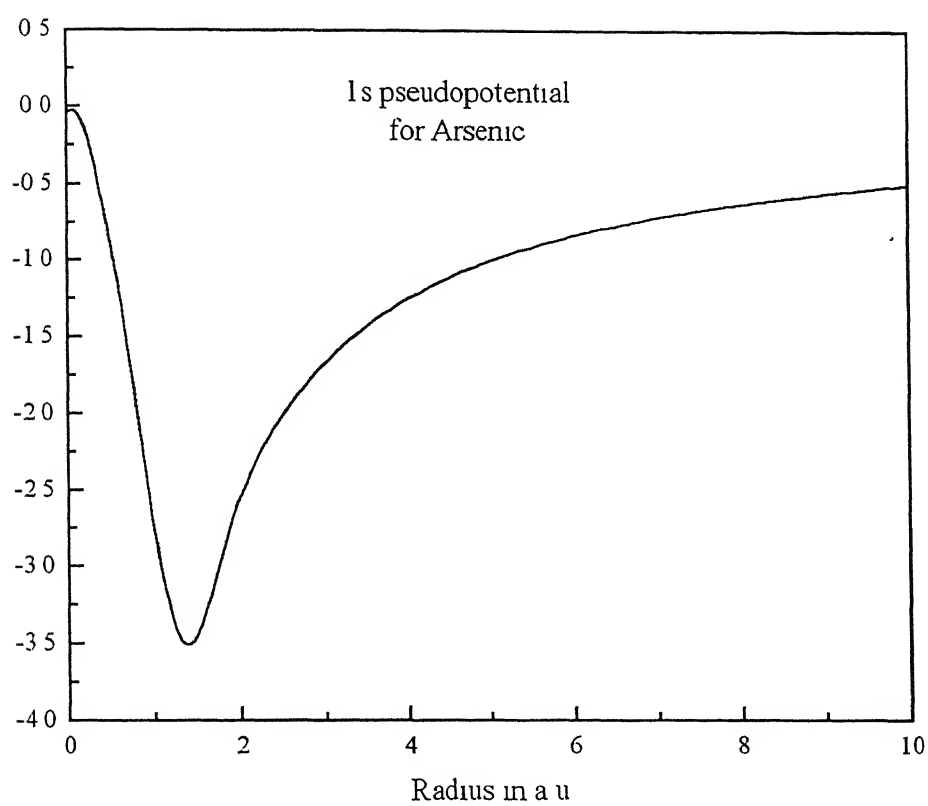


Fig.3.7. Plot for Arsenic 1s pseudopotential

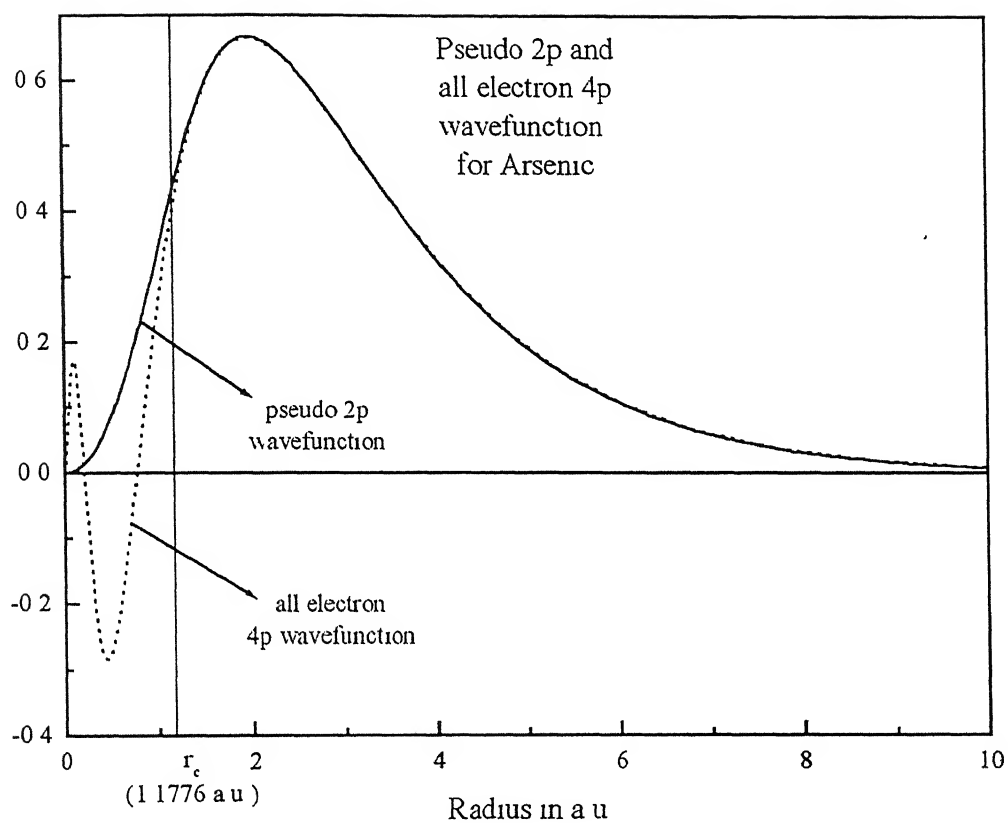


Fig.3.8. Plot for Arsenic pseudo 2p and all electron 4p wavefunction

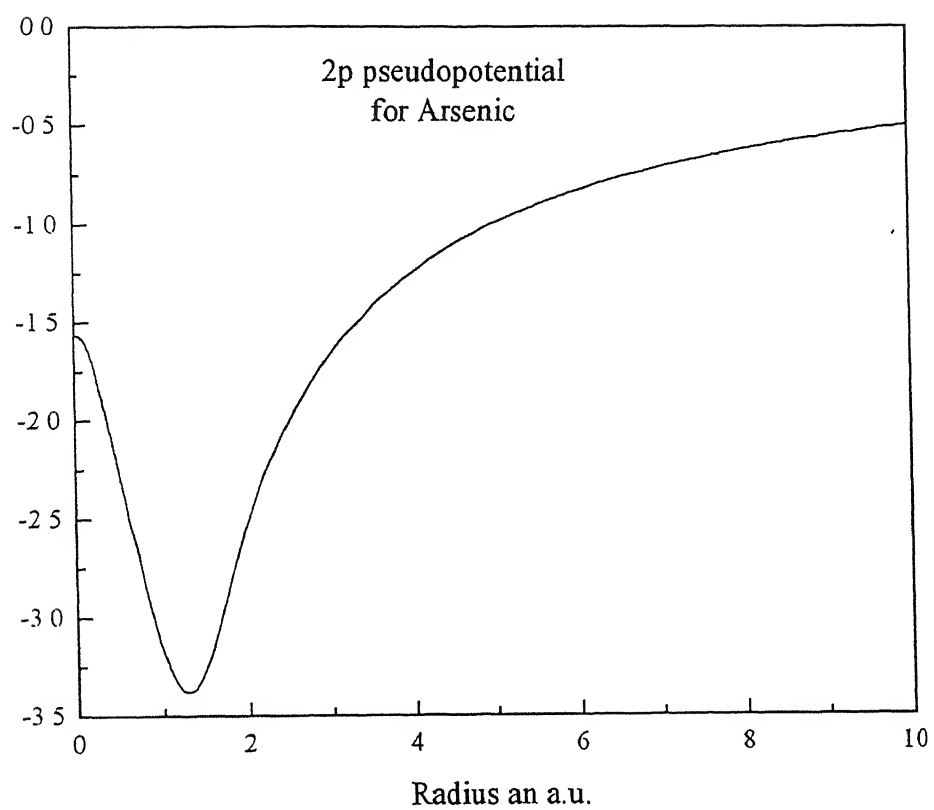


Fig.3.9. Plot for Gallium 2p pseudopotential

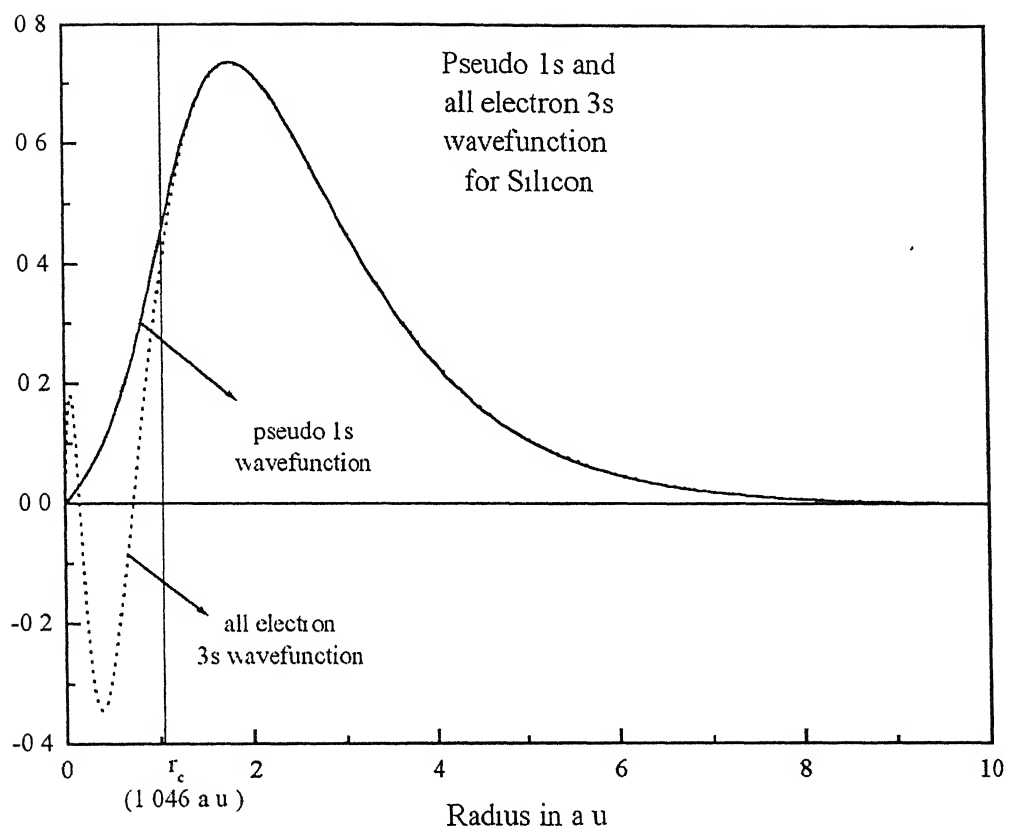


Fig.3.10. Plot for Silicon pseudo 1s and all electron 3s wavefunction

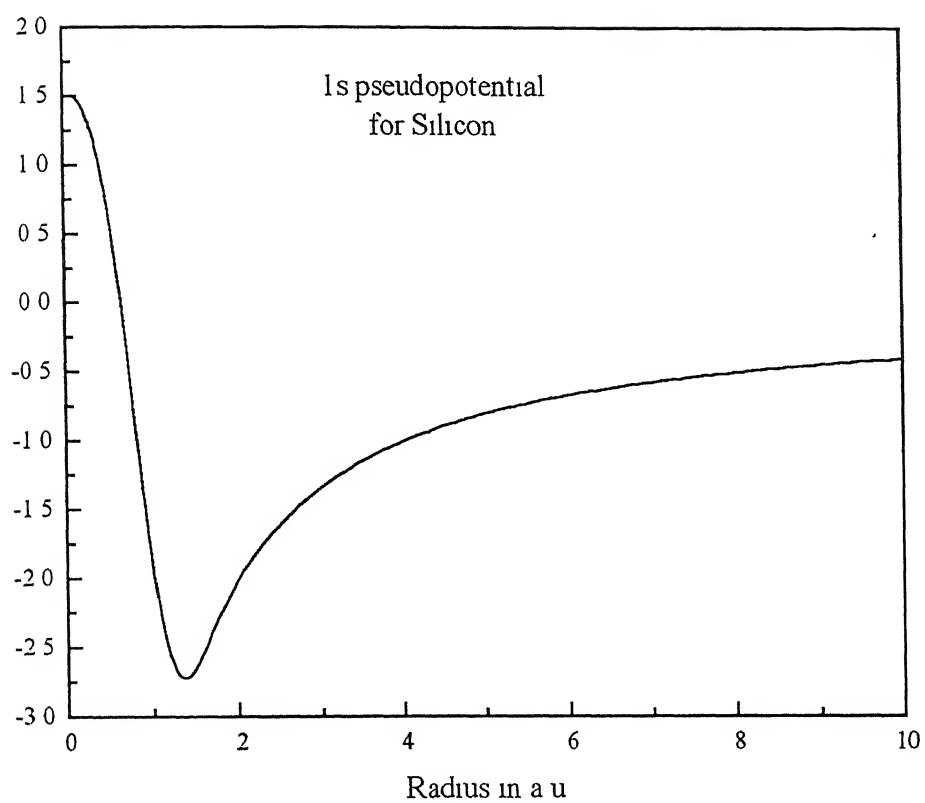


Fig.3.11. Plot for Silicon 1s pseudopotential

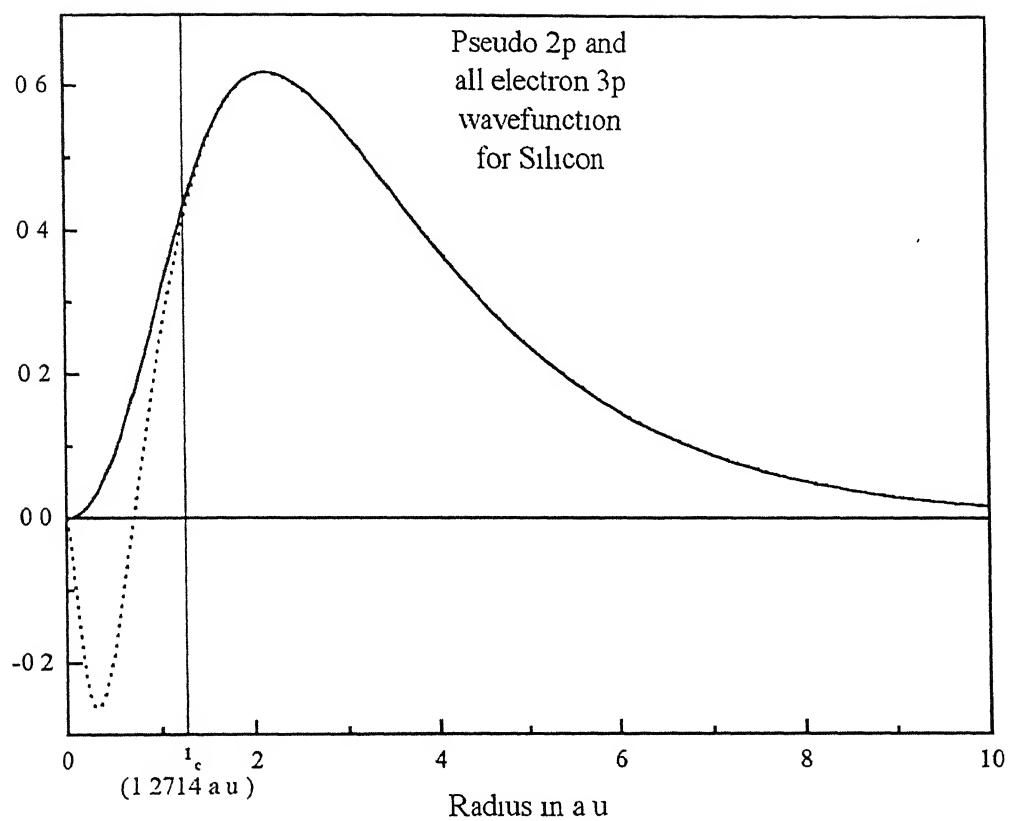


Fig.3.12. Plot for Silicon pseudo 2p and all electron 3p wavefunction

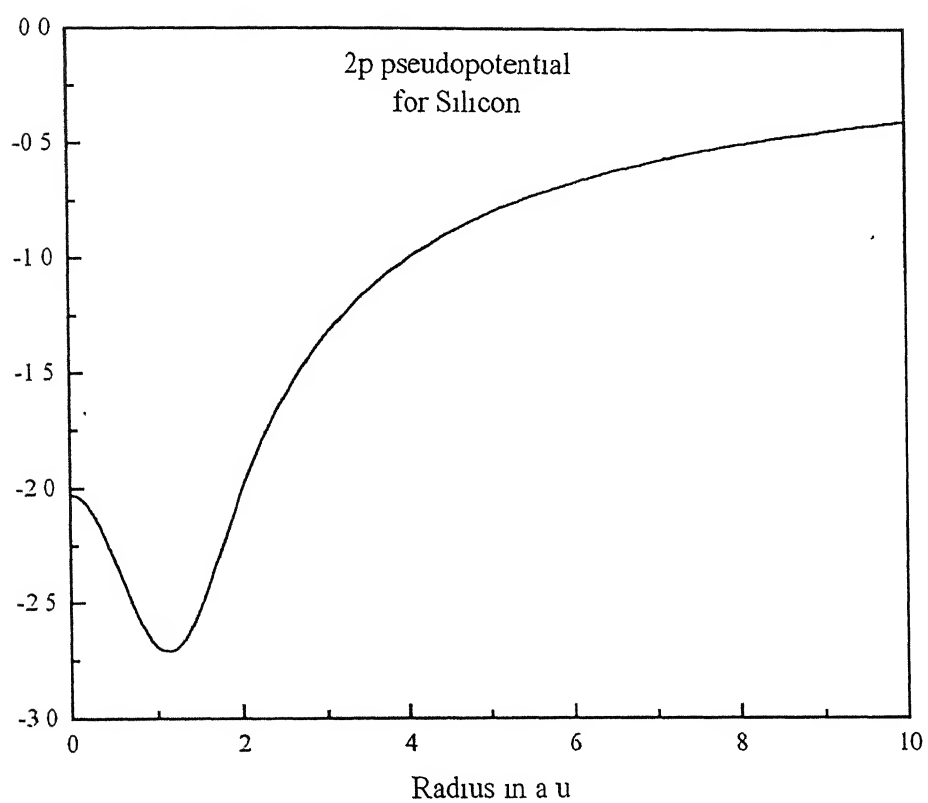


Fig.3.13. Plot for Silicon 2p pseudopotential

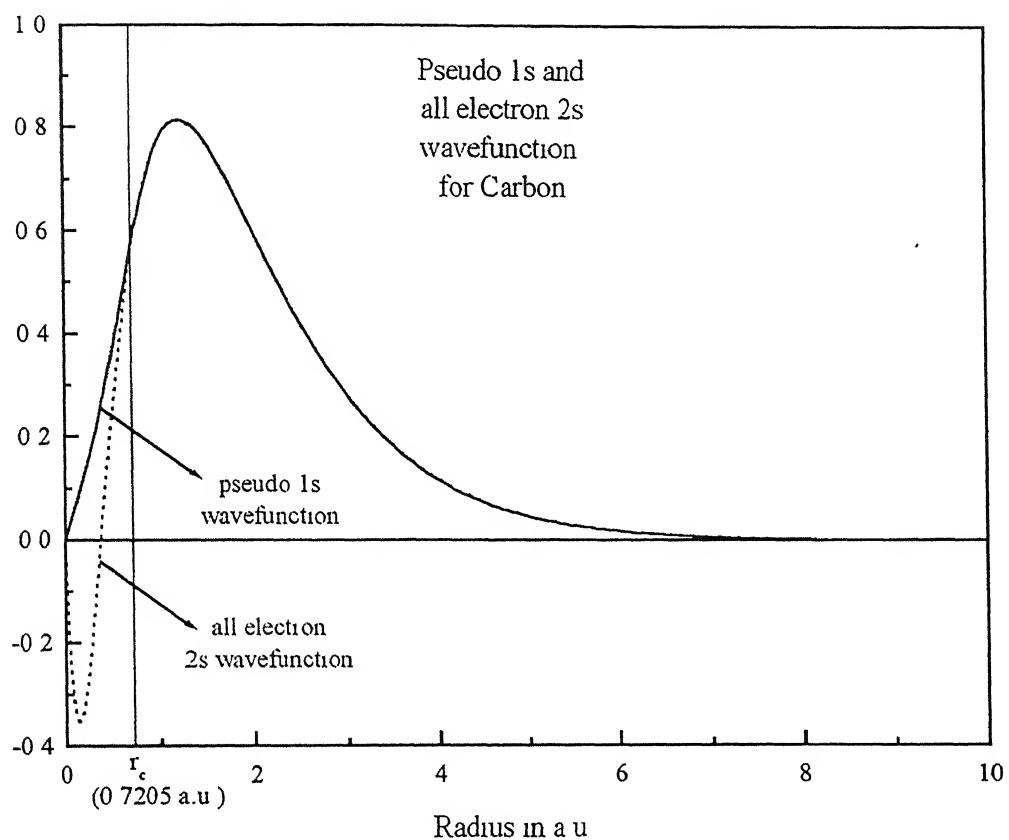
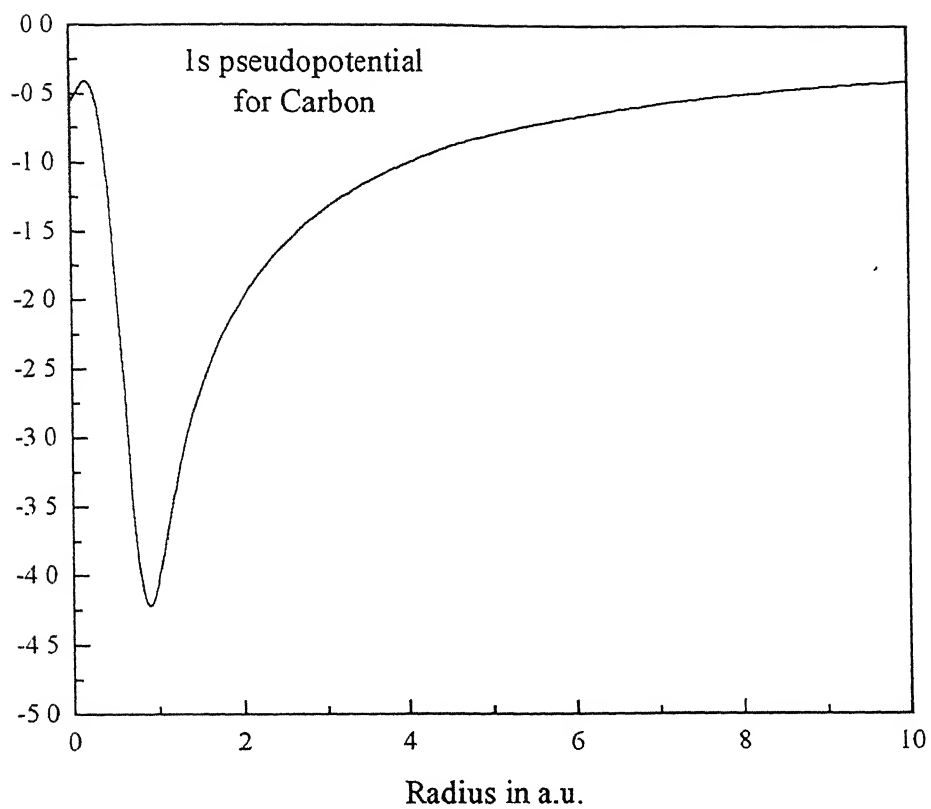


Fig.3.14. Plot for Carbon pseudo 1s and all electron 2s wavefunction



3.15. Plot for Carbon 1s pseudopotential

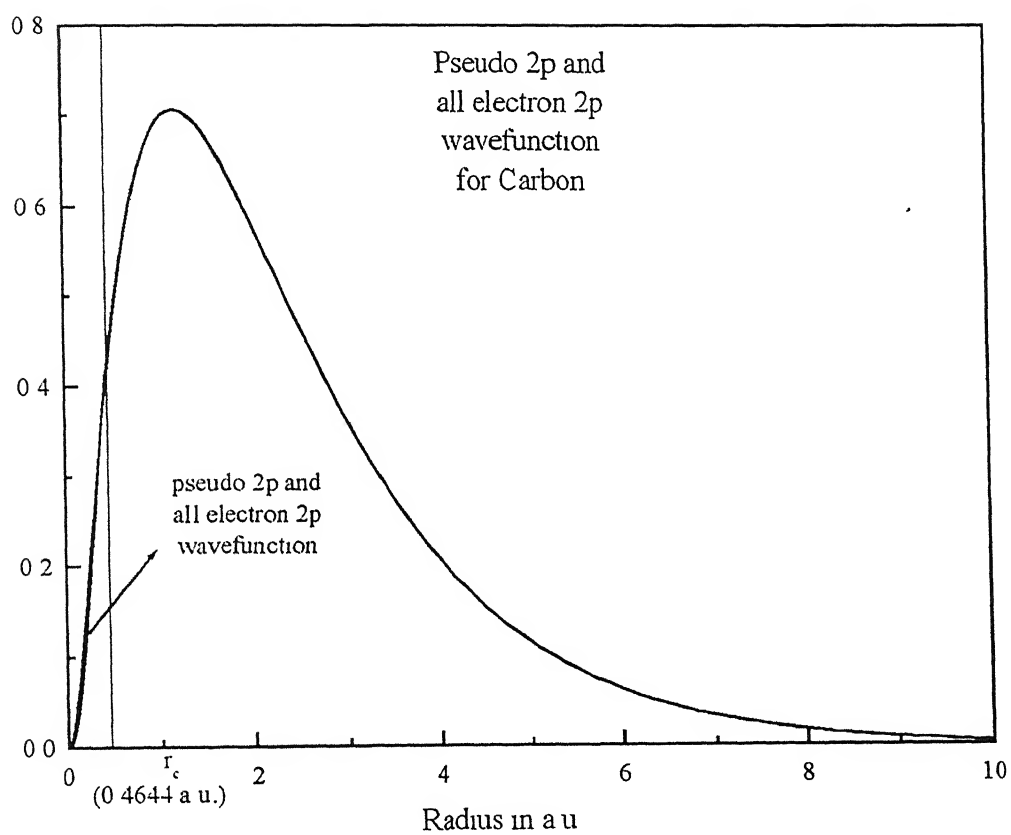


Fig.3.16. Plot for Carbon pseudo 2p and all electron 2p wavefunction

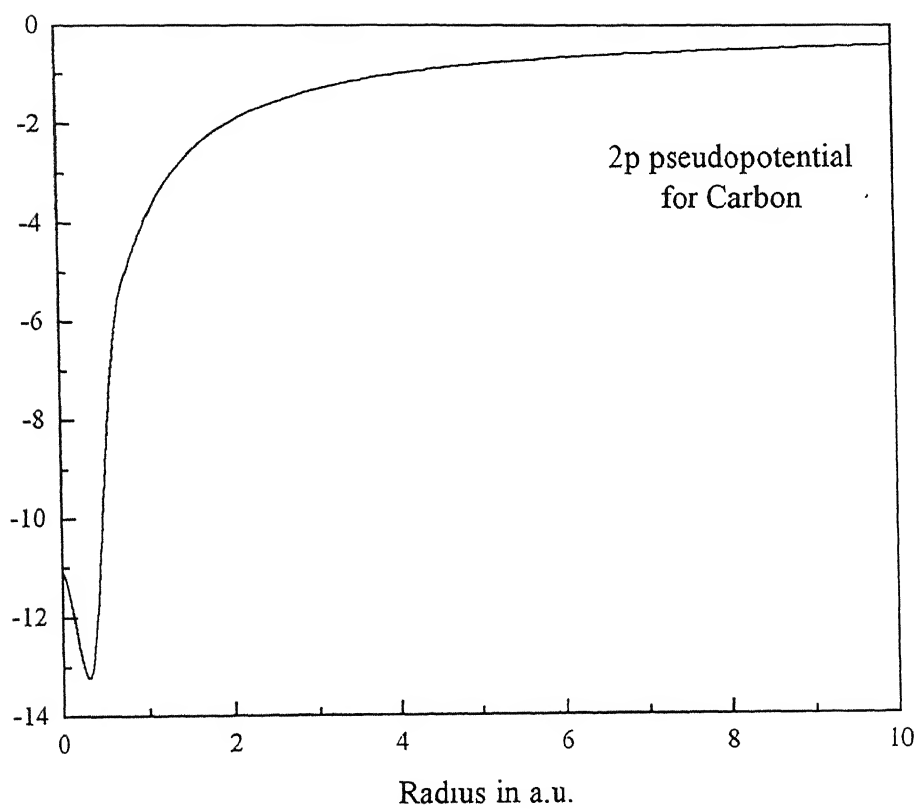


Fig.3.17. Plot for Carbon 2p pseudopotential

Chapter 4

Results and Discussion

4.1 Optimization of the Gallium Arsenide structure

Gallium arsenide (GaAs) has the well known zinc blende (ZnS) structure. In a gallium-arsenide unit cell, four gallium atoms are placed at $(0,0,0)$ $(\frac{1}{2}, \frac{1}{2}, 0)$ $(\frac{1}{2}, 0, \frac{1}{2})$ $(0, \frac{1}{2}, \frac{1}{2})$ while the four arsenic atoms are placed at $(\frac{1}{4}, \frac{1}{4}, \frac{1}{4})$ $(\frac{3}{4}, \frac{3}{4}, \frac{1}{4})$ $(\frac{3}{4}, \frac{1}{4}, \frac{3}{4})$ $(\frac{1}{4}, \frac{3}{4}, \frac{3}{4})$. The supercell for computation is made up of 8 unit cells containing 32 atoms of Ga and As each. In order to optimize the structure, we first determined the cutoff energy at which the subsequent calculations are to be done. The choice of the cutoff energy is a crucial factor. Ideally, the number of plane waves used in this calculation should be infinite. According to energy cut-off, the number of plane waves are, $n_{\text{gwx}} = \frac{1}{6\pi^2} \Omega E_{\text{cut}}^{3/2}$, where Ω is the volume of the supercell and E_{cut} is the energy cutoff (in Ry). The larger the number of the plane waves, the better is the accuracy of the results. But, a large cutoff energy requires more computational time. Therefore, the cutoff energy is chosen in such a way that at this energy, the variation of the total energy with cutoff energy does not affect the accuracy of the calculation. In order to establish the accuracy of our calculation, we will compare our results with a measured value of 0.74 eV for heat of formation of GaAs molecule. Thus, allowable value of energy in all minimization problems is for the condition that energy does not change by more than 0.01 eV per atom (molecule) (i.e. 0.001 a.u., 1 a.u. = 27.211 eV) upon changing the parameters in the minimization problem.

The total energy is calculated at different cutoff radii and the results are plotted to get an optimum value. The results are shown in table 4.1 and the corresponding plot is shown in fig 4.1

For our calculation, we have chosen the cutoff energy as 20 Ry. This choice is made because of following considerations. The time taken for the calculation of the total energy at 18, 20 and 22 Ry cutoff energy were approximately 5, 7 and 12 hours, respectively. Though the total energy at 22 Ry is lower than that at 20 Ry cutoff, but only by 0.04 a.u., and calculations at 22 Ry consumed extra computational time. Also note that, this chosen cutoff is already higher than the equivalent calculations reported in literature [1.7]. Bachlet, Hamann and Schlüter [3.2] had done the calculation of heat of formation at 18 Ry cutoff and estimated it at 0.73 eV, while Chadi and others [1.7] had done the same calculation with a soft pseudopotential at 6 Ry cutoff and got an error of ~ 0.35 eV in energy. Thus, it can be expected that for our calculation, a 20 Ry cutoff energy is sufficient. The input files *start.inp* and *inp.mod* used for the optimization of the GaAs structure is given in appendix C. The supercell was constructed by assuming a simple cubic lattice and atomic positions of all 32 atoms of As and Ga are specified in *start.inp*.

Once the cutoff energy is determined, the optimization for the lattice parameter is straightforward. Again we plot total energy against the lattice parameter. The minimum of the curve gives the required optimum point. The optimum value of the lattice constant (the lattice constant of the supercell, $2a$) obtained at this cutoff is 20.98 a.u. and calculated total energy at this point is -277.113509 a.u. Since this energy is for 32 pairs of Ga and As atoms, the total energy per pair is -8.659797 a.u. (-235.64174 eV). Also, since

the supercell is made up of 8 actual Zinc blend GaAs unit cells, the lattice parameter for GaAs is 10.49 a.u.

Table 4.1 Variation of total energy with the cutoff energy

Cutoff Energy (a.u.)	Total Energy (a.u.)
8	-274.712182
10	-275.601537
12	-276.320312
14	-276.747908
16	-276.953976
18	-277.048783
20	-277.110737
22	-277.151251

Table 4.2 Variation of total energy with the lattice parameter

Lattice Parameter (a.u)	Total Energy (a.u.)
20	-276.837322
20.2	-276.943782
20.4	-277.024203
20.6	-277.077615
20.8	-277.107448
20.9	-277.111396
20.95	-277.110575
20.98	-277.113509
20.985	-277.113289
20.99	-277.113163
21	-277.112678
21.1	-277.113194
21.2	-277.103183
21.4	-277.075901
21.6	-277.031815
21.8	-276.976025
22	-276.910593

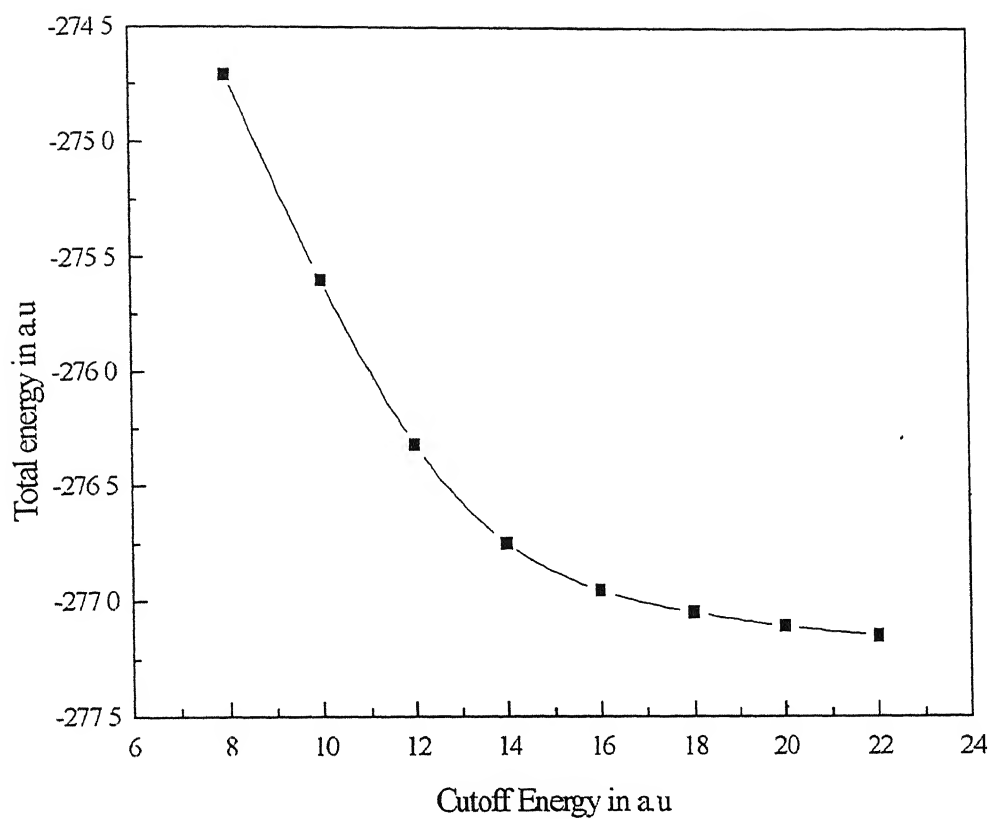


Fig.4.1. Plot for total energy as a function of cutoff energy for a GaAs supercell containing 32 gallium and 32 arsenic atoms

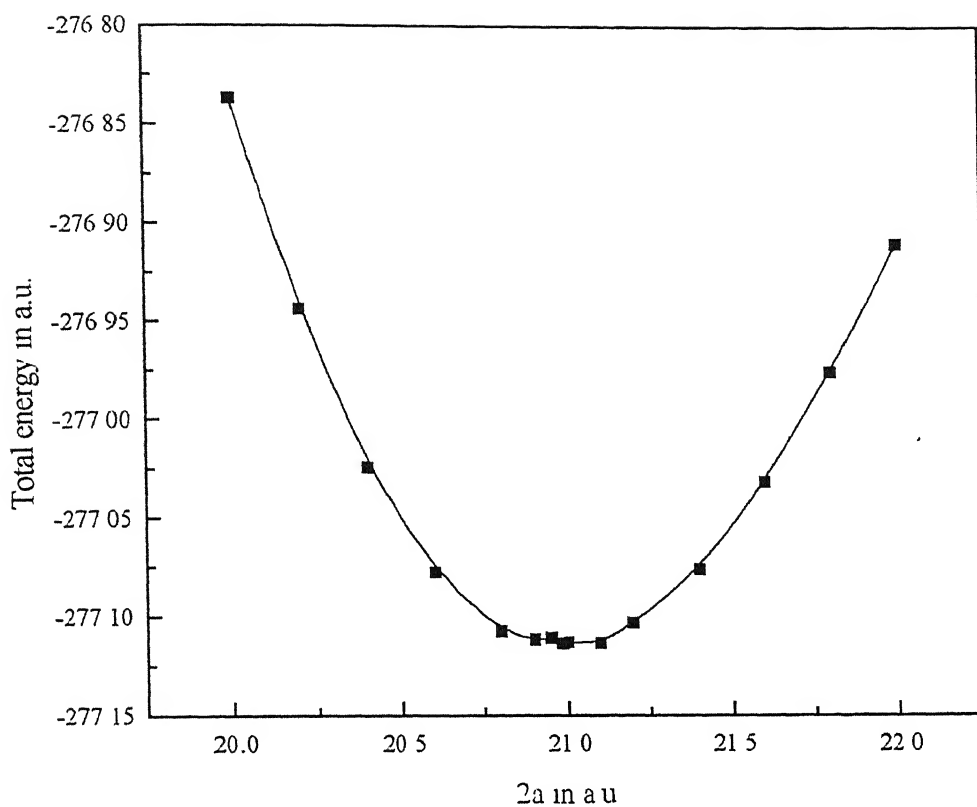


Fig. 4.2. Plot for total energy as a function of lattice parameter for a GaAs supercell containing 32 gallium and 32 arsenic atoms

4.2 Optimization of the Arsenic structure

The structure of arsenic can be described in three different ways [4.1]:

- (1) primitive rhombohedral cell with α slightly less than 60° , two atoms at $\pm(x, x, x)$, where x is less than $\frac{1}{4}$,
- (2) hexagonal unit cell with six atoms at $[(0,0,0)(\frac{2}{3}, \frac{1}{3}, \frac{1}{3})(\frac{1}{3}, \frac{2}{3}, \frac{2}{3})] \pm (0,0,z)$ where z has the same value as that of x , and
- (3) face centered rhombohedral unit cell with α less than 90° and eight atoms at $[(0,0,0)(0, \frac{1}{2}, \frac{1}{2})(\frac{1}{2}, 0, \frac{1}{2})(\frac{1}{2}, \frac{1}{2}, 0)] \pm (\frac{x}{2}, \frac{x}{2}, \frac{x}{2})$, where x is the same as above.

In our calculation, the structure has been described according to the second definition and this structure of As is shown in figure 4.3. The lattice constant and the values of the positional parameter are taken as $a = 3.7599 \text{ \AA}$ (7.10515 a.u.), $c = 10.5478 \text{ \AA}$ (19.9323 a.u.) and $z = 0.2271$ [4.1]. In actual calculation, a supercell is constructed by considering four unit cells of arsenic. These four cells were taken by repeating unit cells in \vec{a} and \vec{b} directions of the lattice, which mean lattice parameter taken in \vec{a} and \vec{b} direction is $2 \times 7.10515 \text{ a.u.} = 14.2103 \text{ a.u.}$ and also the 24 atomic positions for the supercell are given in appendix D. Since the lattice parameters described above are not optimized ones (i.e. the total energy is not minimum at the corresponding values), they are optimized through the following procedure. The total energies were calculated with five different values of lattice constants a (12.7887, 13.4998, 14.2103, 14.9208 and 15.6313 a.u.), c (17.9391, 18.9357, 19.9323, 20.9289 and 21.9255 a.u.) and z (0.2044, 0.2158, 0.2271, 0.2385 and 0.2498) for all their possible combinations. The maximum and the minimum values of these parameters represent $\pm 10\%$ variation about the central value. With the energies

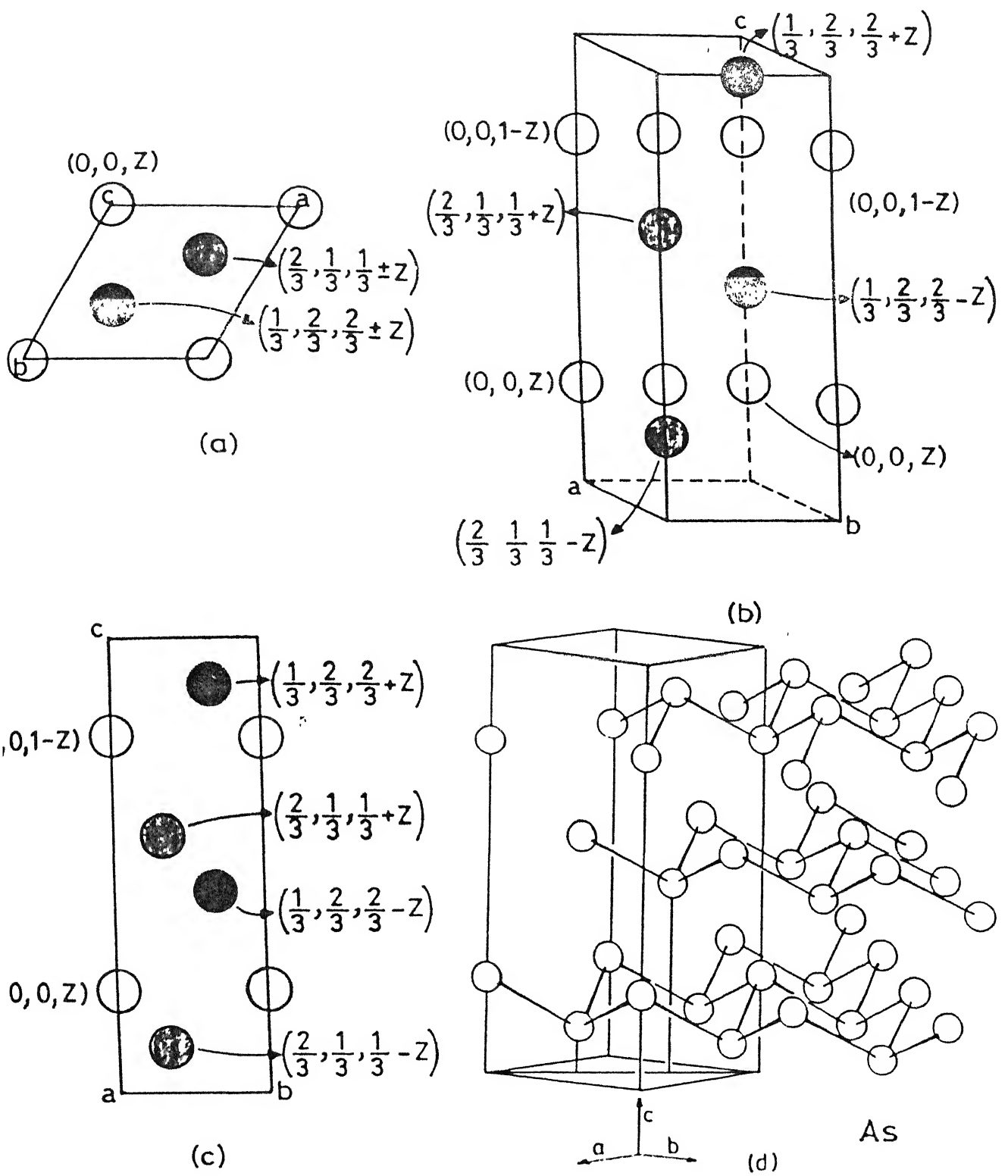


Fig.4.3(a-d). Plot for As structure (Fig. 4.3(d) is taken from Ref. [4.3])

calculated for all 125 sets formed by combinations of $2a$, c and z , the minimum energy condition was obtained by a neural network program. This program trains the network for the given 125 sets of $2a$, c and z values and corresponding energies included in appendix E. From the allowable range of variation for the different parameters, the program then calculates the energy of a large number of points and predicts the point of minimum energy from them. The point of minimum as described by the neural network program in this case is $2a = 15.0994$ a.u., $c = 20.0898$ a.u. and $z = 0.2748$. Here the predicted z value is outside the range of our input data set (z is allowed to vary from 0.2044 to 0.2498). This shows that total energy is a strong function of the parameter z . In order to estimate the accuracy of the prediction by the neural network optimization, we also graphically represent the energy as a function of $2a$, c and z .

Examine the plot of the total energy against the lattice parameter $2a$ in fig. 4.4. For a fix value of c , the total energy becomes independent of the value of a for $2a > 15$ a.u.. Also for $2a > 15$ a.u., the variation in energy with respect to z is minimal when z is large. Like wise, it is clear from fig. 4.5, for $2a$ between 14 and 15 a.u., energies are insensitive to the value of c . Thus prediction of $2a = 15.0994$ a.u. seems acceptable.

From fig. 4.6, it can be seen that in the given range of value of c (17.9391 to 21.9255 a.u.), total energy is insensitive to the variation in the value of z when z is large. Thus the z dependency of the total energy may be eliminated at a higher value of z . The next curve, fig. 4.7, indicates that, for $2a$ between 14.2 and 14.9 a.u., total energy does not change significantly with an increase in the value of c . Since these calculations are done at $z = 0.2498$, it is expected that c dependency of the total energy will be less at a still higher z value.

From plots in fig 4.6 and fig. 4.7, $c = 20.0898$ a.u. does not appear unreasonable as a first estimate

However, a more serious concern is with the prediction of neural network minima for z . But, it is clear from fig. 4.8 and fig. 4.9, only for large values of z , a minimum energy condition is reached. Nonetheless, because the predicted value of z lies outside the range of input data, further investigation is necessary

For this purpose the energy calculation is done in the neighborhood of the approximate minimum point, by varying one parameter at a time. If the calculated energies at the neighboring points are higher than the predicted point, then the predicted value from neural network is accepted. If the energy decreases in any given direction, then further calculations are performed in that direction, till either the energy increases or the variation of the energy with respect to the change in the parameter is 10^{-3} a.u. or less.

Table 4.3 Calculated total energies at the neighboring points of the approximate minimum as predicted by the neural network

Serial No.	2a (a.u.)	c (a.u.)	z	Total Energy (a.u.)
1.	15.0994	20.0898	0.2748	-152.334489
2.	14.9994	20.0898	0.2748	-152.324711
3.	15.1994	20.0898	0.2748	-152.341461
4	15.0994	19.9898	0.2748	-152.334584
5.	15.0994	20.1898	0.2748	-152.334490
6.	15.0994	20.0898	0.2648	-152.394685
7.	15.0994	20.0898	0.2848	-152.166115
8	15.0994	20.0898	0.2548	-152.392038

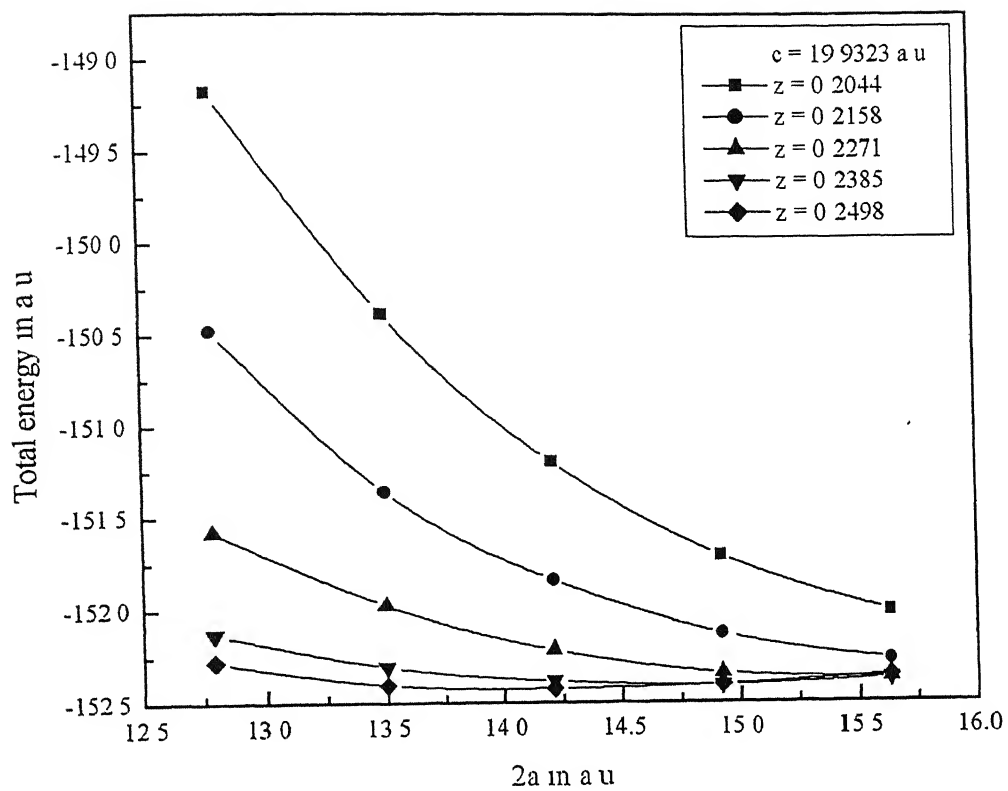


Fig.4.4. Plot for variation of the total energy with $2a$ for a fixed value of c and a family of values of z

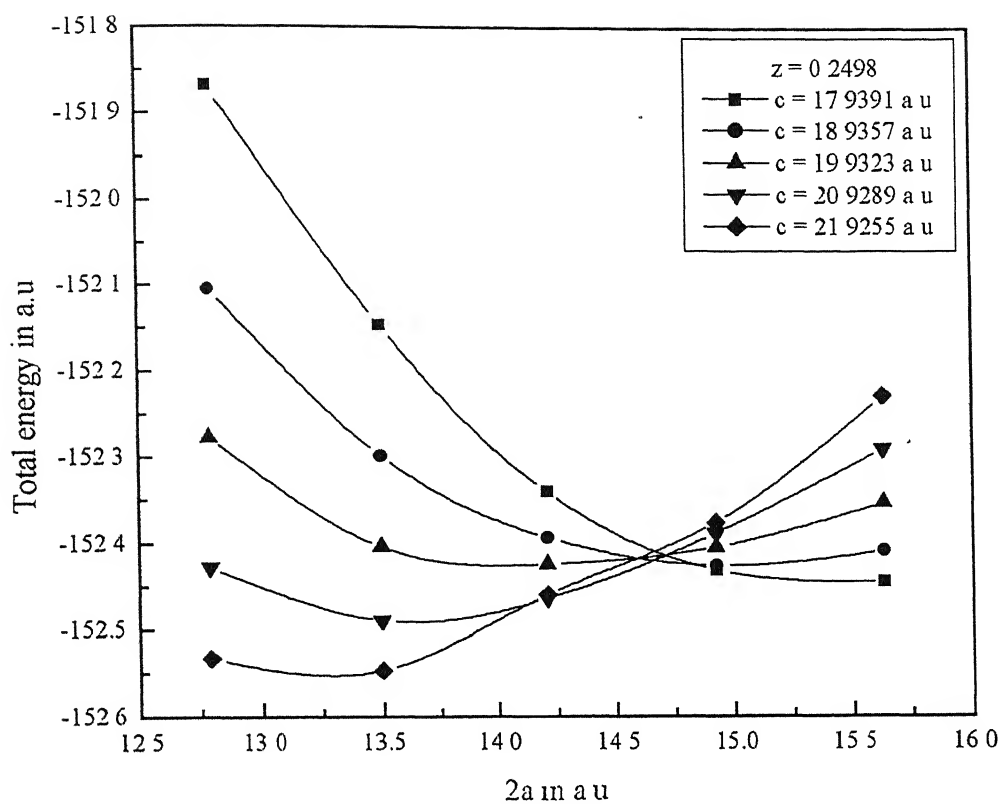


Fig.4.5. Plot for variation of the total energy with $2a$ for a fixed z and a family of values of c

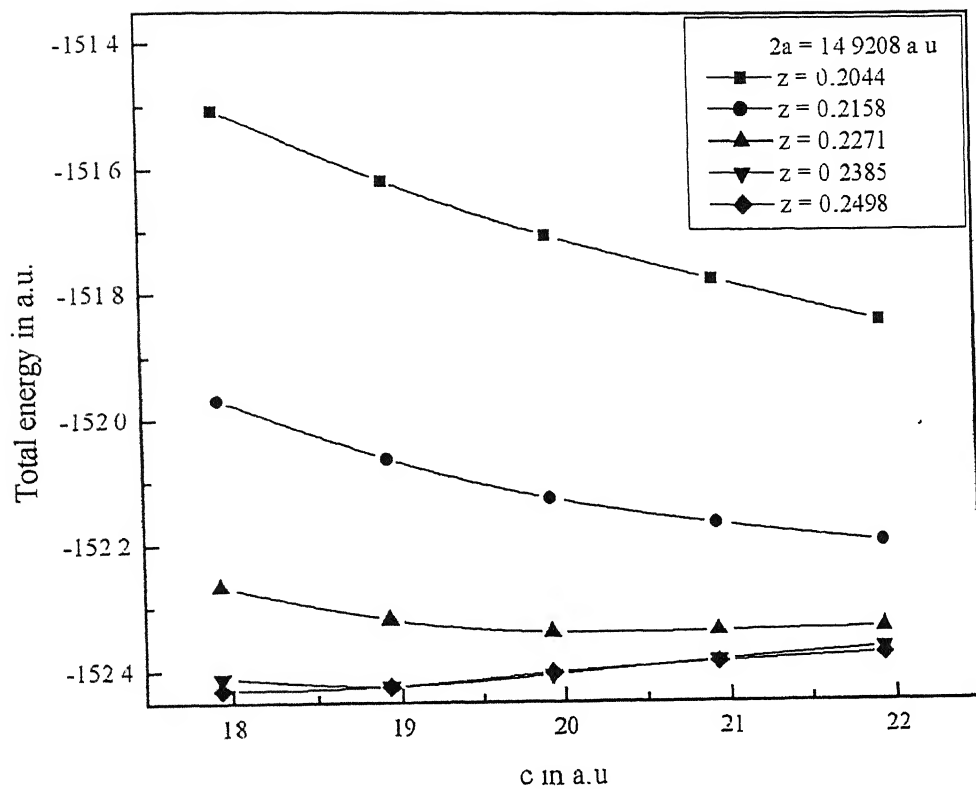


Fig.4.6. Plot for variation of the total energy with c for fixed value of 2a and a family of values of z

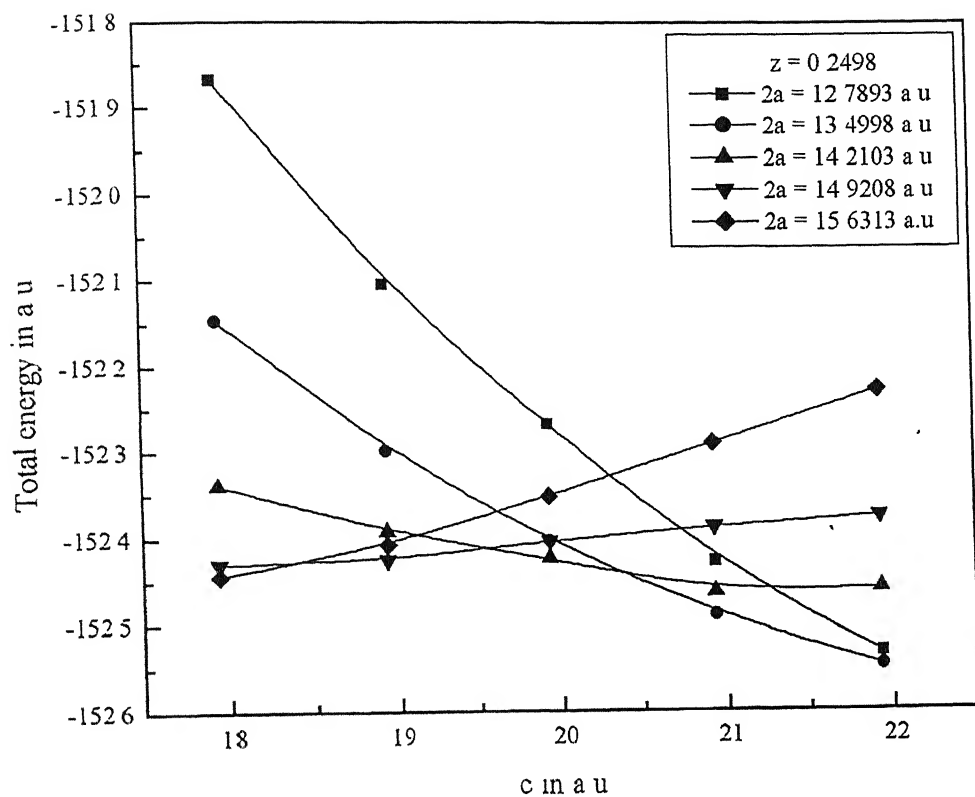


Fig.4.7. Plot for variation of the total energy with c for a fixed value of z and a family of values of $2a$

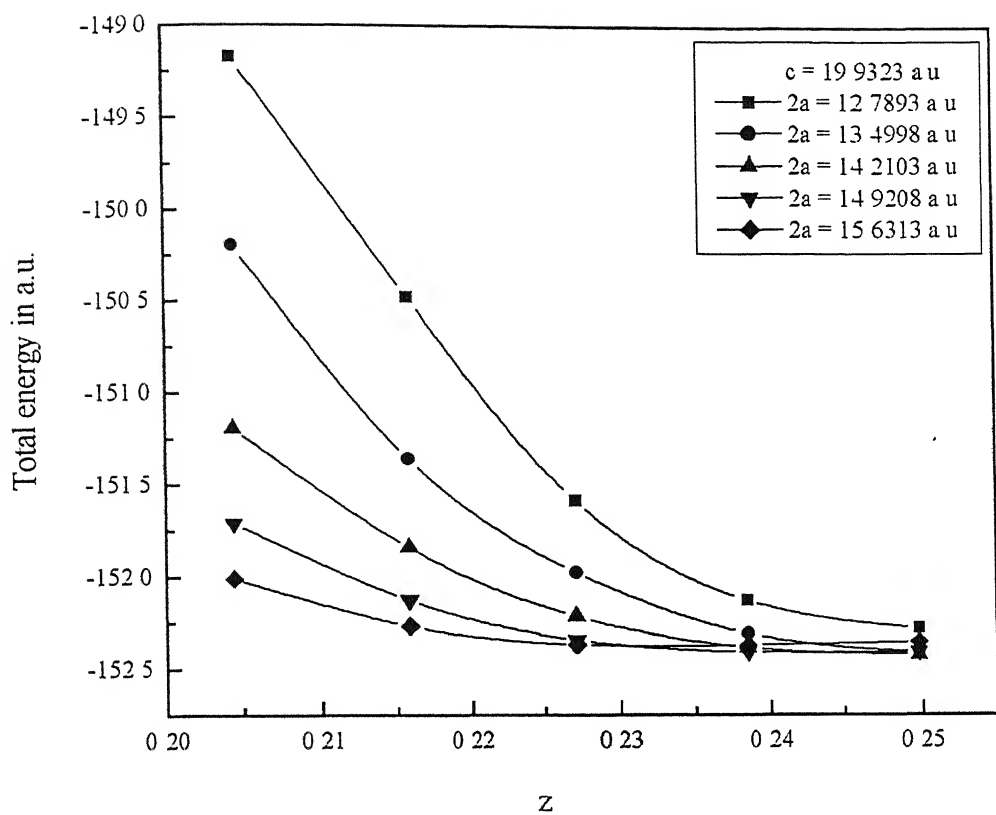


Fig.4.8. Plot for variation of the total energy with z for a fixed value of c and a family of values of $2a$

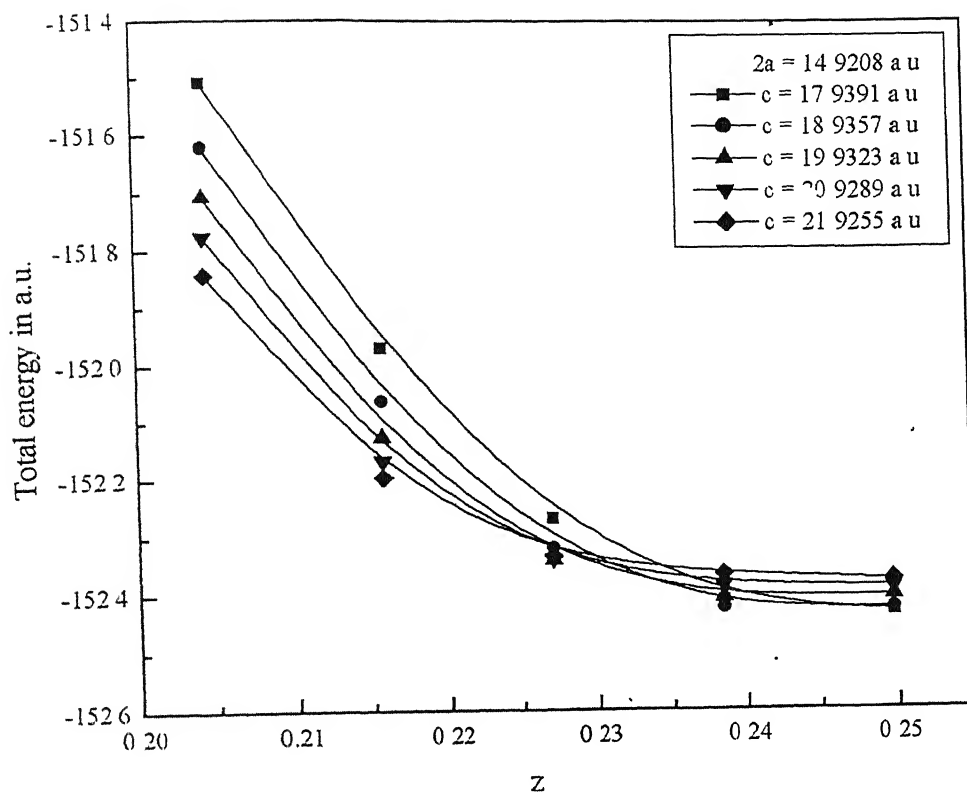


Fig.4.9. Plot for variation of the total energy with z for a fixed value of $2a$ and a family of values of c

From the data in table 4.3, it is clear that the total energy value decreases with the increase in the value of parameter $2a$. The results show that if the parameter a is increased, the total energy decreases. But this decrease in energy is $\sim 10^{-3}$ a.u./atom. A variation of 10^{-3} a.u. in total energy, which is equivalent to 10^{-2} eV, is insignificant in our calculation. No such optimization of the parameter c is required, as when this parameter is changed, total energy of the arsenic remains either constant or increases from that at the neural network minimum (see rows 1, 4 and 5 in table 4.3). Also it is clear from the table 4.3 that the total energy is a strong function of z and needs special attention. We find a more suitable minimum for z at 0.2648 (see rows 1, 6, 7 and 8 in table 4.3). Thus, from this consideration, the point of minimum is fixed at $2a = 15.0994$ a.u., $c' = 20.0898$ a.u. and $z = 0.2648$. We once again repeat the procedure adopted to generate table 4.3 to examine if the sensitivity to a and c has changed at this new value of z . The results are shown in table 4.4. Clearly, $2a = 15.0994$ a.u., $c = 20.0898$ a.u. and $z = 0.2648$ can be accepted as the lattice parameters. Thus the minimum energy for this 24 atom arsenic supercell is -152.394685 a.u. (i.e. -172.783836 eV/atom).

Table 4.4 Total energies around the point of minimum energy

Serial No.	$2a$ (a.u.)	c (a.u.)	z	Total Energy (a.u.)
1.	15.0994	20.0898	0.2648	-152.394685
2.	15.0994	20.0898	0.2848	-152.166115
3.	15.0994	20.0898	0.2548	-152.392038
4.	15.1994	20.0898	0.2648	-152.392158
5.	14.9994	20.0898	0.2648	-152.396238
6.	15.0994	20.1898	0.2648	-152.391698
7.	15.0994	19.9898	0.2648	-152.398110

4.3 Optimization of the Gallium structure

Optimization of the gallium is done in the same way as that of arsenic. Gallium, at room temperature, has orthorhombic symmetry with two of the axes of nearly equal length. The eight gallium atoms are placed at $[(0,0,0) (\frac{1}{2}, \frac{1}{2}, 0)] \pm [(0, y, z) (\frac{1}{2}, y, \frac{1}{2} - z)]$. This structure is plotted in fig. 4.10. At room temperature the lattice parameters are $a = 4.5192 \text{ \AA}$ (8.54 a.u.), $b = 7.6586 \text{ \AA}$ (14.4726 a.u.) and $c = 4.5258 \text{ \AA}$ (8.5525 a.u.) while the offset parameters y and z are 0.1539 and 0.0798 [4.1], respectively. Here the supercell is constructed by considering four gallium unit cells, and therefore, the supercell contains 32 gallium atoms. The lattice parameters of the supercell for computation taken in \bar{a} and \bar{b} direction are $2 \times 8.54 = 17.08 \text{ a.u}$ and $2 \times 14.4726 = 28.9452 \text{ a.u}$. respectively. In order to optimize the structure, the above said structural parameters (a , b , c , y and z) are varied by $\pm 10\%$ about the room temperature value given above. Total energies are calculated for all the combinations of three different values of $2a$ (15.372, 17.08 and 18.788 a.u.), $2b$ (26.0507, 28.9452 and 31.8397 a.u.) and c (7.6973, 8.5525 and 9.4078 a.u.) and two different values of y (0.1385 and 0.1693) and z (0.0718 and 0.0878). The input file for *fh196md*, which also provides the 32 atom positions, is attached in appendix F. The calculated value of total energies, for various combinations of $2a$, $2b$, c , y and z , as mentioned above, are given in appendix G. These 108 set of data containing $2a$, $2b$, c , y , z and total energy are then fed to a neural network program to get the point of minimum energy for a given set of lattice parameters. The point of minimum energy is predicted by the neural network at $2a = 16.514 \text{ a.u.}$, $2b = 28.8253 \text{ a.u.}$, $c = 8.0075 \text{ a.u.}$, $y = 0.1586$ and $z = 0.0566$.

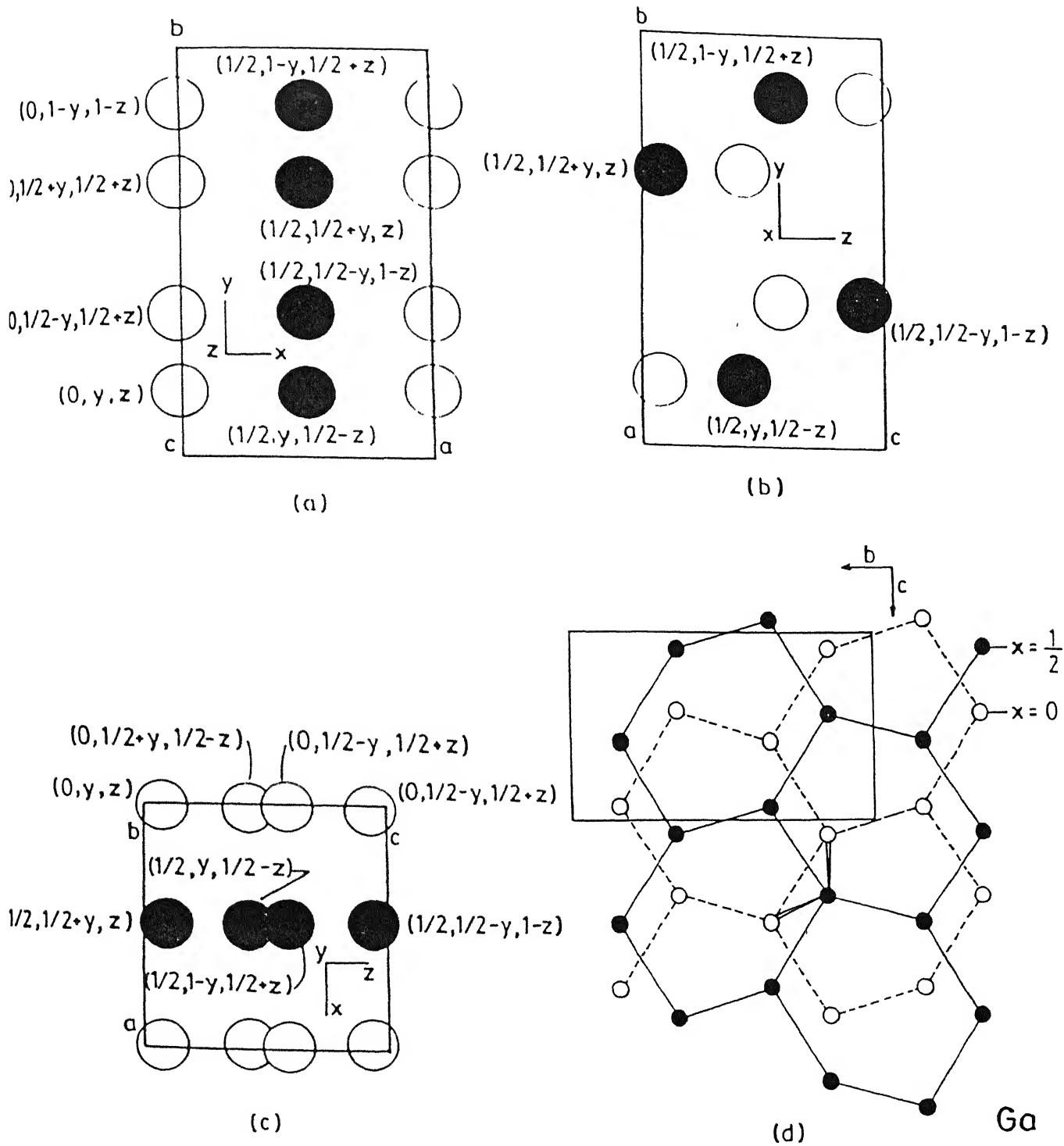


Fig.4.10(a-d). Plot for Ga structure (Fig. 4.10(d) is taken from Ref. [4 3])

Total energies are calculated at the neighboring points of this approximate minimum point by varying one parameter at a time. The results are shown in table 4.5.

Table 4.5 Calculated total energies at the neighboring points of the approximate minimum predicted by the neural network

a (a.u.)	b (a.u.)	c (a.u.)	y	z	Total Energy (a.u.)
16.5140	28.8253	8.0075	0.1586	0.0566	-73.398999
16.6140	28.8253	8.0075	0.1586	0.0566	-73.390369
16.4140	28.8253	8.0075	0.1586	0.0566	-73.407124
16.5140	28.9253	8.0075	0.1586	0.0566	-73.396928
16.5140	28.7253	8.0075	0.1586	0.0566	-73.400781
16.5140	28.8253	8.1075	0.1586	0.0566	-73.379983
16.5140	28.8253	7.9075	0.1586	0.0566	-73.415477
16.5140	28.8253	8.0075	0.1686	0.0566	-73.291836
16.5140	28.8253	8.0075	0.1486	0.0566	-73.360814
16.5140	28.8253	8.0075	0.1586	0.0666	-73.382359
16.5140	28.8253	8.0075	0.1586	0.0466	-73.411612

Clearly, with both increase and decrease in the value of y about the predicted minimum, the cell energy decreases. Thus the predicted minimum for y is acceptable. Whereas, in the case of parameters b, the energy increases with an increase in the value of b. However, for a reasonable change in the value of b, the change in energy is of the order of 10^{-3} a.u. Hence, we accept the predicted minimum for b. However, a change in cell energy as a function of a, c and z is significant. Thus, a better estimate for a, c and z is searched further. At this stage, we vary only one of the parameters a, c and z at a time. To get an optimum value of c, total energies are calculated at different values of c keeping the other parameters constant at predicted minimum of the neural network. The corresponding values are shown in table 4.6. The results are also shown in graphical form

in fig 4.11. It shows a distinct minimum at $c = 7.6075$ a.u., which is now taken as the new optimum value. In order to get the optimum value of z , the same procedure is applied. Total energies are calculated at different points by decreasing the value of z and keeping the other parameters constant at value shown in fig. 4.12. The results are given in table 4.7 and the corresponding graph is shown in fig. 4.12. In this case, instead of a well defined minimum, we get a curve that decreases with the decrease in the value of z . Since a variation of 10^{-3} a.u. in total energy is allowed in our calculation, we chose the point $z = 0.0366$ as the optimum point. Similarly, the total energy value also decreases with a decrease in parameter a . As no distinct minimum was obtained in this case also, the optimum point is chosen at $2a = 16.114$ a.u. The variation of total energy with the lattice parameter a is given in table 4.8 and is plotted in fig. 4.13. Thus, in subsequent calculations, the following optimum values are taken: $2a = 16.114$ a.u., $2b = 28.8253$ a.u., $c = 7.6075$ a.u., $y = 0.1586$ and $z = 0.0366$.

Table 4.6 Variation of total energy with parameter c

c (a.u.)	Total Energy (a.u)
8.1075	-73.379983
8.0075	-73.398999
7.9075	-73.415477
7.8075	-73.427118
7.7075	-73.433446
7.6075	-73.433953
7.5075	-73.428174

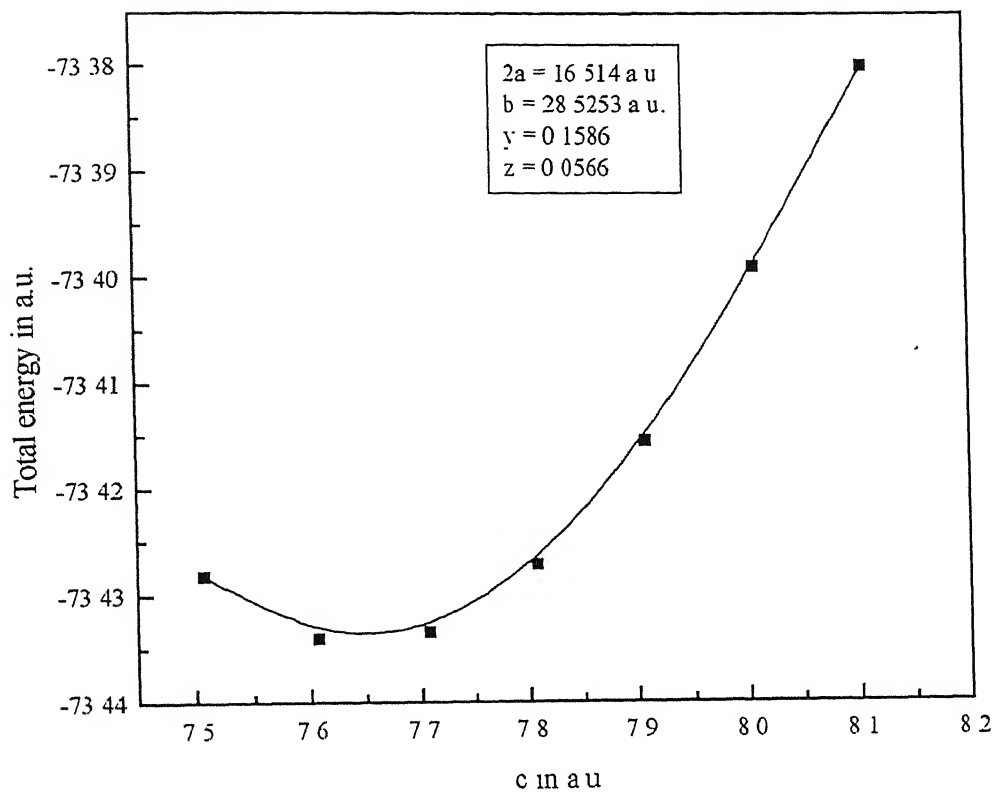


Fig.4.11. Plot for total energy of gallium as a function of parameter c

Table 4.7 Variation of total energy with parameter z

z	Total Energy (a.u.)
0.0798	-73.381665
0.0566	-73.433953
0.0466	-73.448832
0.0366	-73.459965
0.0266	-73.467873
0.0166	-73.473001
0.0066	-73.475657

Table 4.8 Variation of total energy with parameter a

a (a.u.)	Total Energy (a.u.)
16.514	-73.459965
16.414	-73.469243
16.314	-73.477905
16.214	-73.485893
16.114	-73.493255
16.014	-73.499882
15.914	-73.505717
15.814	-73.510774

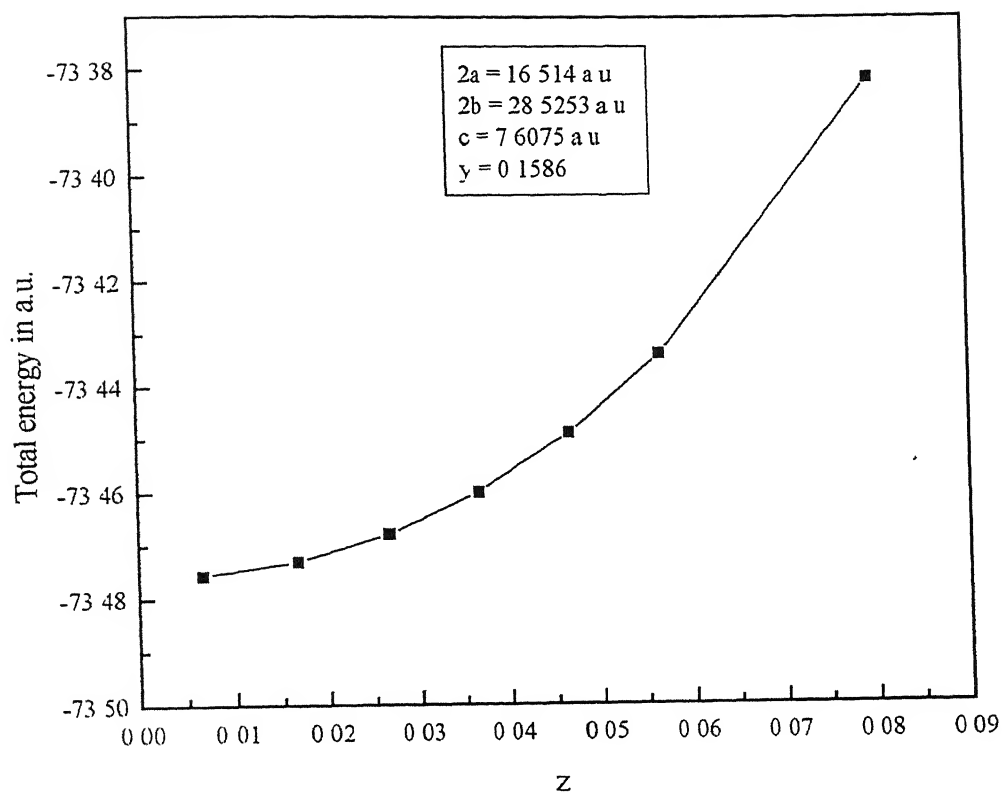


Fig.4.12. Plot for total energy of gallium as a function of parameter z

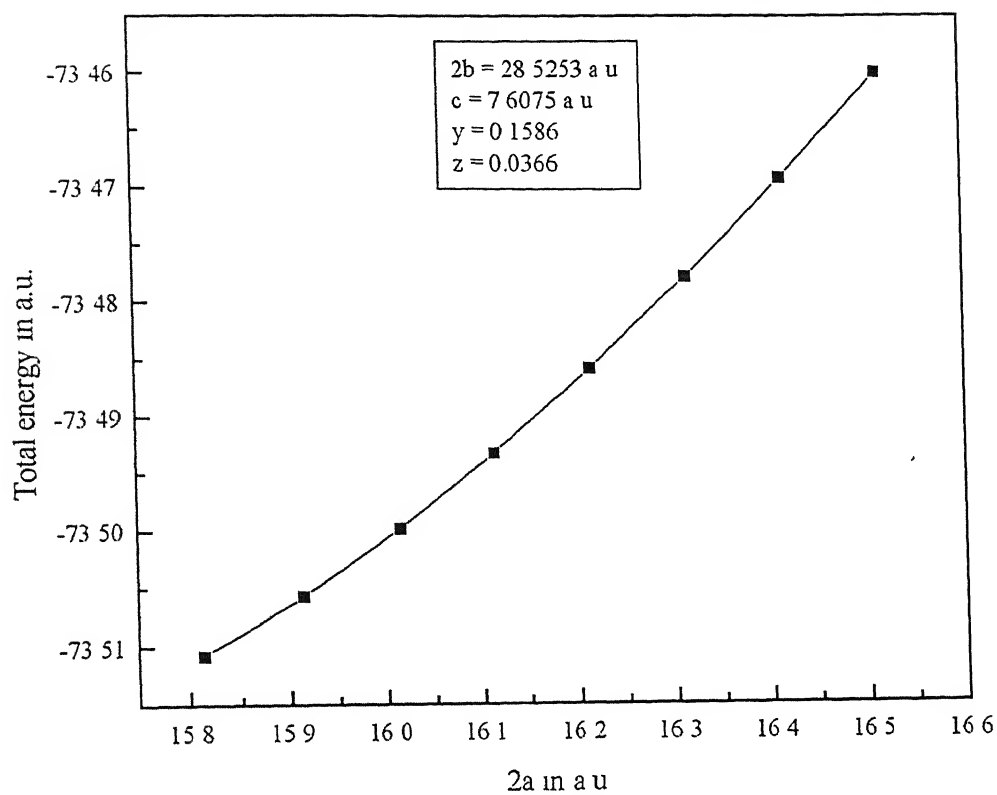


Fig.4.13. Plot for total energy of gallium as a function of parameter a

Finally, we examine the sensitivity of energy around this new point of minimum. These results are shown in table 4.9.

Table 4.9 Total energies around the point of minimum energy

2a (a.u.)	2b (a.u.)	c (a.u.)	y	Z	Total energy (a.u.)
16.1140	28.5253	7.6075	0.1586	0.0366	-73.495423
16.0140	28.5253	7.6075	0.1586	0.0366	-73.501631
16.2140	28.5253	7.6075	0.1586	0.0366	-73.488497
16.1140	28.4253	7.6075	0.1586	0.0366	-73.487144
16.1140	28.6253	7.6075	0.1586	0.0366	-73.495052
16.1140	28.5253	7.5075	0.1586	0.0366	-73.491861
16.1140	28.5253	7.7075	0.1586	0.0366	-73.492762
16.1140	28.5253	7.6075	0.1486	0.0366	-73.461380
16.1140	28.5253	7.6075	0.1686	0.0366	-73.349660
16.1140	28.5253	7.6075	0.1586	0.0266	-73.503096
16.1140	28.5253	7.6075	0.1586	0.0466	-73.484418

It is evident from the results in table 4.9 that the new values of cell parameters are either at a minima, or energy does not change significantly when any of the parameters are changed. The calculated total energy at the point of minimum is -73.495423 a.u.. Since this energy is calculated for a supercell containing 32 Ga atoms, the total energy per atom is -2.296731 a.u. (-62.496374 eV). And the final optimized lattice parameters obtained are $a = 8.57$ a.u., $b = 14.26265$ a.u., $c = 7.6075$ a.u., $y = 0.1586$ and $z = 0.0366$.

4.4 Heat of formation of GaAs

The bulk energies of Ga, As and GaAs are calculated, as mentioned in Section 4.1-4.3, using optimized lattice parameters. To calculate the heat of formation of GaAs, the bulk energies of Ga and As are subtracted from the total bulk energy of GaAs (per pair). The calculated heat of formation of GaAs is compared with a set of published results [1.7], where various pseudopotentials were used in the calculation. The table 4.10 contains those total energy and heat of formation values along with the experimental heat of formation of GaAs [4.2] and our calculated result. The results show that the hard pseudopotentials generated according to the Bachelet, Hamann and Schlüter [2.11] and Kerker [1.8] scheme (0.72 and 0.73 eV respectively) matches well with the experimental result, while the soft pseudo potential gives the heat of formation as 1.08 eV. When these calculations are repeated for both hard and soft pseudopotentials generated according to the Kerker scheme at 6 Ry cutoff energy (modified Kerker scheme as applied by Chadi and others [1.7]), the heat of formation obtained to be 1.76 eV and 1.18 eV respectively. Clearly, the heat of formation for the hard pseudopotential is ~ 1 eV off from that of at 12 Ry. On the other hand, the soft pseudopotential result is off by 0.1 eV. In order to compensate this error at 6 Ry, this soft pseudopotential results are corrected according to the following considerations. The soft pseudopotential heat of formation (1.08 eV) is ~ 0.35 eV off from the experimental result. To correct this, the Ga and As heat reservoirs are lowered by an amount of 0.175 eV ($=0.35/2$ eV), while keeping the energy of GaAs fixed. The other error of 0.1 eV between the 12Ry and 6 Ry cutoff energy is equally distributed between Ga and As. This corrected result is also included in the table 4.10.

The calculated bulk energies of Ga, As and GaAs, in our case, are -62.496374, -172.783836 and -235.64174, respectively. The heat of formation obtained is 0.36 eV,

Table 4.10 Bulk energies of Ga, As and GaAs and the heat of formation of GaAs.

	Cutoff energy (Ry)	Bulk Energy (eV)			Heat of formation (eV)
		GaAs	Ga	As	
Measured ¹					0.74
Hard Ga, As ²	18	-235.379	-61.364	-173.294	0.72
Hard Ga, As ³	12	-235.832	-62.613	-172.490	0.73
	6	-230.825	-60.988	-168.075	1.76
Soft Ga, As ³	12	-235.512	-62.364	-174.070	1.08
	6	-236.168	-62.161	-172.823	1.18
Soft Ga, As	12	-237.512	-62.538	-174.245	0.73
Soft Ga, As ³	6	-236.168	-62.388	-173.051	0.73*
Present calculation	20	-235.64174	-62.496374	-172.783836	0.36

¹ Experimental result [4 2]

² Using Bachelet, Hamann and Schluter pseudopotential at 18 Ry cutoff energy [1 7]

³ Potential generated according to the Kerker scheme [1 7]

* Corrected heat of formation at 6 Ry

which is off by ~0.4 eV from the experimental value. On the other hand, the calculated bulk energies of these materials are close to the corresponding published results. We have also calculated the heat formation for the optimized lattice parameter of GaAs (10.49 a.u.) and experimental lattice parameters of Ga ($a = 8.54$ a.u., $b = 14.4726$ a.u., $c = 8.5525$ a.u., $y = 0.1539$ and $z = 0.0798$) and As ($a = 7.1051$ a.u., $c = 19.9323$ a.u. and $z = 0.2271$). Then the bulk energies obtained are -235.64174 eV/molecule, -62.204163 eV/atom and -172.58352 eV/atom. In this case the heat of formation obtained is 0.85 eV, which is very close to the experimental value. Thus the error in our calculation may be attributed to our adopted lattice parameter optimization procedure of Ga and As. Chadi

and others [1.7] had optimized the Ga structure in a different way. They had kept the ratio $a:b:c$ fixed and then minimized the total energy with respect to the volume and internal parameters y and z . In this way they had reduced the number of variable from 5 (a , b , c , y and z) to 3 ($a/b/c$, y and z). Our optimization procedure is more intensive one where all the 5 variables are allowed to change.

4.5 Defect formation energy in GaAs

We have investigated a Ga vacancy defect in this work. A defect is introduced in the perfect GaAs crystal by physically removing one atom from its lattice. Here the supercell for computation is constructed from 8 unit cells of GaAs. All the subsequent calculations are carried out at the optimized lattice parameter of 10.49 a.u. and at a plane wave cutoff energy of 20 Ry. The special k-point chosen for the calculation is (0.5, 0.5, 0.5).

In our calculation, the supercell is periodic in nature and thus, every defect associated with a single supercell gets repeated. When a defect is created in a single unit cell of GaAs by removing one Ga atom, the defect concentration becomes too high (i.e. we are removing one Ga atom from a GaAs cell containing 4 Ga and 4 As atoms). But we are interested in one vacancy in an infinite lattice. Therefore, all our defect related calculations are based on big supercell containing 32 Ga and 32 As atoms. Removing a single atom from the interior of this big supercell causes repetition of vacancy at a larger distance.

In principle, the total energy of a cell containing a defect should be independent of the position of the defect. In order to check this, first one Ga vacancy defect is created

at (0.5, 0.5, 0.5) and the total energy is calculated for this supercell. The total energy calculated is -274.725388 a.u.. The same calculation is repeated for a Ga vacancy defect at (0.75, 0.75, 0.5) and in that case the energy obtained is -274.725391 a.u.. Since the difference between these two results are $\sim 10^{-6}$ a.u., this error can be neglected. Hence, in all our calculations, Ga vacancy defects are created at (0.5 0.5 0.5).

A vacancy defect, at a Ga site in neutral charge state is denoted by V_{Ga}^0 . When an extra electron is present at the vacancy, created by the removal of the Ga atom, it is denoted by V_{Ga}^1 and so on. Calculated total energies of some Ga vacancy defect cells in different charge states along with the corresponding perfect cell are shown in the table 4.11.

Table 4.11 Calculated total energies of a defect supercell at different charge states along with the perfect cell

Cell type	Total energy (a.u.)
Perfect cell	-277.113509
V_{Ga}^0	-274.725388
V_{Ga}^1	-274.621469
V_{Ga}^2	-274.511415

The defect formation energy is then calculated according to the Eq. 2.41.

$$\Omega(\mu_e, \mu_{\text{Ga}}, \mu_{\text{As}}) = E'_D + Q_D(E_v + \mu_e) - \frac{1}{2}(n_{\text{Ga}} - n_{\text{As}})\Delta\mu \quad (2.41)$$

where,

$$E'_D = E_D - \frac{1}{2}(n_{\text{Ga}} + n_{\text{As}})\mu_{\text{GaAs(bulk)}} - \frac{1}{2}(n_{\text{Ga}} - n_{\text{As}})(\mu_{\text{Ga(bulk)}} - \mu_{\text{As(bulk)}}) \quad (2.42)$$

and

$$\Delta\mu = (\mu_{Ga} - \mu_{As}) - (\mu_{Ga(bulk)} - \mu_{As(bulk)}) \quad (2.43)$$

E_D is the total energy of the defect cell and for a cell containing a Ga defect, n_{Ga} is 31 and n_{As} is 32. Also as described in chapter 1, the chemical potential of the bulk crystal may be equated to the bulk energy per atom (molecule) of the corresponding system. The bulk chemical potentials, as calculated in section 4.4, of GaAs, Ga and As are -235.64174 eV, -62.496374 eV and -172.783836 eV. Accordingly, our calculated results of the formation energies are shown in table 4.12. Our calculated results are then compared with the results obtained by Northrup and Zhang [2.16].

Table 4.12 Calculated defect formation energies of GaAs containing a Ga vacancy defect at different charge states along with the ionization energies

Defect type	Ω (eV)		Ionization energy (eV)	
	From Reference 2.16	Present calculation	From Reference 2.16	Present calculation
V_{Ga}^0	$4.55 + \Delta\mu/2$	$2.306 + \Delta\mu/2$		
V_{Ga}^1	$4.74 - \mu_e + \Delta\mu/2$	$5.1337 - (\mu_e + E_v) + \Delta\mu/2$	0.19	$2.8277 - E_v$
V_{Ga}^2	$4.94 - 2\mu_e + \Delta\mu/2$	$8.128 - 2(\mu_e + E_v) + \Delta\mu/2$	0.2	$2.9943 - E_v$

Here, μ_e can be considered as fermi energy measured from the valence band edge. Therefore, in order to compare our results with that of Northrup and Zhang [2.16], we need to estimate E_v . Furthermore, since calculations of ionization energy involves difference in formation energies of same defect in different charge states, better match with those in [2.16] can be expected.

The ionization energy is calculated according to the following consideration. A defect changes its ionization state in order to minimize the formation energy. For example, in our calculations, we find for fermi energy (μ_e) $2.8277 - E_v$ (eV), the formation energy of V_{Ga}^0 and V_{Ga}^1 is the same. For μ_e less than this value, V_{Ga}^0 is stable and for μ_e greater, V_{Ga}^1 is more stable. Thus, the acceptor level (0/1) due to Ga vacancy lies $2.8277 - E_v$ (eV) above E_v .

Unfortunately, however the E_v energy level for calculation of total energy of a perfect and a defect cell are not the same. And as a result, a band offset correction to this valance band top is needed.

In order to apply these corrections, band structure calculation is done for the Γ point ($k=0, 0, 0$) and the eigenvalue of the highest occupied state is noted. This is the energy of the top of the valance band and in our case it is 2.884 eV. Again, there may be an overall offset of the electrostatic potential that is different in the bulk cell and in the defect cell. To correct for this, the difference in the eigenvalues of the lowest occupied states of these two states are used as a correction. Thus corrected E_v is given by, $E_{v(corrcted)} = E_v - (\epsilon_{perfect} - \epsilon_{defect})$, where $\epsilon_{perfect}$ and ϵ_{defect} are eigenvalues of the lowest occupied states of the perfect and the defect cell calculated at $k=(0.5, 0.5, 0.5)$. The calculated value of $\epsilon_{perfect}$ and ϵ_{defect} (V_{Ga}^0) are -9.505 and -9.694 eV, respectively. Thus, corrected E_v is at 2.695 eV. Accordingly, the ionization levels (0/-1) and (-1/-2) for Ga vacancy are at 0.1227 and 0.2893 eV above the valence band edge.

Pöykkö and others [4.4] had discussed about this correction in detail. According to them, the difference in the energy level of the perfect supercell and the defect supercell

is due to the finite size of the cells. The reference energy level value (which is the valence-band maximum, VBM) is then corrected from the difference of the average potentials of the defect supercell and the perfect supercell, i.e.

$$E_V = E_{V(bulk)} + V_{average(bulklike)} - V_{average(bulk)} \quad (4.1)$$

For a very large supercell, the last two terms in Eq. (4.1) cancels out. However, using such a big supercell for this type of supercell calculation is impossible.

Lakes and others [4.5] had also discussed the effect of the presence of a defect on the reference energy level of total energy calculation. They had used the “model solid” theory as proposed by Van de Walle and Martin [4.6] to calculate the average potential of a system and thus to predict the shift in energy due to the incorporation of the defect.

Chapter 5

Conclusions

In the present work we have studied the defect formation energies of gallium vacancies in GaAs using the computer code *fhi96md*. In the process, we have generated first principle, fully separable norm conserving pseudopotentials using the associated code *fhi98pp*

The pseudopotentials for Ga, As, Si and C are generated according to Bachlet-Hamann-Schlüter scheme. To ensure the accuracy of the pseudopotentials, all electron valance eigenvalues were compared with the corresponding pseudo wavefunctions.

The effects of various parameters appearing in the *fhi96md* code were examined. In order to optimise the GaAs structure, the effect of the two most important parameters, cutoff energy and lattice parameter, were discussed in detail. On the basis of the total energy minimization, the optimised values of cutoff radius and lattice parameter was chosen as 20 Ry and 10.49 a.u., respectively. These two parameters were kept fixed for the subsequent calculations.

To optimise the structures of Ga and As, a neural network program was used. This program gives an approximate point of minimum for the total energy. To check the accuracy of the neural network program, some of the inputs of the neural network program used for the optimization of Ga, were plotted. These plots show the same trend. Finally, total energy calculations were done at the neighbourhood of the approximate point of minimum. Again, on the basis of the total energy minimization, the optimised lattice parameters for these two structures were chosen. The optimised lattice parameters of Ga is chosen as $a = 8.57$ a.u., $b = 14.26265$ a.u., $c = 7.6075$ a.u., $y = 0.1586$ and $z = 0.0366$. For Ga, the total energy per atom, which is also the

chemical potential, is given by, -62.496374 eV. Similarly, for As, the optimised lattice parameters are given by, $a = 7.5497$ a.u., $c = 20.0898$ a.u. and $z = 0.2648$. The chemical potential for As is estimated as -172.783836 eV

The heat of formation for these optimised structures of GaAs, Ga and As are then calculated and compared with the results published in the literature. Our result (0.36 eV) is less than the experimental measure (0.74 eV). The discrepancy is mainly due to the optimization procedure we have adopted to optimize the structure of Ga and As.

Defects were introduced to the perfect GaAs crystal and their total energies were calculated. The calculations were repeated for different charge states of a Ga vacancy defect. To align the reference energy levels of the perfect and the defected cells, band offset correction was applied. Finally the ionization energy of the various defects were calculated and compared with the literature values.

Appendix A

Input file used for the optimization of GaAs

```
#!/bin/csh -xvf

##### define home directory of fhi96md #####

set FHI96MD = "~/fhi96md"

##### set directories #####

set PSEUDO = "${FHI96MD}/pseudo"
set SOURCES = "${FHI96MD}/src"
set WORK = "${FHI96MD}/GaAs/work"

##### change to the working space #####

cd $WORK

#### move pseudopotentials to the working space ####

cp $PSEUDO/ga_aa.cpi fort.11
cp $PSEUDO/as_aa.cpi fort.12

#####
# make input file for cp-program: inp.mod #
# (controlling main features of the fhi96md) #
#####

cat > inp.mod << end_B
-1 100 1000000 : nbeg iprint timequeue
100 1 : nomore nomore_init
20.0 0.9 : delt gamma
4.0 0.2 0.0001 : delt2 gamma2 eps_chg_dlt
400 2 : delt_ion nOrder
0.0 1.0 : pfft_store mesh_accuracy
2 2 : idyn i_edyn
0 .false. : i_xc t_postc
.F. 0.001 .F. 0.002 : trane ampre tranp amprp
.false. .false. .false. 1800 : tfor tdyn tsdp nstepe
.false. : tdipol
0.0001 0.0005 0.1 : epsel epsfor epsekin
0.001 0.001 3 : force_eps max_no_force
1 : init_basis
end_B
```

```
#####
# create input file : inp.ini                                     #
# (controlling the atomic structure and the input)               #
# and parameter.h (used for compiling of fhi96md)               #
# by the help of the program start.f                             #
# make inp for start program                                     #
#####
cat > start.inp << end_A
2          : number of species
0          : excess electrons
5          : number of empty states
1 0       : ibrav pgind
10.6616 0.0 0.0 0 0 0 : celldm
1          : number of k-points
0.5 0.5 0.5 1.0      : k-point coordintes, weight
1 1 1        : fold parameter
.false      : k-point coordinates relative or absolut?
8 4.0       : Ecut [Ry], Ecuti [Ry]
0.004.true. .f.      : ekt tmetal tdegen
.true. .false. 1     : tmold tband nrho
5 2 1234      : npos nthm nseed
873.0 1400.0 1e8 1   : T_ion T_init Q nfi_rescale
.t. .true.     : tpsmesh coordwave
4 3 'Gallium'     : number of atoms, zv, name
1.0 69.72 0.7 3 3   : gauss radius, mass, damping, l_max, l_loc
.t. .t. .f.      : t_init_basis
0.0 0.0 0.0 .t.    : tau0 tford
0.5 0.5 0.0 .t.    : tau0 tford
0.5 0.0 0.5 .t.    : tau0 tford
0.0 0.5 0.5 .t.    : tau0 tford
4 5 'Arsenic'     : number of atoms, zv, name
1.0 74.92 0.7 3 3   : gauss radius, mass, damping, l_max, l_loc
.t. .t. .f.      : t_init_basis
0.25 0.25 0.25 .t.  : tau0 tford
0.75 0.25 0.75 .t.  : tau0 tford
0.75 0.75 0.25 .t.  : tau0 tford
0.25 0.75 0.75 .t.  : tau0 tford
end_A

#####
# run start program and build up parameter.h                     #
# and inp.ini                                                     #
# -in principle one could create inp.ini and                     #
# parameter.h by hand, but start gives a                         #
# consistent and optimized input for fhi96md                     #
#####
```

```

pushd ${SOURCES}/start
make
if ($status) then
    echo 'makes.start: compilation failed'
    exit
endif
popd
cp ${SOURCES}/start.x .
start.x | tee start.out

#####
#    compile fhi96md                                #
#####

cp ${SOURCES}/fhi96md/parameter.h parameter.old
set changes = `cmp parameter.h parameter.old`
pushd ${SOURCES}/fhi96md

if( "$changes" != "" ) then
    cp $WORK/parameter.h .
    make clean
endif

make netlib

if ($status) then
    echo 'makes.fhi96md: compilation failed'
    exit
endif
popd
mv ${SOURCES}/fhi96md.x .

#####
#                run fhi96md                        #
#####

fhi96md.x

```

Appendix B

Input file used for the generation of the Ga pseudopotential

```
31.00 6 2 8 0.00 : z nc nv iexc mlc
 1 0 2.00 : n l f
 2 0 2.00
 2 1 6.00
 3 0 2.00
 3 1 6.00
 3 2 10.00
 4 0 2.00
 4 1 1.00
2 h : lmax s_pp_def
0 1.25 0.00 h : lt rct et s_pp_type
2 2.25 0.00 h
```

Input file used for the generation of the As pseudopotential

```
33.00 6 2 8 0.00 : z nc nv iexc mlc
 1 0 2.00 : n l f
 2 0 2.00
 2 1 6.00
 3 0 2.00
 3 1 6.00
 3 2 10.00
 4 0 2.00
 4 1 3.00
2 h : lmax s_pp_def
0 1.15 0.00 h : lt rct et s_pp_type
2 2.05 0.00 h
```

Input file used for the generation of the Si pseudopotential

```
14.00 3 2 8 0.00 : z nc nv iexc mlc
 1 0 2.00 : n l f
 2 0 2.00
 2 1 6.00
 3 0 2.00
 3 1 2.00

2 h : lmax s_pp_def
```

Input file used for the generation of the C pseudopotential

```
6.00 1 2 8 0.00 : z nc nv iexc mlc
  1 0 2.00 : n l f
  2 0 2.00
  2 1 2.00

2 h : lmax s_pp_def
0 0.00 0.00 h : lt rct et s_pp_type
```


Appendix C

Files *start.inp* and *inp.mod* used in the total energy calculation of GaAs

```
#####
start inp
#####
2          : number of species
0          : excess electrons
5          : number of empty states
1 0        : ibrav pgind
20.98 0 0 0.0 0 0 0 : celldm
1          : number of k-points
0 5 0 5 0.5 1 0     : k-point coordintes, weight
1 1 1          : fold parameter
.false.       : k-point coordinates relative or absolut?
20 4.0        : Ecut [Ry], Ecuti [Ry]
0.004 .true. .f.    : ekt tmetal tdegen
.true. .false. 1    : tmold tband nrho
5 2 1234       : npos nthm nseed
873.0 1400.0 1e8 1 : T_ion T_init Q nfi_rescale
.t. .true.      : tpsmesh coordwave
32 3 'Gallium'    : number of atoms, zv, name
1.0 69.72 0.7 3 3 : gauss radius, mass, damping,l_max,l_loc
.t. .t. .f.      : t_init_basis
0.0 0.0 0.0 .t.   : tau0 tford
0.25 0.25 0.0 .t. : tau0 tford
0.25 0.0 0.25 .t. : tau0 tford
0.0 0.25 0.25 .t. : tau0 tford
0.5 0.0 0.0 .t.   : tau0 tford
0.75 0 25 0.0 .t. : tau0 tford
0.75 0.0 0.25 .t. : tau0 tford
0.5 0.25 0.25 .t. : tau0 tford
0.0 0.0 0.5 .t.   : tau0 tford
0.25 0.25 0.5 .t. : tau0 tford
0.0 0.25 0.75 .t. : tau0 tford
0.25 0.0 0.75 .t. : tau0 tford
0.0 0.5 0.0 .t.   : tau0 tford
0.25 0.75 0.0 .t. : tau0 tford
0.25 0.5 0.25 .t. : tau0 tford
0.0 0.75 0.25 .t. : tau0 tford
0.5 0.5 0.0 .t.   : tau0 tford
0.75 0.75 0.0 .t. : tau0 tford
0.75 0.5 0.25 .t. : tau0 tford
0.5 0.75 0.25 .t. : tau0 tford
0.5 0.0 0.5 .t.   : tau0 tford
```

```

0.75 0 25 0.5 .t. : tau0 tford
0.75 0.0 0 75 .t. : tau0 tford
0.5 0.25 0.75 .t. : tau0 tford
0.0 0.5 0.5 .t. : tau0 tford
0.25 0.75 0.5 .t. : tau0 tford
0.25 0.5 0.75 .t. : tau0 tford
0.0 0.75 0.75 .t. : tau0 tford
0.5 0.5 0.5 .t. : tau0 tford
0.75 0.75 0.5 .t. : tau0 tford
0.75 0.5 0.75 .t. : tau0 tford
0.5 0.75 0.75 .t. : tau0 tford
32 5 'Arsenic' : number of atoms, zv, name
1.0 74.92 0.7 3 3 : gauss radius, mass, damping, l_max, l_loc
.t. .t. .f. : t_init_basis
0.125 0.125 0.125 .t. : tau0 tford
0.375 0.375 0.125 .t. : tau0 tford
0.375 0.125 0.375 .t. : tau0 tford
0.125 0.375 0.375 .t. : tau0 tford
0.625 0.125 0.125 .t. : tau0 tford
0.875 0.375 0.125 .t. : tau0 tford
0.875 0.125 0.375 .t. : tau0 tford
0.625 0.375 0.375 .t. : tau0 tford
0.125 0.125 0.625 .t. : tau0 tford
0.375 0.375 0.625 .t. : tau0 tford
0.125 0.375 0.875 .t. : tau0 tford
0.375 0.125 0.875 .t. : tau0 tford
0.125 0.625 0.125 .t. : tau0 tford
0.375 0.875 0.125 .t. : tau0 tford
0.375 0.625 0.375 .t. : tau0 tford
0.125 0.875 0.375 .t. : tau0 tford
0.625 0.625 0.125 .t. : tau0 tford
0.875 0.875 0.125 .t. : tau0 tford
0.875 0.625 0.375 .t. : tau0 tford
0.625 0.875 0.375 .t. : tau0 tford
0.625 0.125 0.625 .t. : tau0 tford
0.875 0.375 0.625 .t. : tau0 tford
0.875 0.125 0.875 .t. : tau0 tford
0.625 0.375 0.875 .t. : tau0 tford
0.125 0.625 0.625 .t. : tau0 tford
0.375 0.875 0.625 .t. : tau0 tford
0.375 0.625 0.875 .t. : tau0 tford
0.125 0.875 0.875 .t. : tau0 tford
0.625 0.625 0.625 .t. : tau0 tford
0.875 0.875 0.625 .t. : tau0 tford
0.875 0.625 0.875 .t. : tau0 tford
0.625 0.875 0.875 .t. : tau0 tford

```

inp mod

```
.....#  
.....#  
-1 100 1000000 : nbeg iprint timequeue  
1000 1 : nomore nomore_init  
20 0 0.9 : delt gamma  
4.0 0.2 0.0001 : delt2 gamma2 eps_chg_dlt  
400 2 : delt_ion nOrder  
0.0 1.0 : pfft_store mesh_accuracy  
2 2 : idyn i_edyn  
0 false. : i_xc t_postc  
F 0.001 .F. 0.002 : trane ampre tranp amprp  
.false. .false. .false. 1800 : tfor tdyn tsdp nstepe  
false. : tdipol  
0 0001 0.0005 0.1 : epsel epsfor epsekinc  
0 001 0 001 3 : force_eps max_no_force  
1 : init_basis
```

Appendix D

Input file used for the optimisation of As

```
#!/bin/csh -xvf
##### define home directory of fhi96md #####

set FHI96MD  "  fhi96md"

                set directories #####

set PSEUDO  "$ {FHI96MD}/pseudo"
set SOURCES "$ {FHI96MD}/src"
set WORK    "$ {FHI96MD}/As/work"

                change to the working space #####

cd $WORK

##### move pseudopotentials to the working space #####

cp SPSEUDO/as_aa.cpi fort.11

#####
# make input file for cp-program:  inp.mod      #
# (controlling main features of the fhi96md)    #
#####

cat < inp.mod >> end_B
-1 100 1000000          : nbeg  iprint timequeue
1000 1                  : nomore nomore_init
20.0 0.9                : delt  gamma
4.0 0.2 0.0001          : delt2 gamma2 eps_chg_dlt
400 2                   : delt_ion nOrder
0.0 1.0                 : pfft_store mesh_accuracy
2 2                     : idyn i_edyn
0 .false.               : i_xc t_postc
.F. 0.001 .F. 0.002     : tranc ampre tranp amprp
.false. .false. .false. 1800 : tfor tdyn tsdp nstepe
.false.                 : tdipol
0.0001 0.0005 0.3       : epsel epsfor epsekin
0.001 0.001 3           : force_eps max_no_force
1                       : init_basis
end_B
```

```
#####
# create input file : start.ini                                     #
# (controlling the atomic structure and the input)                 #
# and parameter.h (used for compiling of fhi96md)                 #
# by the help of the program start.f                               #
# make inp for start program                                       #
#####

cat > start.inp << end_A
1          : number of species
0          : excess electrons
5          : number of empty states
4 0        : ibrav pgind
14.2102 1 4027 0.0 1 1 1 : celldm
1          : number of k-points
0.33 0.33 0.25 1.0       : k-point coordintes, weight
1 1 1        : fold parameter
.true.       : k-point coordinates relative or absolut?
20 4.0       : Ecut [Ry], Ecuti [Ry]
0.1 .true. .f. : ekt tmetal tdegem
.true. .false. 1 : tmold tband nrho
5 2 1234      : npos nthm nseed
873.0 1400.0 1e8 1 : T_ion T_init Q nfi_rescale
.t. .true.    : tpsmesh coordwave
24 5 'Arsenic' : number of atoms, zv, name
1.0 74.92 0.7 3 3 : gauss radius, mass, damping,l_max,l_loc
.t. .t. .f.    : t_init_basis
0.0 0.0 4.5260 .t. : tau0 tford
0.0 0.0 -4.5260 .t. : tau0 tford
2.3684 4.7368 17.8143 .t. : tau0 tford
2.3684 4.7368 8.7622 .t. : tau0 tford
4.7368 2.3684 11.1702 .t. : tau0 tford
4.7368 2.3684 2.1181 .t. : tau0 tford
7.1051 0.0 4.5260 .t. : tau0 tford
7.1051 0.0 -4.5260 .t. : tau0 tford
9.4735 4.7368 17.8143 .t. : tau0 tford
9.4735 4.7368 8.7622 .t. : tau0 tford
11.8419 2.3684 11.1702 .t. : tau0 tford
11.8419 2.3684 2.1181 .t. : tau0 tford
0.0 7.1051 4.5260 .t. : tau0 tford
0.0 7.1051 -4.5260 .t. : tau0 tford
2.3684 11.8419 17.8143 .t. : tau0 tford
2.3684 11.8419 8.7622 .t. : tau0 tford
4.7368 9.4735 11.1702 .t. : tau0 tford
4.7368 9.4735 2.1181 .t. : tau0 tford
7.1051 7.1051 4.5260 .t. : tau0 tford
```

```

7.1051 7.1051 -4.5260 .t. : tau0 tford
9.4735 11.8419 17.8143 .t. : tau0 tford
9.4735 11.8419 8.7622 .t. : tau0 tford
11.8419 9.4735 11.1702 .t. : tau0 tford
11.8419 9.4735 2.1181 .t. : tau0 tford
end_A

```

```

#####
# run start program and build up parameter.h #
# and inp.ini #
# -in principle one could create inp.ini and #
# parameter.h by hand, but start gives a #
# consistent and optimized input for the #
# fhi96md #
#####

```

```

pushd ${SOURCES}/start
make
if ($status) then
    echo 'makes.start: compilation failed'
    exit
endif
popd
cp ${SOURCES}/start.x .
start.x |tee start.out

```

```

#####
# compile fhi96md #
#####

```

```

cp ${SOURCES}/fhi96md/parameter.h parameter.old
set changes = `cmp parameter.h parameter.old`
pushd ${SOURCES}/fhi96md

```

```

if( "$changes" != "" ) then
    cp $WORK/parameter.h .
    make clean

```

```

endif

```

```

make netlib

```

```

if ($status) then
    echo 'makes.fhi96md: compilation failed'
    exit
endif

```

```
popd
mv S{SOURCES}/fhi96md.x .
```

```
#####
#           run fhi96md                               #
#####
```

```
fhi96md.x
```

Appendix E

Neural network inputs used for the optimization of arsenic

2a (a.u.)	c (a.u.)	z	Total Energy (a.u.)
12.7893	17.9391	0.2044	-148.592756
12.7893	17.9391	0.2158	-148.597763
12.7893	17.9391	0.2271	-149.685384
12.7893	17.9391	0.2385	-151.652316
12.7893	17.9391	0.2498	-151.867524
12.7893	18.9357	0.2044	-148.900903
12.7893	18.9357	0.2158	-150.334842
12.7893	18.9357	0.2271	-151.335916
12.7893	18.9357	0.2385	-151.928675
12.7893	18.9357	0.2498	-152.104528
12.7893	19.9323	0.2044	-149.174143
12.7893	19.9323	0.2158	-150.476578
12.7893	19.9323	0.2271	-151.580436
12.7893	19.9323	0.2385	-152.125691
12.7893	19.9323	0.2498	-152.276857
12.7893	20.9289	0.2044	-149.436043
12.7893	20.9289	0.2158	-150.881858
12.7893	20.9289	0.2271	-151.810842
12.7893	20.9289	0.2385	-152.290418
12.7893	20.9289	0.2498	-152.427439
12.7893	21.9255	0.2044	-149.405347
12.7893	21.9255	0.2158	-151.12387
12.7893	21.9255	0.2271	-151.996896
12.7893	21.9255	0.2358	-152.413284
12.7893	21.9255	0.2498	-152.532102
13.4998	17.9391	0.2044	-149.966719
13.4998	17.9391	0.2158	-150.947268
13.4998	17.9391	0.2271	-151.648953
13.4998	17.9391	0.2358	-152.034279
13.4998	17.9391	0.2498	-152.145701

2a (a u)	c (a u)	z	Total Energy (a.u.)
13 4998	18.9357	0.2044	-150 190956
13 4998	18 9357	0.2158	-151 168662
13.4998	18 9357	0.2271	-151 830942
13 4998	18.9357	0 2385	-152 182843
13 4998	18 9357	0 2498	-152 297785
13.4998	19.9323	0.2044	-150.190956
13.4998	19.9323	0.2158	-151 353098
13.4998	19 9323	0.2271	-151 973077
13 4998	19 9323	0 2385	-152 305185
13 4998	19.9323	0.2498	-152 403676
13.4998	20.9289	0.2044	-150 549596
13 4998	20.9289	0 2158	-151.510053
13.4998	20.9289	0.2271	-152.093085
13 4998	20 9289	0.2385	-152.402923
13.4998	20.9289	0.2498	-152.489102
13.4998	21.9255	0.2044	-150.704569
13.4998	21.9255	0.2158	-151 655003
13 4998	21.9255	0 2271	-152.206141
13.4998	21 9255	0 2385	-152.47314
13 4998	21.9255	0.2498	-152.546772
14.2103	17.9391	0.2044	-150.896989
14.2103	17.9391	0.2158	-151.574875
14.2103	17.9391	0.2271	-152.041176
14 2103	17.9391	0.2385	-152.283256
14.2103	17.9391	0.2498	-152.3393
14 2103	18.9357	0.2044	-150.998672
14 2103	18.9357	0.2158	-151.686898
14 2103	18.9357	0.2271	-152.12534
14.2103	18.9357	0.2385	-152 338327
14 2103	18.9357	0.2498	-152 392332

2a (a u)	c (a.u.)	z	Total Energy (a.u.)
14.2103	19.9323	0.2044	-151.190622
14.2103	19.9323	0.2158	-151.837567
14.2103	19.9323	0.2271	-152.214004
14.2103	19.9323	0.2385	-152.382564
14.2103	19.9323	0.2498	-152.423512
14.2103	20.9289	0.2044	-151.300884
14.2103	20.9289	0.2158	-151.92332
14.2103	20.9289	0.2271	-152.263325
14.2103	20.9289	0.2385	-152.417692
14.2103	20.9289	0.2498	-152.463261
14.2103	21.9255	0.2044	-151.381373
14.2103	21.9255	0.2158	-152.036796
14.2103	21.9255	0.2271	-152.309305
14.2103	21.9255	0.2385	-152.426381
14.2103	21.9255	0.2498	-152.458771
14.9208	17.9391	0.2044	-151.507124
14.9208	17.9391	0.2158	-151.96845
14.9208	17.9391	0.2271	-152.267596
14.9208	17.9391	0.2385	-152.410306
14.9208	17.9391	0.2498	-152.430264
14.9208	18.9357	0.2044	-151.618496
14.9208	18.9357	0.2158	-152.062044
14.9208	18.9357	0.2271	-152.318991
14.9208	18.9357	0.2385	-152.423884
14.9208	18.9357	0.2498	-152.425016
14.9208	19.9323	0.2044	-151.705588
14.9208	19.9323	0.2158	-152.125665
14.9208	19.9323	0.2271	-152.339689
14.9208	19.9323	0.2385	-152.407047
14.9208	19.9323	0.2498	-152.403438

2a (a u)	c (a u)	z	Total Energy (a u)
14 9208	20 9289	0.2044	-151.774869
14 9208	20 9289	0.2158	-152.166093
14 9208	20 9289	0.2271	-152.337961
14 9208	20 9289	0.2385	-152.384107
14 9208	20.9289	0.2498	-152.387221
14 9208	21 9255	0.2044	-151.841269
14 9208	21 9255	0 2158	-152 195787
14 9208	21 9255	0.2271	-152 33325
14.9208	21 9255	0.2385	-152 364998
14.9208	21 9255	0.2498	-152.374562
15 6313	17 9391	0.2044	-151 884662
15.6313	17.9391	0 2158	-152 188452
15.6313	17.9391	0.2271	-152 371035
15.6313	17 9391	0 2385	-152 442035
15.6313	17 9391	0.2498	-152.443712
15.6313	18.9357	0 2044	-151.956486
15.6313	18.9357	0 2158	-152.23994
15.6313	18 9357	0.2271	-152.381797
15.6313	18 9357	0.2385	-152.41976
15.6313	18.9357	0 2498	-152 407368
15 6313	19.9323	0.2044	-152.008415
15.6313	19 9323	0.2158	-152.267179
15 6313	19.9323	0 2271	-152.366205
15 6313	19.9323	0.2385	-152.370041
15.6313	19.9323	0.2498	-152.351764
15 6313	20.9289	0.2044	-152.047868
15 6313	20 9289	0.2158	-152.27578
15.6313	20.9289	0 2271	-152.335951
15.6313	20 9289	0 2385	-152.313594
15.6313	20.9289	0 2498	-152.289382

2a (a.u.)	c (a.u.)	z	Total Energy (a.u.)
15.6313	21.9255	0.2044	-152.078463
15.6313	21.9255	0.2158	-152.272436
15.6313	21.9255	0.2271	-152.297813
15.6313	21.9255	0.2385	-152.251902
15.6313	21.9255	0.2498	-152.227326

Appendix F

Input file used for the optimisation of Ga

```
#!/bin/csh -xvf
##### define home directory of fhi96md #####

set FHI96MD = "~/fhi96md"

##### set directories #####

set PSEUDO = "${FHI96MD}/pseudo"
set SOURCES = "${FHI96MD}/src"
set WORK = "${FHI96MD}/Ga/work"

##### change to the working space #####

cd $WORK

#### move pseudopotentials to the working space ####

cp $PSEUDO/ga_aa.cpi fort.11

#####
# make input file for fhi96md: inp.mod #
# (controlling main features of the fhi96md) #
#####

cat > inp.mod << end_B
-1 100 1000000      : nbeg iprint timequeue
5000 2              : nomore nomore_init
30.0 0.9            : delt gamma
4.0 0.2 0.0001      : delt2 gamma2 eps_chg_dlt
400 2               : delt_ion nOrder
0.0 1.0             : pfft_store mesh_accuracy
2 2                 : idyn i_edyn
0 .false.           : i_xc t_postc
.F. 0.001 .F. 0.002 : trane ampre tranp amprp
.false. .false. .false. 1800 : tfor tdyn tsdp nstepe
.false.             : tdipol
0.0001 0.0005 0.2   : epsel epsfor epsekinc
0.001 0.001 3        : force_eps max_no_force
3                     : init_basis
end_B
```

```

#####
# create input file : inp.ini                                     #
# (controlling the atomic structure and the input)               #
# and parameter.h (used for compiling of fhi96md)               #
# by the help of the program start.f                             #
# make inp for start program                                     #
#####

cat > start.inp << end_A
1          : number of species
0          : excess electrons
5          : number of empty states
8 0        : ibrav pgind
17.08 28.946 8.552 1 1 1 : celldm
1          : number of k-points
0.5 0.5 0.5 1.00        : k-point coordintes, weight
1 1 1          : fold parameter
.true.         : k-point coordinates relative or absolut?
20 5.0         : Ecut [Ry], Ecuti [Ry]
0.1 .true. .f.   : ekt tmetal tdegen
.true. .false. 1 : tmold tband nrho
5 2 1234        : npos nthm nseed
873.0 1400.0 1e8 1 : T_ion T_init Q nfi_rescale
.t. .true.      : tpsmesh coordwave
32 3 'Gallium'   : number of atoms, zv, name
1.0 69.72 0.7 3 3 : gauss radius, mass, damping,l_max,l_loc
.t. .t. .f.     : t_init_basis
0.0 2.2274 0.6824 .t. : tau0 tford
0.0 -2.2274 -0.6824 .t. : tau0 tford
4.27 2.2274 3.5936 .t. : tau0 tford
4.27 -2.2274 4.9584 .t. : tau0 tford
4.27 9.4639 0.6824 .t. : tau0 tford
4.27 5.0091 -0.6824 .t. : tau0 tford
0.0 5.0091 4.9584 .t. : tau0 tford
0.0 9.4639 3.5936 .t. : tau0 tford
8.54 2.2274 0.6824 .t. : tau0 tford
8.54 -2.2274 -0.6824 .t. : tau0 tford
12.81 2.2274 3.5936 .t. : tau0 tford
12.81 -2.2274 4.9584 .t. : tau0 tford
12.81 9.4639 0.6824 .t. : tau0 tford
12.81 5.0091 -0.6824 .t. : tau0 tford
8.54 5.0091 4.9584 .t. : tau0 tford
8.54 9.4639 3.5936 .t. : tau0 tford
0.0 16.7004 0.6824 .t. : tau0 tford
0.0 12.2456 -0.6824 .t. : tau0 tford
4.27 16.7004 3.5936 .t. : tau0 tford

```

```

4.27 12.2456 4.9584      .t. : tau0 tford
4.27 23.9369 0.6824      .t. : tau0 tford
4.27 19.4821 -0.6824     .t. : tau0 tford
0.0  19.4821 4.9584      .t. : tau0 tford
0.0  23.9369 3.5936      .t. : tau0 tford
8.54 16.7004 0.6824      .t. : tau0 tford
8.54 12.2456 -0.6824     .t. : tau0 tford
12.81 16 7004 3.5936     .t. : tau0 tford
12.81 12.2456 4.9584     .t. : tau0 tford
12.81 23.9369 0.6824     .t. : tau0 tford
12 81 19 4821 -0.6824    .t. : tau0 tford
8.54 19.4821 4.9584      .t. : tau0 tford
8.54 23.9369 3.5936      .t. : tau0 tford
end_A

```

```

#####
# run start program and build up parameter.h      #
# and inp.in                                         #
# -in principle one could create inp.ini and       #
# parameter.h by hand, but start gives a           #
# consistent and optimized input for               #
# fhi96md                                           #
#####

pushd ${SOURCES}/start
make
if ($status) then
    echo 'makes.start: compilation failed'
    exit
endif
popd
cp ${SOURCES}/start.x .
start.x |tee start.out

#####
# compile fhi96md                                   #
#####

cp ${SOURCES}/fhi96md/parameter.h parameter.old
set changes = `cmp parameter.h parameter.old`
pushd ${SOURCES}/fhi96md

if( "$changes" != "" ) then
    cp $WORK/parameter.h .
    make clean

```

```

endif

make netlib

if ($status) then
    echo 'makes.fhi96md. compilation failed'
    exit
endif
popd
mv ${SOURCES}/fhi96md.x .

#####
#           run fhi96md                               #
#####

fhi96md.x

```


Appendix G

Neural network inputs used for the optimization of gallium

2a (a u.)	2b (a u.)	c (a u.)	y	z	Total energy (a u.)
15.372	26.0507	7.6973	0.1385	0.0718	-72.946632
15.372	26.0507	7.6973	0.1385	0.0878	-73.00116
15.372	26.0507	7.6973	0.1693	0.0718	-73.17925
15.372	26.0507	7.6973	0.1693	0.0878	-73.116578
15.372	26.0507	8.5525	0.1385	0.0718	-72.717299
15.372	26.0507	8.5525	0.1385	0.0878	-72.802232
15.372	26.0507	8.5525	0.1693	0.0718	-73.042343
15.372	26.0507	8.5525	0.1693	0.0878	-73.01291
15.372	26.0507	9.4078	0.1385	0.0718	-72.325745
15.372	26.0507	9.4078	0.1385	0.0718	-72.4347
15.372	26.0507	9.4078	0.1693	0.0878	-72.649952
15.372	26.0507	9.4078	0.1693	0.0878	-72.630669
15.372	28.9452	7.6973	0.1385	0.0718	-73.282178
15.372	28.9452	7.6973	0.1385	0.0878	-73.274833
15.372	28.9452	7.6973	0.1693	0.0718	-73.301977
15.372	28.9452	7.6973	0.1693	0.0878	-73.25467
15.372	28.9452	8.5525	0.1385	0.0718	-73.104797
15.372	28.9452	8.5525	0.1385	0.0878	-73.108821
15.372	28.9452	8.5525	0.1693	0.0718	-73.149786
15.372	28.9452	8.5525	0.1693	0.0878	-73.119617
15.372	28.9452	9.4078	0.1385	0.0718	-72.650385
15.372	28.9452	9.4078	0.1385	0.0878	-72.686652
15.372	28.9452	9.4078	0.1693	0.0718	-72.764318
15.372	28.9452	9.4078	0.1693	0.0878	-72.748086

2a (a.u.)	2b (a.u.)	c (a.u.)	y	z	Total Energy (a.u.)
15.372	31.8397	7.6973	0.1385	0.0718	-73.210365
15.372	31.8397	7.6973	0.1385	0.0878	-73.20457
15.372	31.8397	7.6973	0.1693	0.0718	-73.280907
15.372	31.8397	7.6973	0.1693	0.0878	-73.248118
15.372	31.8397	8.5525	0.1385	0.0718	-73.013472
15.372	31.8397	8.5525	0.1385	0.0878	-73.029739
15.372	31.8397	8.5525	0.1693	0.0718	-73.126805
15.372	31.8397	8.5525	0.1693	0.0878	-73.112496
15.372	31.8397	9.4078	0.1385	0.0718	-72.646568
15.372	31.8397	9.4078	0.1385	0.0878	-72.681739
15.372	31.8397	9.4078	0.1693	0.0718	-72.759612
15.372	31.8397	9.4078	0.1693	0.0878	-72.762634
17.08	26.0507	7.6973	0.1385	0.0718	-72.87244
17.08	26.0507	7.6973	0.1385	0.0878	-72.95765
17.08	26.0507	7.6973	0.1693	0.0718	-73.174164
17.08	26.0507	7.6973	0.1693	0.0878	-73.137081
17.08	26.0507	8.5525	0.1385	0.0718	-72.670453
17.08	26.0507	8.5525	0.1385	0.0878	-72.775988
17.08	26.0507	8.5525	0.1693	0.0718	-72.067294
17.08	26.0507	8.5525	0.1693	0.0878	-73.037114
17.08	26.0507	9.4078	0.1385	0.0718	-72.312578
17.08	26.0507	9.4078	0.1385	0.0878	-72.431531
17.08	26.0507	9.4078	0.1693	0.0718	-72.706837
17.08	26.0507	9.4078	0.1693	0.0878	-72.674234
17.08	28.9452	7.6973	0.1385	0.0718	-73.152382
17.08	28.9452	7.6973	0.1385	0.0878	-73.163748

2a (a.u.)	2b (a.u.)	c (a u)	y	z	Total Energy (a u)
17.08	28.9452	7.6973	0.1693	0.0718	-73 198104
17 08	28.9452	7.6973	0.1693	0 0878	-73 153634
17 08	28 9452	8.5525	0.1385	0 0718	-72 927961
17 08	28 9452	8.5525	0.1385	0 0878	-72 95572
17.08	28.9452	8.5525	0.1693	0.0718	-73 077214
17.08	28 9452	8 5525	0.1693	0.0878	-73 038365
17.08	28.9452	9.4078	0.1385	0.0718	-72 580664
17 08	28.9452	9.4078	0.1385	0.0878	-72 613028
17.08	28.9452	9.4078	0.1693	0.0718	-72.721315
17.08	28.9452	9.4078	0 1693	0.0878	-72 685313
17.08	31.8397	7.6973	0 1385	0.0718	-73 023889
17.08	31.8397	7 6973	0.1385	0.0878	-73.027779
17.08	31.8397	7.6973	0 1693	0.0718	-73.095547
17 08	31.8397	7.6973	0 1693	0.0878	-73 065969
17 08	31.8397	8.5525	0 1385	0.0718	-72 854404
17 08	31.8397	8.5525	0.1385	0.0878	-72 869299
17 08	31.8397	8.5525	0 1693	0.0718	-72 9741
17.08	31.8397	8.5525	0.1693	0.0878	-73.95221
17 08	31.8397	9.4078	0.1385	0.0718	-72 521119
17.08	31.8397	9.4078	0 1385	0 0878	-72 543919
17 08	31.8397	9.4078	0 1693	0.0718	-72 637968
17 08	31.8397	9.4078	0 1693	0.0878	-72.623488
18.788	26.0507	7.6973	0 1385	0.0718	-72 653423
18.788	26.0507	7.6973	0 1385	0.0878	-72.754084
18.788	26.0507	7.6973	0 1693	0 0718	-72 99646
18.788	26.0507	7.6973	0 1693	0 0878	-72 943921

2a (a.u.)	2b (a.u.)	c (a.u.)	y	z	Total Energy (a u)
18 788	26.0507	8.5525	0.1385	0 0718	-72.478426
18.788	26 0507	8.5525	0.1385	0 0878	-72 595728
18 788	26.0507	8 5525	0 1693	0 0718	-72.916775
18 788	26 0507	8.5525	0.1693	0 0878	-72 88746
18 788	26 0507	9.4078	0 1385	0.0718	-72.152547
18 788	26.0507	9 4078	0.1385	0.0878	-72.279387
18 788	26 0507	9.4078	0 1693	0 0718	-72 581597
18 788	26 0507	9.4078	0 1693	0 0878	-72 548741
18 788	28 9452	7.6973	0.1385	0 0718	-72 918081
18 788	28.9452	7.6973	0.1385	0 0878	-72.937145
18 788	28.9452	7.6973	0.1693	0 0718	-72.969414
18 788	28 9452	7.6973	0.1693	0.0878	-72.926379
18.788	28 9452	8 5525	0.1385	0.0718	-72 796325
18 788	28 9452	8.5525	0 1385	0 0878	-72.810759
18 788	28 9452	8 5525	0.1693	0.0718	-72.875041
18 788	28.9452	8.5525	0 1693	0.0878	-72.832872
18 788	28 9452	9.4078	0 1385	0.0718	-72 410677
18.788	28.9452	9 4078	0 1385	0.0878	-72 441576
18 788	28 9452	9.4078	0.1693	0.0718	-72.548506
18 788	28.9452	9 4078	0 1693	0.0878	-72 504717
18 788	31 8397	7.6973	0 1385	0.0718	-72 760679
18.788	31 8397	7.6973	0 1385	0 0878	-72 758218
18 788	31.8397	7 6973	0 1693	0.0718	-72 802653
18 788	31.8397	7.6973	0.1693	0.0878	-72 767385
18.788	31.8397	8 5525	0 1385	0.0718	-72.623396
18.788	31 8397	8.5525	0.1385	0.0878	-72 625656

2a (a u)	2b (a u)	c (a u.)	y	z	Total Energy (a.u)
18.788	31 8397	8 5525	0.1693	0 0718	-72.710581
18.788	31 8397	8 5525	0.1693	0 0878	-72.677826
18 788	31 8397	9.4078	0 1385	0.0718	-72.328431
18.788	31 8397	9.4078	0 1385	0.0878	-72.331826
18 788	31 8397	9.4078	0.1693	0.0718	-72.405067
18 788	31 8397	9.4078	0.1693	0.0878	-72.374261

Bibliography

Chapter 1

- [1.1] P. Hohenberg and W. Kohn, Phys. Rev. **136**, B864 (1964)
- [1.2] M. Born and J. R. Oppenheimer, Ann. der Phys. **84**, 457 (1927)
- [1.3] W. kohn and L. J. Sham, Phys. Rev. **140**, A1133 (1965)
- [1.4] J. P. Perdew, *Electronic Structure of Solids '91*, edited by P. Ziesche and H. Eschrig, Akademie-Verlag, Berlin (1990)
- [1.5] M. Bockstedte, A. Kley, J. Neugebauer and M. Scheffler, Comput. Phys. Commun. **107**, 187 (1997)
- [1.6] M. Fuchs and M. Scheffler, Comput. Phys. Commun. **119**, 67 (1999)
- [1.7] G. Qian, R. Martin and D. J. Chadi, Phys. Rev. B **38**, 7649 (1988)
- [1.8] G. P. Kerker, J. Phys. C **13**, L189 (1980)
- [1.9] R. J. Needs, R. M. Martin and O. H. Nielsen, Phys. Rev. B **33**, 3778 (1986)

Chapter 2

- [2.1] D. R. Hartree, Proc. Cambridge. Philos. Soc. **24**, 89 (1928)
- [2.2] V. Fock, Z. Phys. **61**, 126 (1930)
- [2.3] J. C. Slater, Phys. Rev. **35**, 210 (1930)
- [2.4] L. H. Thomas, Proc. Cambridge. Philos. Soc. **23**, 542 (1927)
- [2.5] E. Fermi, Z. Phys. **48**, 73 (1928)
- [2.6] D. M. Ceperley and B. J. Alder, Phys. Rev. Lett. **45**, 566 (1980)
- [2.7] J. P. Perdew and A. Zunger, Phys. Rev. B **23**, 5048 (1981)
- [2.8] L. Verlet, Phys. Rev. **159**, 98 (1967)
- [2.9] M. P. Allen and D. J. Tildesley, *Computer Simulation of Liquids*, Clarendon Press,

Oxford, (1990)

- [2.10] D. R. Hamann, M. Schlüter and C. Chiang, Phys. Rev. Lett. **43**, 1494 (1979)
- [2.11] G. B. Bachlet, D. R. Hamann and M. Schlüter, Phys. Rev. B **26**, 4199 (1982)
- [2.12] N. Troullier and L. J. Martins, Phys. Rev. B **43**, 1993(1991)
- [2.13] D. Vanderbilt, Phys. Rev. B **32**, 8412(1985)
- [2.14] G. D. Mahan, *Many Particle Physics*, Plenum, NY, (1990)
- [2.15] L. Kleinman and D. M. Bylander, Phys. Rev. B **48**, 1425 (1982)
- [2.16] J. E. Northrup and S. B. Zhang, Phys. Rev. B **47**, 6791(1993)
- [2.17] L. Kleinman, Phys. Rev. B **24**, 7412(1981)

Chapter 3

- [3.1] M.C. Payne, J. D. Joannopoulos, D. C. Allen, M. P. Teter and D. H. Vanderbilt,
Phys. Rev. Lett. **56**, 2656 (1986)
- [3.2] A. Williams and J. Soler, Bull. Am. Phys. Soc. **32**, 562 (1987)
- [3.3] D. J. Chadi and M. L. Cohen, Phys. Rev. B **8**, 5747 (1973)
- [3.4] H. J. Monkhorst and J. D. Pack, Phys. Rev. B **13**, 5188 (1976)
- [3.5] *Handbook of Electronic Materials*, vol.2, III-V Semiconducting Compounds, M.
Neuberger, IFI/PLENUM, New York-Washington-London (1971)

Chapter 4

- [4.1] J. Donohue, *The Structure of Elements*, John Wiley and Sons 303 (1974)
- [4.2] *Large's Handbook of Chemistry*, 12th edition, edited by J. A. Dean (McGraw Hill,
New York, 1979) pp. 9-23 and 9-8
- [4.3] W. B. Pearson, *The Crystal Chemistry and Physics of Metals and Alloys*, Wiley –
Interscience (1972)

- [4.4] S. Pöykkö, M. J. Puska and R. M. Nieminen, Phys. Rev. B **53**, 3813 (1996)
- [4.5] D. B. Lakes, C.G. Van de Walle, G. F. Neumark, P.E. Blöchl and S.T. Pantelides,
Phys. Rev. B **19**, 10965 (1992)
- [4.6] C.G. Van de Walle and R. M. Martin, Phys. Rev. B **35**, 8154 (1987)

132703

This book is to be returned on
the date last stamped.

This image shows a blank sheet of white paper with horizontal ruling lines. A solid vertical line runs down the left side of the page, creating a narrow margin. The rest of the page is filled with evenly spaced horizontal dashed lines, typical of notebook paper. There are no markings or text on the page.

A133733

TH

MS/2001/M

N153f